2020•2021
Faculteit Industriële Ingenieurswetenschappen
master in de industriële wetenschappen: elektromechanica

Masterthesis

Optimisation of wheelchairs for Paralympic athletes: design of a flexible carbon fibre backrest

PROMOTOR :
Prof. dr. ir. Kris HENRIOULLE

PROMOTOR :
Prof. dr. Yann LANDON

Tim Biesmans

Scriptie ingediend tot het behalen van de graad van master in de industriële wetenschappen: elektromechanica

▶▶ UHASSELT   KU LEUVEN

▶▶ UHASSELT   KU LEUVEN

2020•2021
Faculteit Industriële Ingenieurswetenschappen
master in de industriële wetenschappen: elektromechanica

Masterthesis

Optimisation of wheelchairs for Paralympic athletes: design of a flexible carbon fibre backrest

PROMOTOR :
Prof. dr. ir. Kris HENRIOULLE

PROMOTOR :
Prof. dr. Yann LANDON

Tim Biesmans
Scriptie ingediend tot het behalen van de graad van master in de industriële wetenschappen: elektromechanica

►► UHASSELT   KU LEUVEN

Preface

When I was a child, I dreamed of becoming an astronaut or a pilot. Unfortunately, I discovered that this would be very difficult for someone with asthma. However, I had an interest in engineering already from a young age, when I built crazy creations with my favourite Lego-bricks. Therefore, I swore that I would one day be involved in developing an airplane or spaceship or by working together with the aerospace industry.

Fast forward 19 years into the future during the COVID-pandemic. I loathed staying at home in my room, constantly following online seminars and working on several group projects in lockdown, without being able to visit the campus to socialise with my peers. Although I could always rely on my family for relaxation, love, and support, I felt like my room had become an unfulfilling workstation. One day, I heard that there were still students signing up and experiencing Erasmus exchanges abroad, despite the global lockdown and unrest. Frightened of the prospect of another year in confinement at home, I made a spontaneous decision to **sign up for an Erasmus exchange**. I could picture no better location than Toulouse: this would help me attain my goal of becoming fluent in French and perhaps fulfil a lifelong dream.

The exchange wasn't without difficulty. It was a lot of work solely to arrive in Toulouse, let alone rent a student residence. But I have learned more in the past three months about myself than in the rest of my twenty-three-year-old life. I have made amazing friends, become far more self-sufficient and fallen in love with Toulouse and all its charms. I thoroughly enjoyed worked on this master's thesis because of its challenges and context. I even fulfilled a lifelong dream to work together with the company Airbus…

Table of contents

List of tables

List of figures

Glossary of terms

Design parameter	Parameter related to the design of the sheet/section. Examples include the section length L and the thickness t for the section of the different models. This may also include the beam length H for the sheet design.
FEM	Finite Elements Method
FEA	Finite Elements Analysis
Rigidity	The relationship between the load and the deformation caused by that load. For example: an elastic spring has a linear relation between the load F and deformation v, characterised by the formula $F = k * v$. In this formula, k is the spring constant or the rigidity of that spring. The higher the rigidity, the less the spring will deform given a given load. In the context of this thesis, this principle is applied for a beam under a distributed charge. It is further explained in chapter two: theoretical background.

Abstract in English

The research lab ICA is working on a global project of designing a wheelchair for a Paralympic badminton athlete. Because this athlete has no abdominal muscles, the backrest of this wheelchair requires elastic bands to support the athlete's back. The goal of this master's thesis is to investigate if the elastic bands could be replicated with thin carbon fibre sheets with a variable rigidity.

There are three objectives in the design of such a sheet. Firstly, the relationship between the design of the sheet and the deformation is unknown. The rigidity varies depending on the position on the sheet. Therefore, a method to calculate the deformation characteristic in function of the position is developed. Secondly, the impact of varying a design parameter on the deformation is investigated. Thirdly, the desired deformation is converted to a sheet design and prototype.

To investigate the deformation, various designs for the section of the sheet are made, for each of which a mathematical model is developed. After selecting the preferred model, the deformation in function of the position is calculated. By varying design parameters, the impact on the deformation characteristic is found. Subsequently, the desired deformation can be converted by varying the design parameters of the model, resulting in a final sheet design. Finally, the results of finite element analyses (FEA) on the design are discussed and physical tests are prepared. The linear and non-linear FEA show that the proposed design is feasible for a limited charge.

Abstract in Dutch

Het onderzoekslab ICA werkt aan een globaal project om een rolstoel te ontwerpen voor een Paralympische batmintonatleet. Omdat deze atleet geen buikspieren heeft, gebruikt de rugsteun van de rolstoel elastieken om de atleet zijn rug te ondersteunen. Het doel van deze Masterproef is te onderzoeken of de elastieken gerepliceerd kunnen worden door dunne carbonvezel platen met een variërende stijfheid.

Er zijn drie doelstellingen in het ontwerpen van een dergelijke plaat. Ten eerste is de relatie tussen het ontwerp van de plaat en de vervorming onbekend. De stijfheid varieert afhankelijk van de positie op de plaat. Daarom is een methode ontwikkeld om de vervormingskarakteristiek in functie van de positie te tonen. Ten tweede wordt voor elke ontwerpparameter het effect getoond op de vervormingskarakteristiek. Ten slotte, wordt de gewenste vervorming omgezet worden in een plaatontwerp en prototype.

Om de vervorming te onderzoeken, worden verschillende ontwerpen voor de sectie van de plaat gemaakt, waarvoor elk een wiskundig model wordt opgesteld. Na de selectie van de modellen, wordt de vervorming berekend. Door elk van de ontwerpparameters te variëren, kan de impact op de vervorming bekomen worden. Vervolgens, kan de gewenste vervorming omgezet worden door ontwerpparameters te optimaliseren, wat leidt tot een eindontwerp. Ten slotte, worden eindige-elementanalyses (EEA) op het ontwerp besproken en fysieke testen voorbereid. De lineaire en non-lineaire EEA tonen aan dat dit ontwerp haalbaar is voor een beperkte belasting.

1. Introduction

1.1 Context of the thesis

The aerospace company Airbus is currently designing a wheelchair for a Paralympic badminton athlete to compete in the 2024 Paralympic games. For the design of specific components of the wheelchair, they are working together with the research centre Institute Clément Ader (ICA), who granted this thesis subject in cooperation with Université Toulouse III Paul Sabatier. This thesis focusses specifically on the backrest of the athlete. Because of his injury, the Paralympic athlete has no abdominal muscles left.

Therefore, the athlete currently uses a backrest made entirely from elastic bands. The purpose of these bands is to support the back of the athlete and to give more power during strokes. Because Para-badminton games require high agility and fast acceleration, the mass of the components of the wheelchair also need to be minimised. Elastic bands fit this constraint perfectly, since their mass is negligible compared to the frame of the wheelchair. A 3D scan of the current backrest, made by a previous Master's student Mathias Lambrecht and his colleagues, is shown on the following figure (Fig. 1). [1]
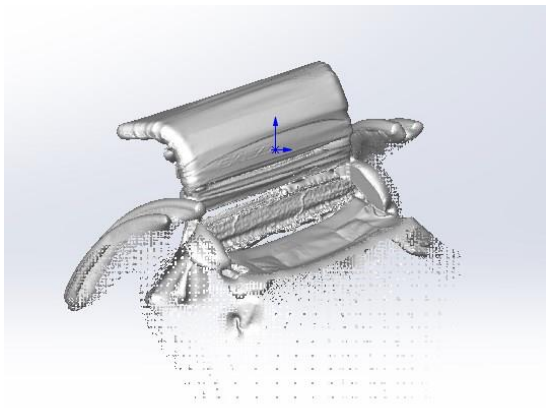
Figure 1: 3D-scan of the backrest of the current wheelchair

Because the athlete requires more support at his lower back and more flexibility at the top of his backrest, each elastic band has a different rigidity. This is illustrated on the following image (Fig. 2).
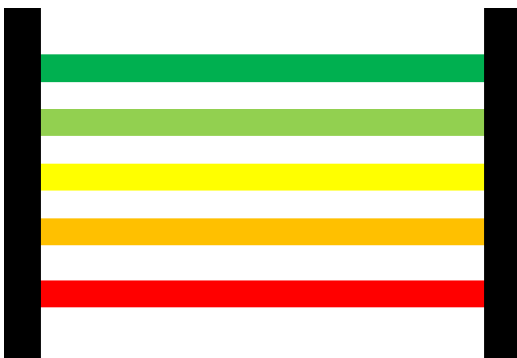
Figure 2: Schematic representation of the elastic bands

The colours on figure 2 represent the different levels of rigidity. A redder colour means a higher rigidity is required, whilst a greener colour means a lower rigidity is required. Thus, **a higher rigidity is required at the base and a lower rigidity at the top**. However, utilising these elastic bands is not an ideal solution for three key reasons:

1. It takes a long time to calibrate these elastic bands.
2. The bands are stretched beyond their limits. This means they are prone to permanent deformation even during the match.
3. Because of the high stress on the elastic bands, they must be replaced and recalibrated after each match. This also means that the configuration might be inconsistent or suboptimal.

These disadvantages would be remedied by designing thin elastic panels made from carbon fibre epoxy resin, which mimic the rigidity of the elastic bands. Utilising these carbon fibre sheets would yield the following advantages:

-   Because of its design, practically no calibration would be necessary before the match.
-   If designed properly, the carbon sheets will only deform elastically under the loads of the match. This means the rigidity of the backrest does not change during matches and the backrest can be used for multiple matches without a decrease in performance.
-   Because of the utilised material category (carbon fibre/epoxy resin), difference in mass for replacing the elastic bands would be negligible, thus satisfying the goal of minimizing the mass of the wheelchair.
-   Because the backrest is already calibrated in its design, the rigidity will be more consistent during matches and could be optimised on the physiology of the athlete. In theory, this would yield consistent optimal results.

A design concept for this carbon fibre backrest proposed by Mathias Lambrecht is shown on figure 4.
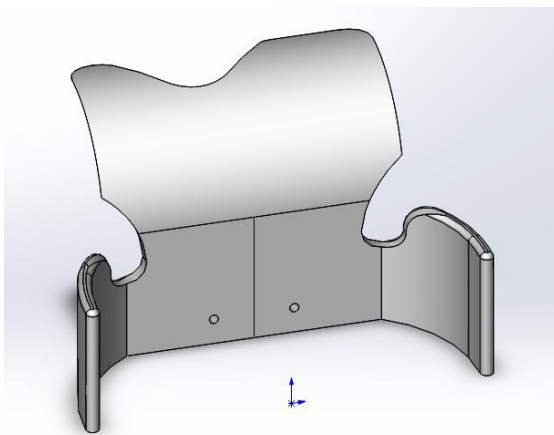
Figure 3: New concept for the backrest

As visible in the figure, the back panel is slanted and does not rely on elastic bands. Because the rigidity of the elastic band is different depending on the height, the carbon fibre replication must vary in rigidity in function of the height of the panel. This means that the rigidity of the backrest must be calibrated to match the rigidity of the elastic bands at each given height.

Although it is proposed to create a backrest from a single carbon fibre sheet, this is not the most ideal option. The deformation is different for each side of the backrest: in the middle the deformation will be the highest, whilst at the sides the deformation would be minimal. To achieve this, the rigidity must vary within the single sheet from the centre to the side. A single sheet could in theory address this concern by varying the thickness of the sheet. However, since carbon fibre sheets are produced layer by layer, it is far harder to vary the thickness during production.

This problem is resolved by designing a backrest consisting of multiple carbon fibre sheets connected by a solid piece. To vary the rigidity in function of the height of the backrest, the section of the sheet can be altered. This way, the deformations, and rigidities from side to centre could be reproduced by the individual sheets. Therefore, it would be **more beneficial to create a backrest from multiple carbon fibre sheets with a varying section**. This principle is shown on the following figure (Fig. 4).
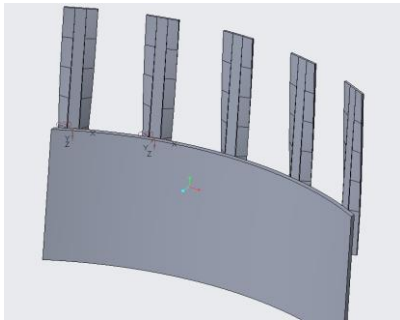
Figure 4: The new design concept, a backrest made from multiple carbon fibre sheets with a variable section

1.2 Problem definition

Although the goal is to replicate elastic bands by a fully carbon fibre backrest, it is still unknown if it is possible to replicate the characteristics of the elastic bands by multiple carbon fibre sheets. Design an entirely carbon fibre backrest has too many variables to take into consideration, such as rigidity, design parameters (like section design, sheet length), the applied load, etc…

Therefore, this Master's thesis poses the following research question:

"Can the characteristics of the elastic bands of the current backrest be replicated by flexible thin carbon fibre epoxy resin sheets with a variable rigidity?"

To know if it is possible to design a whole backrest from carbon fibre sheets, it must be known if it is possible to design **one single carbon fibre sheet** based on a desired deformation and rigidity at a given position. If this is possible, the same methodology can be applied to design multiple sheets. Because of this reasoning, this Master's thesis will focus on replicating one single sheet. This reasoning is shown on the following figure (Fig. 5).
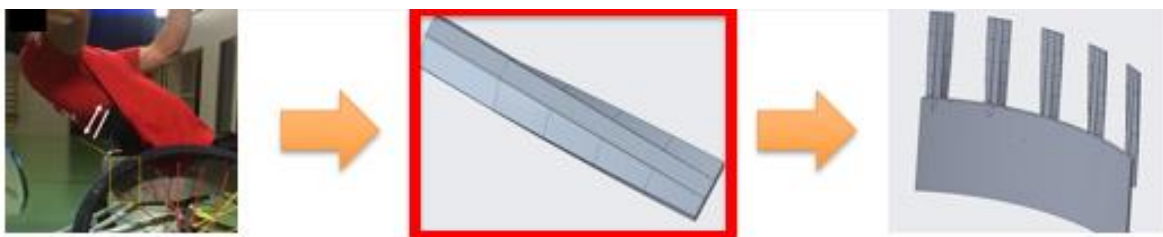
Figure 5: The design process – 1) Calculate/measure the desired deformation (left); 2) Recreate the deformation for a single sheet (centre); 3) Design the entire backrest based on the same methodology (right)

This study is **based on estimations and approximations** of real values, since no concrete data was available on the forces on the elastic bands, the rigidity, the deformation, etc… Therefore, the goal of the thesis is not to accurately recreate the deformation and rigidity based on the given data. The goal of this study is **to develop the methodology and mathematical framework to recreate the rigidity for a sheet**, to be applied when the necessary data becomes available. This thesis functions as the **foundation for the development of each individual carbon fibre sheet** and consequently the backrest.

1.3 Objectives

The overarching goal of recreating the characteristics of the elastic bands can be achieved by first recreating the rigidity. To measure if the rigidity is successfully recreated, we need to **measure the deformation**, since this is related to the rigidity. The relationship between the rigidity and the deformation is further explained in **paragraph 3.1**.

Therefore, the goal of recreating the elastic bands by a single carbon fibre sheet can be divided into three subgoals:

1. Find the relation between the sheet design and the deformation.
2. Visualise the impact of varying each design parameter on the resulting deformation.
3. Convert the desired deformation into a functional prototype.

By measuring the deformation of a prototype, which is designed to replicate the deformation of the elastic bands for a given point, it is possible to check if the result matches the designed deformation and therefore the designed rigidity.

1.4 Methodology

1.4.1 Simplifications

To design a carbon fibre sheet based on the rigidity and deformation of the backrest, some simplifications are necessary. Because a single sheet is fixed at the backrest at a single point, the sheet can be considered as an embedded beam. Therefore, this thesis adopts the first simplification, that **classical beam theory** [2] **is applicable on the carbon fibre sheet.** This means that there is a linear relationship between the applied load and the deformation of the sheet, which makes calculations far easier. If the deformation is limited, this is a good simplification. If, however, the desired deformation is relatively great, it should be calculated for which range beam theory is applicable. When beam theory is applied, the carbon fibre sheet can be mechanically represented in a 2D plane as in the following figure (Fig. 6).
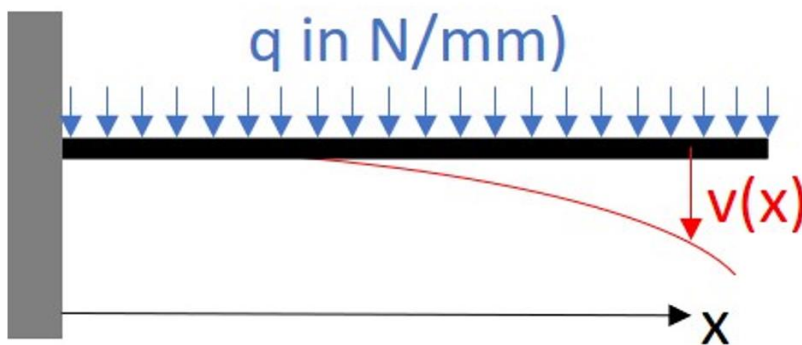
Figure 6: Mechanical representation of the carbon fibre sheet for beam theory

Since the backrest will be used in a competitive environment, the sheet will be subjected to a varying load at different positions in the x-axis. However, it is not yet measured how this load is distributed and which order of magnitude is applicable. Therefore, the second simplification states that **the charge on the carbon fibre sheet is uniform.**

Since the real charge is unknown, it is far easier to replace a varying charge with a constant charge q. In essence, the function for the charge in function of the position q(x) can be described with the following equation (1.1):

$$q(x) = q \tag{1.1}$$

With q(x) the charge at any given position of x and q the constant charge. Since in all the following mathematical calculations the charge is assumed as constant, the charge can easily be updated by a function of x when the charge is measured/quantified. This makes it relatively easy to expand the mathematical models calculated in this thesis and the Excel calculations.

1.4.2 Concrete methodology

The methodology of this thesis follows the following schematic (Fig. 7).
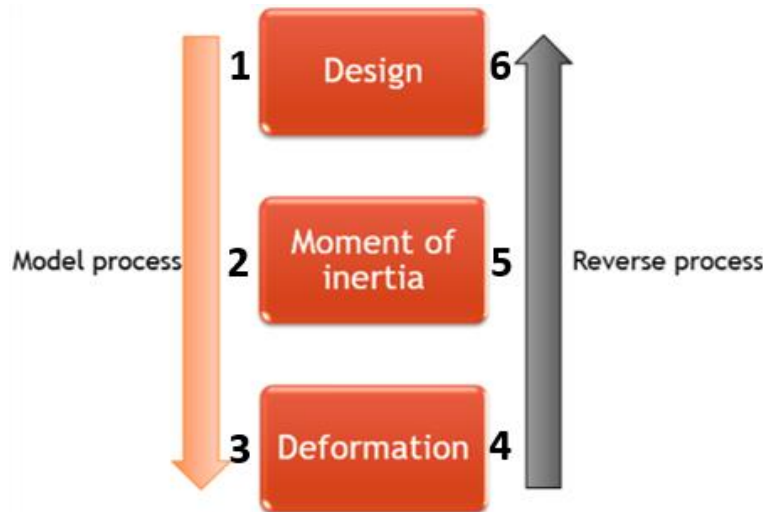
Figure 7: Schematic representation of the methodology

To design the carbon fibre sheet, the methodology can be divided into two processes. The first process is the 'Model process', which aims to check which mathematical models for the section yield a favourable relationship with the deformation. The steps in the model process are:

1. Design: the design of multiple mathematical models of the section of the hypothetical sheet.
2. Moment of inertia: the calculation of the moment of inertia, based on the models of the section.
3. Deformation: the calculation of the deformation, based on the previously calculated moments of inertia. This includes checking the effects of each design parameter on the deformation.

When these three steps are completed, a direct relationship between the sheet design and the deformation will be found. It is important to note that the effect of varying each design parameter is studied. This would enable the recreation of the desired deformation in a discrete manner during the reverse process.

The 'Reverse process' aims to reverse the previous three steps to find the optimal design of the sheet. By reversing the process and starting from the desired deformation, the sheet parameters can be calculated to mimic this desired deformation. This process consists of the following steps:

4. Deformation: the calculation of the desired deformation for one point of the backrest.
5. Moment of inertia: by utilising the model of the moment of inertia, the design parameters are calculated based on the deformation. This can be completed analytically or discretely.
6. Design: the conversion of the design parameters into an actual prototype and mould design for the sheet. This design should be tested with FEM-software and physical tests to see if the replication of the deformation is successful.

It could be argued that the model process could be sidestepped by directly trying to calculate the sheet design from the desired deformation, but this would be less effective. First and foremost, the relation between the section design (by mathematical models) and the deformation is necessary to calculate the shape of the sheet. Secondly, the model process is a way of testing multiple sections designs to see which shape is easily utilised and altered to replicate the elastic bands. Thirdly, by calculating the deformation based on the different section models, it is possible to find the effect of each design parameter of the sheet on the deformation. If the analytical calculation of the design parameters in step four is not possible/hard, the result can be found discretely by tweaking parameters until the correct deformation is found.

2. Theoretical background

The overarching goal of the master's thesis is to check if a carbon fibre sheet can replicate the desired deformation. This requires important theoretical insights and literature. This chapter aims to provide a base of reference for the insights required to finish the project.

Firstly, this chapter will discuss how to create a design utilising Finite Element Modelling. Secondly, the theoretical concept of rigidity is discussed. Thirdly, literature is reviewed to perform an estimation for certain material characteristics in this thesis. Finally, the chapter is closed by stating the conclusions.

2.1 Designing using Finite Element Modelling

This thesis is in essence a design study entirely based on FEM analyses. Because there are no physical tests performed, the results are entirely based on these analyses, which should confirm the preformed calculations. A study with an equivalent methodology is researched to check if the methodologies align and to find possible difficulties with this study.

In 2018, a study was conducted to design a carbon-fibre ankle-foot prosthetic by only utilising Finite Element Modelling [3]. It aims to design a prosthetic foot from carbon fibre sheets, based on biomechanics and numerical data available. No physical tests were conducted to verify the FEA from this study, which means this is a good comparison with this thesis.

The methodology is divided into three main chapters (excluding the introduction):

- Design considerations
- Methods
- Results and discussion

The chapter 'Design considerations' focusses on the theoretical background necessary for designing such a study, such as ISO standards, biomechanics, anthropometry, … This indicates that a theoretical framework must be clearly defined at the start of the thesis. Applied to this thesis, this means explaining the theoretical concepts of rigidity, deformation, and the underlying theory beneath it.

The chapter 'Methods' focusses on the actual design of the prosthetics and creating the CAD model. It also discusses how the FEM software is used. This can be related to this study: there are multiple chapters dedicated to calculating the theoretical results and one chapter implements these results into a prototype design. Results and discussion focus on showing and discussing the FEM results. This should be applied in the final chapter before the conclusion.

There are aspects that are not applied in this study. The source is dependent on biomechanical theory, whilst this study is focussed primarily on beam theory from mechanics. This study does not utilise measurements on the backrest or the athlete to predict the results. This should be taken into consideration when comparing these studies.

2.2 Defining rigidity

The concept of rigidity is the resistance to deformation: The more rigid an object is, the less it will deform when subjected to a given load. In this thesis, it is related to the bending stiffness of a material, which is the resistance against bending deformation [4]. The stiffness, and in essence the rigidity, can be calculated based on the formula's related to classic beam theory. The course "Mechanics of Materials" by Russel C. Hibbeler [5] is consulted for the required formulas for the calculations and this concept will be explained based on these formulas.

In classical beam theory, the rigidity of a thin sheet can be compared to the rigidity of a beam. The rigidity can be concluded as the relation between the applied load and the resulting deformation. This relation is described by the following differential equations (2.1 and 2.2):

$$E * I * \frac{d^4v}{dx^4} = q(x) \tag{2.1}$$

$$E * I * \frac{d^2v}{dx^2} = M(x) \tag{2.2}$$

Containing:

E: Young's Modulus of the selected material, more specifically the **Flexural Modulus**
I: moment of inertia of the beam section
v: deformation of the beam for a position x
M: flexural moment in the beam for a position x
q: distributed load applied at the beam for a position x

The deformation v (also a function of x) and the load q(x) can be determined by experimental data on the elastic bands. The Young's Modulus/Flexural Modulus is entirely dependent on the material used (in this case, carbon fibre epoxy resin) and is a constant. Because the goal is to vary the section of the sheet, **the moment of inertia will not be a constant, but a function of x**. Because of the previously stated simplifications, the charge is defined as a constant q. This means (by double integrating the differential in formula 2.1) that **M(x) is a second order polynomial**. This means the functions change to the following (2.3 and 2.4):

$$E * I(x) * \frac{d^4v(x)}{dx^4} = q \tag{2.3}$$

$$E * I(x) * \frac{d^2v(x)}{dx^2} = M(x) \sim q * x^2 \tag{2.4}$$

Formula 2.4 is the basis for every calculation in this thesis. For the model process, the formula is used to calculate the deformation, whilst for the reverse process it is used to calculate the design parameters of the moment of inertia.

The relation between the load and the deformation, is known as the rigidity. Therefore, **the rigidity of a beam is equal to the Young's modulus of the material multiplied by the moment of inertia of the beam section (2.5):**

$$Rigidity = E * I(x) \tag{2.5}$$

Because the Flexural Modulus is a constant, it can be stated that the bending stiffness and rigidity of the carbon fibre sheet is directly related to the moment of inertia of the section. Therefore, the moment of inertia will be used to characterise the rigidity of the sheet at any position for x.

2.3 Estimating material characteristics

From chapter 4 onwards, the calculations for the rigidity and the reverse require an estimation of the Flexural Modulus of the material. However, the exact material used to produce the prototype was not yet determined, since there are multiple variants for producing carbon fibre epoxy resin. Therefore, the Flexural Modulus should be estimated based on studies that test the flexural modulus of this material.

In the calculations, a Modulus of 75 GPa is used as a reference value. This was first based on the Tensile Modulus of a peer reviewed study from the 2nd International Conference on Nanomaterials and Technologies in 2014 [6]. In this study, the average value of the Tensile Modulus was calculated at 75.095 GPa. Therefore, a value of 75 GPa was used during the first calculations.

However, the stress on this sheet is primarily flexural stress instead of tensile strength because of the applied load on the sheet. This means the Flexural Modulus should be used to calculate the deformation in formula 2.4. In this study, an average flexural modulus of 69.63 GPa was found. To check if this value was up to date, another study specifically focussing on the flexural properties from 2020 was consulted [7]. For 0% glass/epoxy plies, a flexural modulus of around 70 GPa is indeed found. From this study, the value for the flexural strength of 950 MPa is utilised as a reference during the discussion of the FEM analyses.

Since this is still an estimate of the real flexural modulus and close to the reference value of 75 GPA, it was decided to keep using 75 GPa as reference modulus. Because this is an estimation, the FEA results must be regarded critically. The flexural modulus and the flexural strength should be tested with an extra carbon fibre sheet during the physical tests to modify the references for the mathematical calculations. Therefore, the test results should be used to recalculate the deformation and rigidity. This is one of the key reasons why physical testing is very important.

2.4 Conclusions

- To design the sheet, a structure of Theory-Design-Discussion is necessary. This is the best approach to replicating an object with another material.
- The flexural moment is a function of the position x and should be second order polynomial according to the utilised simplifications. This is an important control for the calculations.
- The rigidity on a given position x is directly related to the moment of inertia of the section in x. The rigidity is also dependant on the flexural modulus of the material.
- The flexural modulus is estimated at 75 GPa and the flexural strength at 950 MPa. These values should be checked by physical tests on the used material. The test results should be used to recalculate the deformation and rigidity.

3. Calculating the rigidity

To create a successful design for the section of the sheet, the relationship between the section design and the rigidity must be found. As stated previously in chapter 2, the rigidity is defined by the moment of inertia of the section of the sheet. To calculate the rigidity for each position of the sheet, a relation between the shape of the sheet and the moment of inertia must first be defined. This relation should be simple enough to allow for easier calculations using formula 2.4. Therefore, mathematical models for the section of the sheet are established to calculate the moment of inertia using Microsoft Excel. Afterwards, an interpolation equation is established with excel to find the best fitting function to use in further calculations. In this chapter, these calculations are summarised and the resulting characteristics of the moment inertia are discussed.

3.1 Creating mathematical models

3.1.1   Analytical circular model

The first impulse to defining a model for the section, was to use a sheet in the form of a circular arc and calculate the moment of inertia analytically. This sheet would have a fixed section length and thickness because it is easier to produce a sheet with a fixed length and thickness. To vary the rigidity (and the moment of inertia), the radius would increase. This is illustrated by the following image (Fig. 8).
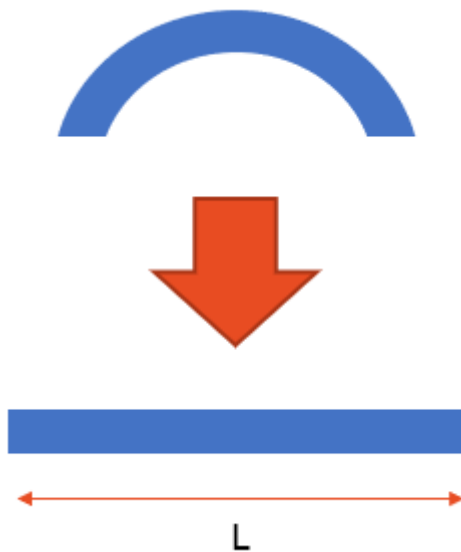
Figure 8: Principle of the variation of a circular section when increasing the radius R

The model was based entirely on analytical calculations and integrations. However, the calculation of the moment of inertia showed great errors when the radius R increased. Mathematically, the model is correct, but it is inapplicable in this scenario. This model is very hard to use because of the complex calculations and is practically unusable for calculating the deformation. A lesson was learned: the most intuitive solution is not always the correct/best solution.

The next model approximates this circular arc by a 2nd order Least Squares Solution of for the circular arc. Although the error remained for lower values of the radius, the error diminished when the radius increased. This is the first model that successfully approximated the circular arc, but the error remains too great to be used consistently.

The lessons learned when calculating these two models are implemented into the next three models. Each of these models has successfully calculated the moment of inertia in relation to their section.

3.1.2 Polynomial model

The first model to effectively calculate the moment of inertia in relation to the section design. It is also based on a circular arc. The section design is shown on figure 9 below.
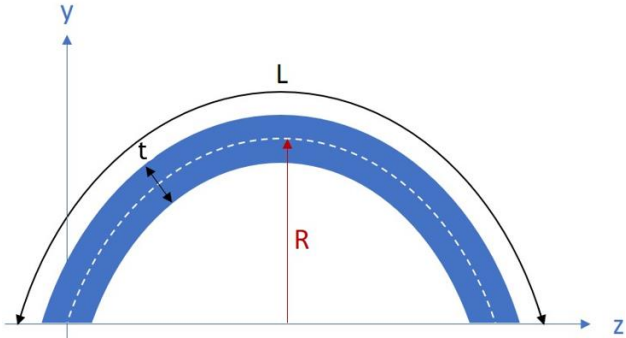
Figure 9: Principle of the polynomial model

In essence, this model is based on a 2nd polynomial approximation of a circular arc (as shown by the white striped line). This polynomial has a constant thickness based on the development of the polynomial function. This model has the following constant parameters for each position of x:

L: Section length and the length of the polynomial.
t: Thickness of the sheet.

The variable parameter of this model is the radius R. When the radius increases, the section becomes more flat and less bent. The evolution of the section is the same as illustrated on figure 8.

3.1.3 U-model

The second successful section model is the U-model. This model works by varying the shape of a U where each leg has the same length as the top base. This principle is illustrated on figure 10.
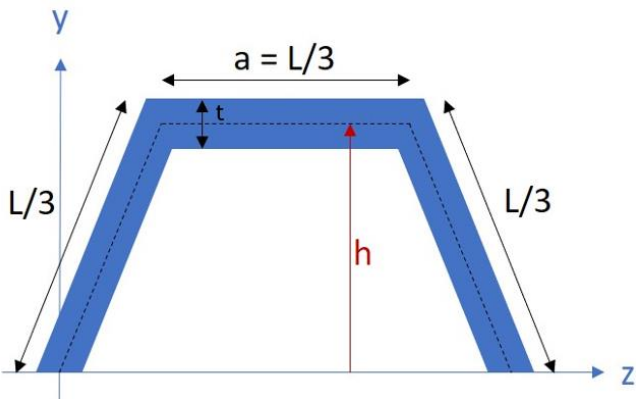
Figure 10: Principle of the U-model

For this model, the top base and the length of each leg has the same length. Thus, the section length L, the thickness t and the top base a are constant parameters. The variable parameter is the height h. By

26

decreasing the height, the shape of the model can be changed to a straighter surface. This evolution is shown on the following figure (Fig. 11).
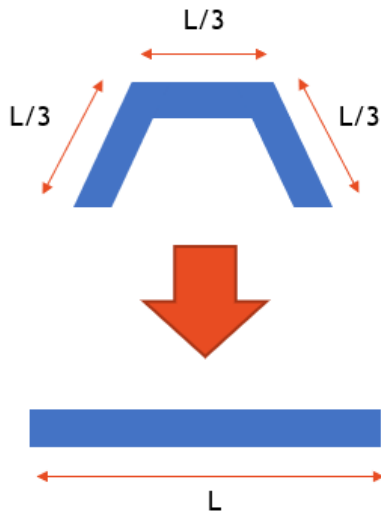
Figure 11: Evolution of the U-model when lowering the height h

3.1.4 U-model with a constant base

The final successful section model has the same principle as the U-model, but has one key difference: **the base is always constant in length**. This principle is shown in figure 12.
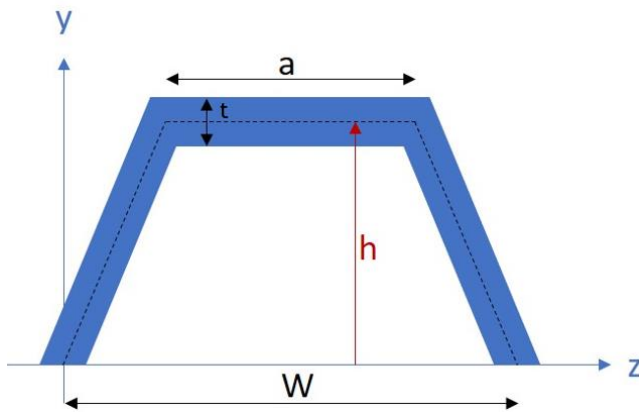
Figure 12: Principle of the U-model with a constant base

For this model, the parameters section length L, thickness t and base W are constant, while the parameters top base a and height h can change. The most important aspect about this model is the relation between the base W and the section length L, characterised by the following formula (3.1):

$$\frac{L - a}{2} = \frac{W}{2} \tag{3.1}$$

The height h is directly related to the top base a and can be calculated by the following formula:

$$\left(\frac{L - a}{2}\right)^2 = \left(\frac{W - a}{2}\right)^2 + h^2 \tag{3.2}$$

Although it is easier to vary the section by varying the top base, the moment of inertia is directly related to the height of the section. Therefore, the height h is chosen as the variable parameter.

Although the top base a also varies, it will thus vary depending of the height. When decreasing the height, the moment of inertia will increase. This evolution of the section is shown on figure 13.
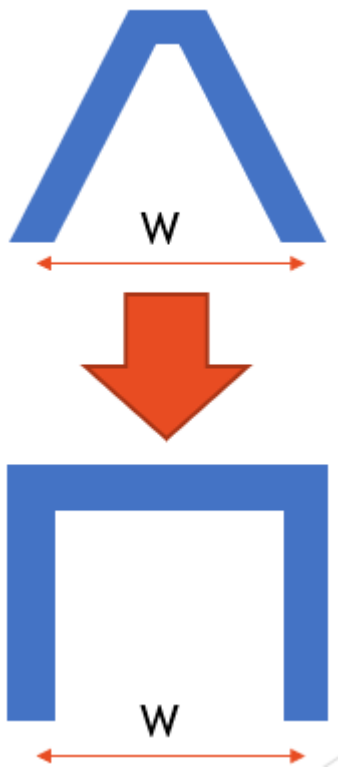
Figure 13: Evolution of the U-model with a constant base when lowering the height h

3.2 Calculating moment of inertia for each model

The goal of this paragraph is to calculate the moment of inertia in the centre of gravity in function of the varying parameter (R or h). This will indicate a clear relationship between the rigidity and the varying parameter. This relationship can later be used in the calculation of the deformation.

3.2.1 Polynomial model

The calculation for the moment of inertia for the centre of gravity of the section I_{gz} is summarised in this chapter. The full written calculation is added in Appendix A. Note that in the appendix the thickness is defined as e because the French for thickness is the word 'epaisseur'.

To calculate the moment of inertia, it is first necessary to define the polynomial approximation of the circular arc. This can be done by creating a point O on a 2D plane and defining it as the base for the circular arc and the approximating 2nd order polynomial. This principle is shown in figure 14.
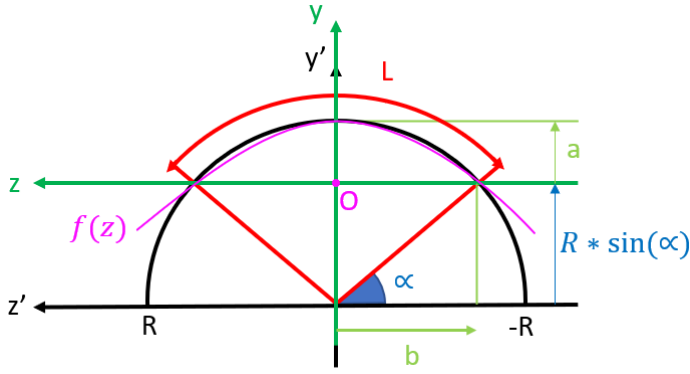
Figure 14: Defining the circular arc and approximating by a polynomial

After calculating each parameter, the function for the approximation of the circular arc can be described by the following formula (3.3):

$$f(z) = \frac{-a}{b^2} * z^2 + a \tag{3.3}$$

With:

$$a = R * \left(1 - \cos\left(\frac{L}{2R}\right)\right) \tag{3.4}$$

$$b = R * \sin\left(\frac{L}{2R}\right) \tag{3.5}$$

The section of the model can be calculated by creating a line integral [8] for an infinitesimal piece of the length, as shown in appendix A. This leads to the following value of the section area:

$$S = b * t < L * t \tag{3.6}$$

This is not a good approximation, since the section area should always be equal to L*t. Utilising the same integral approximation, the moment of inertia for the point O I_{oz} is calculated as:

$$I_{oz} = \frac{(32 * a^2 + 5 * t^2) * b * t}{30} \tag{3.7}$$

Calculating the moment of inertia for the centre of gravity I_{gz} by calculating the height of the centre of gravity, leads to the following result:

$$I_{gz} = \frac{(16 * a^2 + 15 * t^2) * b * t}{90} \tag{3.8}$$

Note that the moment of inertia in formula 3.8 is stated in the parameters a and b, as defined by formula 3.4 and 3.5. This means that the parameters a and b must be calculated to calculate the moment of inertia. In Excel, this can be accomplished by creating a column structure and calculating each parameter based on the given radius R.

The model is checked by calculating the moment of inertia for given parameters and comparing this with the real moment of inertia for these parameters. The used software to calculate the real moment of inertia in the centre of gravity is CATIA V5. This control is shown in the following table (Tab. 1).

R(mm)	L(mm)	t(mm)	Measured I_{gz} (mm^4)	Calculated I_{gz} (mm^4)	Error (mm^4)	Relative error (%)
10	10	1	2,109	2,076	0,033	1,550
50	10	1	0,890	0,887	0,003	0,302
100	10	1	0,847	0,847	0,000	0,016
200	10	1	0,837	0,837	0,000	0,034
500	10	1	0,834	0,834	0,000	0,015

As shown on the table, the error decreases significantly for a higher radius and the starting error is relatively low. This means that this model is a good approximation for the section of a circular arc.

3.2.2   U-model

The calculation for the moment of inertia for the centre of gravity of the section I_{gz} is summarised in this chapter. The full written calculation is added in Appendix C. Note that in the appendix the thickness is defined as e because the French for thickness is the word 'epaisseur'. Note also that this calculation is based on the x-y coordinate system to make calculations easier.

To calculate the moment of inertia for the U-model, the moment of inertia must be defined for a trapezoid. This is calculated in **Appendix B.** This results in the following formula for the moment of inertia at the height of the lower base:

$$I_{ox,trapezoïd} = \frac{3 * a * h^3}{12} + \frac{b * h^3}{12}$$

(3.9)

With b the lower base, a the top base and h the height of the trapezoid.

The moment of inertia in the origin for the U-model, as shown in figure 10, can be calculated by subtracting two trapezoids. The larger trapezoid has a height of h+t/2 whilst the lower trapezoid has a height of h-t/2. By calculating the variables of the two trapezoids, the moment of inertia in the origin O can be calculated for both trapezoids. This principle is shown on the following figure (Fig. 15).
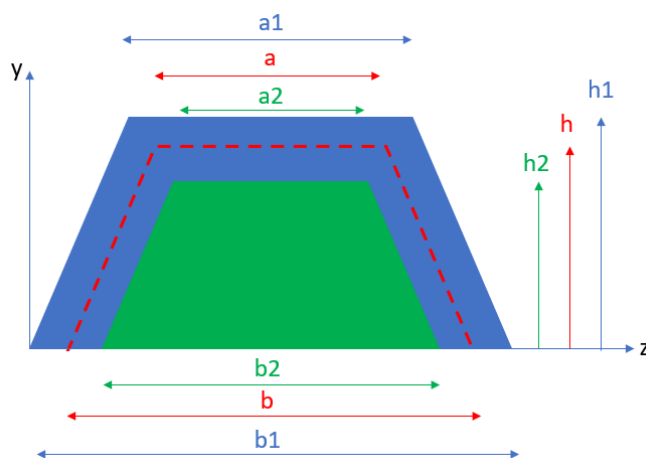
Figure 15: Principle of calculating the two trapezoids to create the U-model, by subtracting trapezoid 2 from trapezoid 1

Afterwards, the values for the moments of inertia in the origin can be subtracted. By calculating the height of the centre of gravity and the section area, the moment of inertia in the centre of gravity I_{gx} can be calculated.

The numerical control calculations made in Appendix C show that the moment of inertia is correct for both extreme states. These controls were made utilising a calculator (TI-nspire CX CAS) and a calculation website [9].

3.2.3   U-model with constant base

The full written calculation is added in Appendix D. Note that in the appendix the thickness is defined as e because the French for thickness is the word 'epaisseur'. Note also that this calculation is based on the x-y coordinate system to make calculations easier.

The methodology to calculate the moment of inertia for the U-model with a constant base is the same as for the U-model. It is important to note that both calculations are verified by calculations in CATIA V5 on the last page of Appendix D.

3.3 Discussion of the results

Each of the models will be calculated for a section length L of 30 mm and a thickness t of 1 mm. For the U-model with a constant base, a base W of 10 mm is chosen. The moment of inertia is calculated for the whole range of the varying parameter (R or h). Hereafter, the calculation of the moment of inertia is completed in Excel by implementing the methodology described in the previous chapter and Appendix A, B and D. The results are discussed in the next paragraphs.

3.3.1 Polynomial model

Figure 16 shows the results for the polynomial model.
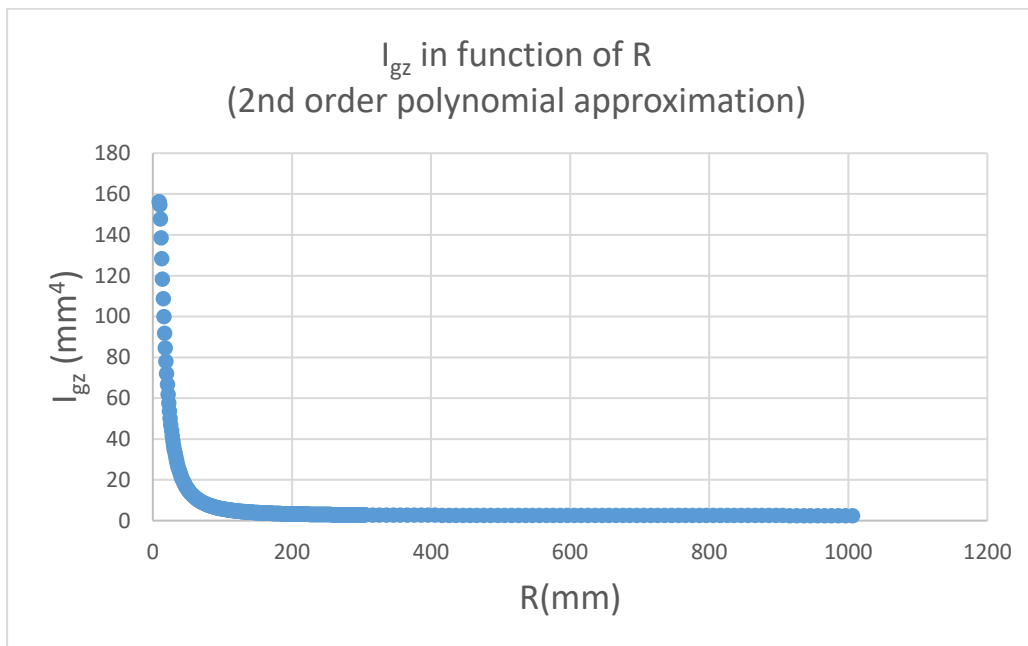
Figure 16: Resulting function polynomial model

This is not a desirable result for three key reasons:

1. The range is low in comparison to the other models.
2. The moment of inertia changes very quickly for a small change of the radius R. This yields a lot of uncertainty when utilising this model in calculating the deformation.
3. It is difficult to use this model in calculations and in the reverse process. To find an interpolation equation for these results, a complex least squares approximation needs to be calculated. This results in an equation in function of $1/R^2$, which is very hard to use.

For these reasons, the polynomial model will no longer be used in further calculations.

32

3.3.2 U-model

Figure 17 shows the results for the U-model.

I_{gz} in function of h (U-model)

$I(x) = 3,3454 \ast h^2 - 0,0402 \ast h + 1,4229$

$R^2 = 1$
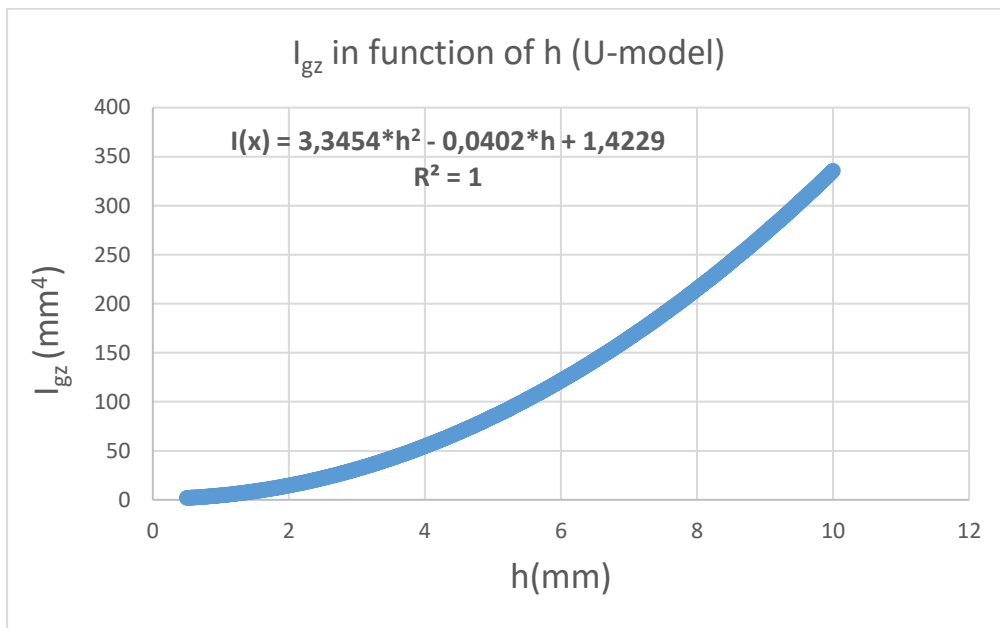
Figure 17: Results for the U-model.

The results for the U-model are desirable:

- The characteristic can be approximated easily by the interpolation equation. This equation of second order interpolation correlates highly with the results.
- The range is almost three times as high as for the polynomial model for the same utilised values. This means this model can be used to convey a larger change in rigidity than the polynomial model.
- Because of the simplified interpolation equation, this is easier to implement in the calculations.

3.3.3 U-model with a constant base

Figure 18 shows the results for the U-model with a constant base.
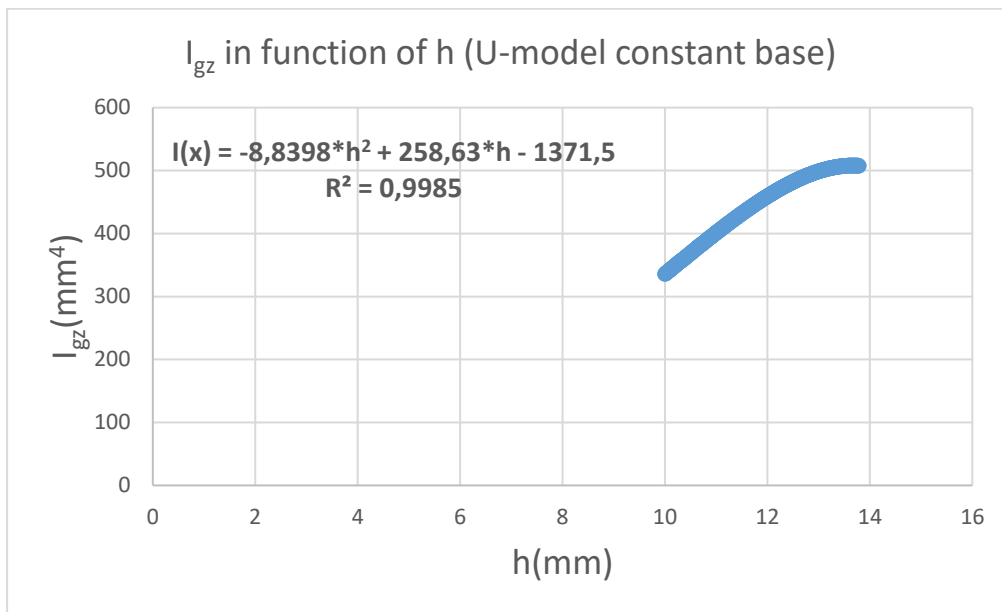
Figure 18: Results for the U-model with a constant base.

The results for this model are also desirable:

- The characteristic can be approximated easily by the interpolation equation. This equation of second order interpolation correlates highly with the results.
- The range is slightly lower than the polynomial model, but a higher rigidity can be achieved. The range can also supplement the range of the U-model (since it starts at ~ 350 mm^4).
- Because of the simplified interpolation equation, this is easier to implement in the calculations.

Conclusion:

The polynomial model is not desirable for the next step in the calculations. Therefore, only the U-model and U-model with a constant base will be used to calculate the deformations.

4. Calculating the deformation

4.1 Calculation of the deformation in function of position x

To calculate the deformation, the following formula from chapter two (formula 2.4) must be utilised:

$$E * I(x) * \frac{d^2 v(x)}{dx^2} = M(x) \tag{4.1}$$

Containing:

E: Young's Modulus of the selected material, more specifically the **Flexural Modulus**

I(x):   moment of inertia of the beam section in function of position x

v(x):   deformation of the beam for a position x

M(x):   flexural moment in the beam for a position x

q: the applied charge

To use formula 4.1 in calculations, the flexural moment M(x) and moment of inertia in function of x I(x) must be defined.

Calculating flexural moment M(x)

To calculate the flexural moment, the mechanical situation of the sheet must be clarified (Fig. 19).
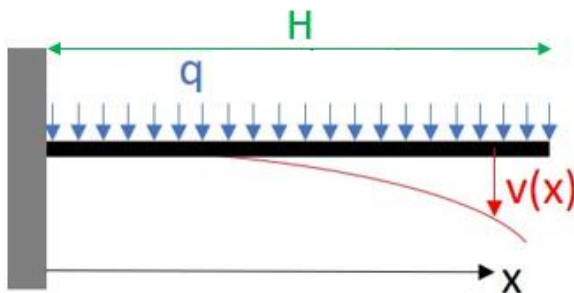
Figure 19: Mechanical situation for the sheet.

In figure 19 the mechanical situation is clarified as an imbedded beam. The following parameters are of importance:

H: sheet/beam length

q: charge on the sheet

Calculating the flexural moment of the imbedded beam results in the following equation:

$$M(x) = \frac{q}{2} * (H - x)^2 \tag{4.2}$$

As described in chapter two, the flexural moment should be a 2nd order polynomial in function of x because of the constant charge. Formula 4.2 satisfies that condition.

For the beam length, a reference value of 400 mm is chosen. The charge to be used as reference value is 300 N/m. This value is chosen to compensate a load of 12 kg on the sheet, as shown by the following calculation:

$$12 \ kg \sim 120 \ N = 0.400 \ m * 300 \ N/m \tag{4.3}$$

Calculating moment of inertia in function of the position x I(x)

For formula 4.1, the moment of inertia in function of the position in the x-axis is required. However, the previously calculated moment of inertia is calculated in function of the total range of the dependant parameter (height h). Therefor it should be converted into a function of x.

Because of the excellent fit of the 2nd order interpolation equation, the moment of inertia of each model can be described by the following equation:

$$I(h) = \bar{u} * h^2 + \bar{v} * h + \bar{w} \tag{4.4}$$

With $\bar{u}$, $\bar{v}$ and $\bar{w}$ the coefficients for the polynome in function of the height of the model. To utilise the moment of inertia in formula 4.1, it needs to be described in function of x. To resolve this and to control the variation of the rigidity in function of the position, the height can be varied in function of x. This leads to the following equation:

$$h(x) = A * x + B \tag{4.5}$$

Because the rigidity needs to be the highest at the base (x = 0), h(x) needs to decrease linearly. To achieve this, the parameters A and B can be defined as follows:

$$A = -\frac{\Delta h}{H} \tag{4.6}$$

$$B = h_{min} + \Delta h \tag{4.7}$$

Containing:

Δh: chosen difference in height ($= h_{final} - h_{min}$)
H: sheet/beam length
h_{min}:   minimal possible height for the model

The chosen difference in height Δh is added as a parameter to control the difference in rigidity. This is useful for recreating the desired deformation, since this is a parameter that can be easily changed in the calculations. The maximal possible difference in height is thus defined as $h_{max} - h_{min}$.

Since x varies between zero and H, the final height of the model h(H) will be:

$$h(H) = -\frac{\Delta h}{H} * H + h_{min} + \Delta h = h_{min} \tag{4.8}$$

This calculation is correct, since the rigidity should be lowest at the top of the sheet. Now, formulas 4.5, 4.6 and 4.7 can be unified in one single function for the height:

$$h(x) = -\frac{\Delta h}{H} * x + h_{min} + \Delta h \tag{4.9}$$

When combining formula 4.6 with formula 4.3, the moment of inertia in function of x is found. It should be noted that B could also be defined as h_{max}. However, this resulted in an unfavourable sheet design because of the high rigidity of the function. Therefore, a B of $h_{min} + \Delta h$ is preferred.

Calculating the deformation v(x) analytically

To calculate the deformation, formula 4.1 can be transformed into the following equation:

$$\frac{d^2v(x)}{dx^2} = \frac{M(x)}{E * I(x)} \tag{4.10}$$

Logically, the deformation could be calculated by double integrating formula 4.10:

$$v(x) = \int\int \frac{M(x)}{E * I(x)} * dx^2 + C_1 * x + C_2 \mid x \in [0, H] \tag{4.11}$$

The integration constant C_1 and C_2 can be calculated by calculating the first and second integral of formula 4.7 for x = 0 respectively. v(x = 0) = 0 and $\frac{dv(x=0)}{dx} = 0$ applies for an imbedded beam. In theory, this should result into the most accurate values for the deformation and yield consistent results.

However, the solution of formula 4.7 is very complex. The solution was calculated by using a TI-nspire CX calculator and by using MATLAB. Both yielded different results and were far too complex to implement in the calculations. The used MATLAB code and the results of these calculations can be found in Appendix E.

The calculations made with the calculator echoed the results from calculating fff(x) in Appendix E, but yielded not the same results. It can therefore be concluded that **it is too difficult to calculate the deformation analytically**. However, the deformation can be calculated discretely by utilising the differential equation 4.7.

Calculating the deformation v(x) discretely

To calculate the deformation discretely, the differential equation should be converted to a formula to be used in calculating each individual value of the deformation, devoid of differentials and integrals. Therefor the definition of the derivative is needed. The derivative of v(x) is defined as:

$$\frac{dv(x)}{dx} = \frac{v(x + \Delta x) - v(x)}{\Delta x} \; for \; \Delta x \approx 0 \tag{4.12}$$

This reasoning can also be applied for the second derivative of v(x):

$$\frac{d^2v(x)}{dx^2} = \frac{1}{\Delta x} * \left(\frac{dv(x + \Delta x)}{dx} - \frac{dv(x)}{dx} \right) for \; \Delta x \approx 0 \tag{4.13}$$

Combining formulas 4.12 and 4.13 results in the following equation:

$$\frac{d^2v(x)}{dx^2} = \frac{1}{\Delta x^2} * \left(v(x + 2\Delta x) - 2 * v(x + \Delta x) + v(x) \right) \tag{4.14}$$

Combining formula 4.10 and 4.14, yields the following result:

$$\frac{M(x)}{E * I(x)} = \frac{1}{\Delta x^2} * \left(v(x + 2\Delta x) - 2 * v(x + \Delta x) + v(x) \right) \tag{4.15}$$

Formula 4.15 is completely devoid of derivatives. This formula can be transformed to find the equation to calculate v(x + 2Δx):

$$v(x + 2 * \Delta x) = \frac{M(x)}{E * I(x)} * \Delta x^2 + 2 * v(x + \Delta x) - v(x) \tag{4.16}$$

Define the deformation at a given point v_i as followed:

$$v_i = v(x_i) = v(i * \Delta x) \; for \; i \; \epsilon \; n \; with \; n * \Delta x = H \tag{4.17}$$

An imbedded beam has two constraints for the deformation:

1. The deformation in x = 0 is 0, or v(x=0) = 0 (= v_0).
2. The change in deformation in x = 0 is 0, or $\frac{dv(x=0)}{dx} = 0$.

Because the deformation does not change because of the second constraint, the deformation at a position of x = Δx should also be zero. Therefore, the values for v_0 and v_1 are calculated as:

$$v_0 = v(0 * \Delta x) = 0 \tag{4.19}$$

$$v_1 = v(1 * \Delta x) = 0 \tag{4.20}$$

With equation 4.19 and 4.20, v_2 can be calculated with formula 4.16. This process can be repeated until every value of i ϵ [0,n] is calculated. For every value of i ϵ [0,n], the following applies:

$$v_i = \frac{M(x_{i-2})}{E * I(x_{i-2})} * \Delta x^2 + 2 * v_{i-1} - v_{i-2} \; for \; n * \Delta x = H \tag{4.21}$$

Formula 4.21 is used to calculate every value of the deformation for i > 1. An Excel sheet is made to apply this formula for every x value. Because Δx should be as close to zero as possible, a value for n of 1000 is chosen for the following calculations. For the study of the parameter variance, a n of 500 is used to limit the required computing power. An example of the first five values of the sheet is shown in the following table (Tab. 2):

Table 2: Example of the Excel sheet for the U-model with a constant base, to show the application of formula 4.21

i	x	M(x)	I(x)	v(x)
[0,n]	=i*Δx	=M(x,q,H)	=I(x,u,v,w,A,B)	=M(i-2)/(E*I(i-2))*dx²+2v(i-1)-v(i-2)
0	0	-24000	298,0244315	0
1	0,4	-23952,024	297,9870124	0
2	0,8	-23904,096	297,9494566	-0,000171798
3	1,2	-23856,216	297,911764	-0,000515072
4	1,6	-23808,384	297,8739346	-0,001029501
5	2	-23760,6	297,8359684	-0,001714763

In the final column, v(x) is calculated as defined by formula 4.21. It should be noted that M(x, q, H) and I(x, u, v, w, A, B) are macros written in VBA to mimic the formulas 4.2 and 4.4 (with 4.9 applied) respectively.

Calculating the deformation v(x) for the U-model

The following reference values are used to calculate the deformation of the U-model (Tab. 3):

Table 3: Values for the used parameters to calculate v(x) for the U-model

E(GPa)	75,00
q(N/m)	300,00
H(mm)	400,00
L(mm)	25,00
t(mm)	1,00
Δh(mm)	7,83
--> Δh$_{max}$	7,83
u	2,7923
v	-0,0404
w	1,1849
n	1000

Δh$_{max}$ is the maximal possible value for the deformation. This value is equal to h$_{max}$ − h$_{min}$ as calculated in Appendix C. Note that the parameters u, v and w are the coefficients used in formula 4.4. Thus, to calculate the deformation with these parameters, it is first necessary to calculate the interpolation equation for the moment of inertia in function of the height. In this case, the moment of inertia can be defined as:

$$I(h) = 2.7923 * h^2 − 0.0404 * h + 1.1849 \qquad (4.22)$$

Using the values for the parameters in table 3, the deformation characteristic in function of x can be calculated. The result is shown in figure 20.
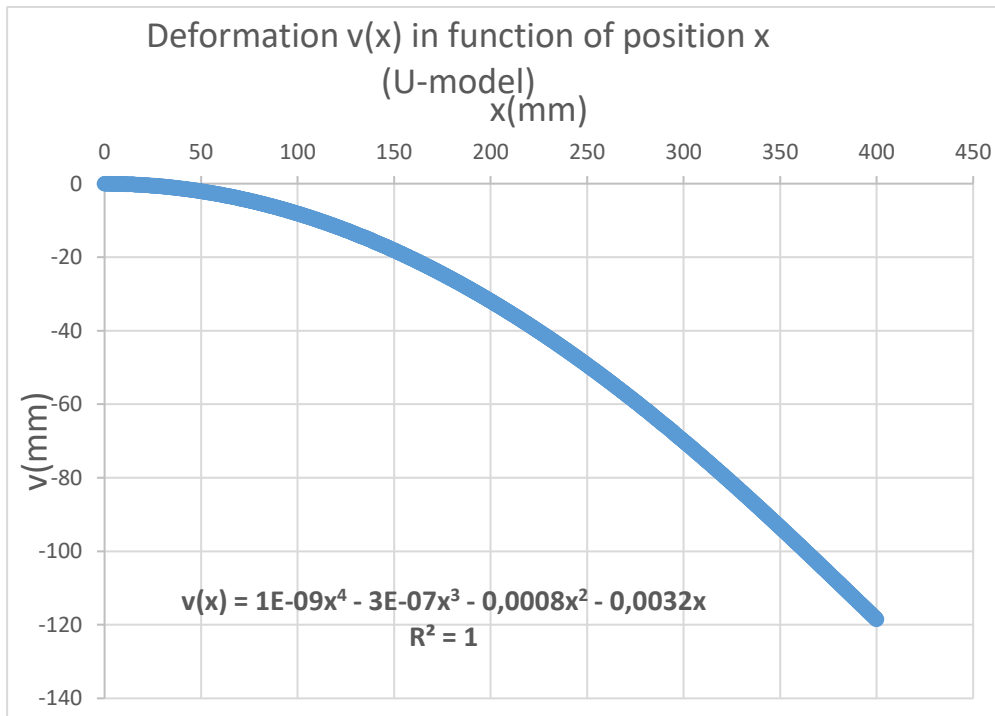
Figure 20: Deformation characteristic for the U-model

The deformation characteristic looks realistic:

- The deformation for x = 0 is zero, since the function starts at the origin.
- The tangent to the curve in x = 0 looks like it has an angle of 0° with the x-axis. This means the derivative of the deformation for x = 0 is zero, satisfying both constraints of an imbedded beam.
- The tangent of the curve seems to have a constant value with the x-axis when approaching x = 400 = H. This is correct, since the flexural moment at this point is zero, which means that the second derivative of the deformation is zero.

Calculating the deformation v(x) for the U-model with a constant base

The following values are used to calculate the deformation of the U-model with a constant base (Tab. 4):

Table 4: Values for the used parameters to calculate v(x) for the U-model with a constant base

E(GPa)	75,00
q(N/m)	300,00
H(mm)	400,00
L(mm)	25,00
W(mm)	8,33
t(mm)	1,00
Δh(mm)	3,09
-->Δhmax	3,09
u	-7,1622
v	175,72
w	-774,67
n	1000

Δh_{max} is the maximal possible value for the deformation. This value is equal to $h_{max} - h_{min}$ as calculated in Appendix D. Note that the parameters u, v and w are the coefficients used in formula 4.3. Thus, to calculate the deformation with these parameters, it is first necessary to calculate the interpolation equation for the moment of inertia in function of the height. In this case, the moment of inertia can be defined as:

$$I(h) = -7.1622 * h^2 + 175.72 * h - 774.67 \qquad (4.23)$$

Using the values for the parameters in table 4, the deformation characteristic in function of x can be calculated. The result is shown in figure 21.
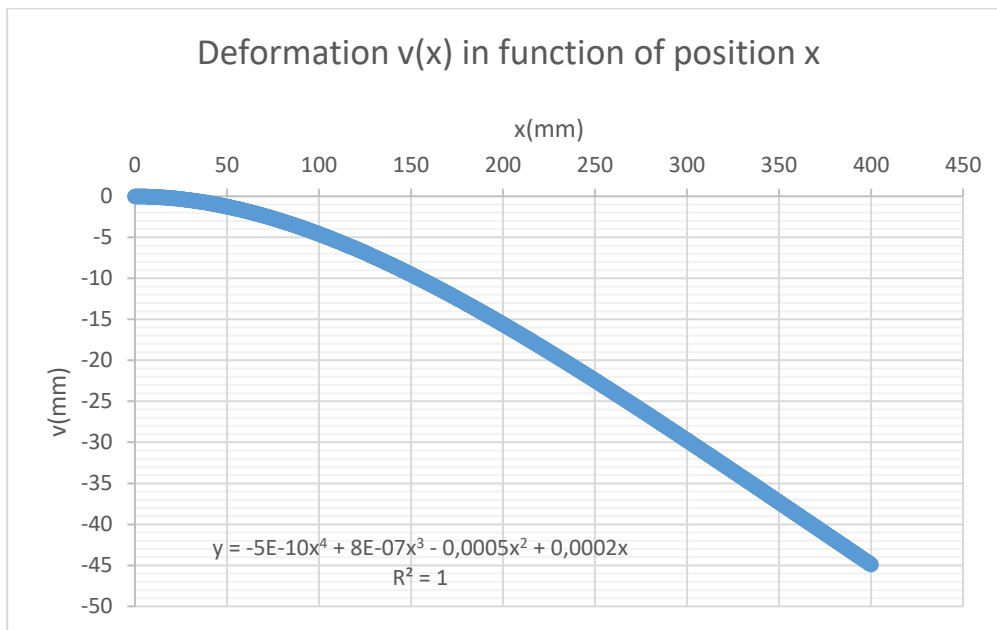
Figure 21: Deformation characteristic for the U-model with constant base

The deformation characteristic looks realistic:

- The deformation for x = 0 is zero, since the function starts at the origin.
- The tangent to the curve in x = 0 looks like it has an angle of 0° with the x-axis. This means the derivative of the deformation for x = 0 is zero, satisfying both constraints of an imbedded beam.
- The tangent of the curve seems to have a constant value with the x-axis when approaching x = 400 = H. This is correct, since the flexural moment at this point is zero, which means that the second derivative of the deformation is zero.

It should be noted that the deformation for the U-model with a constant base is less when compared to the U-model. This is the result of the higher overall rigidity of the U-model with a constant base.

4.2 Parameter variance impact on the deformation

Since the deformation characteristics are successfully calculated for each model, it is now possible to check the impact of varying each individual parameter on the deformation characteristic. By knowing the relation between the varied parameter and the deformation, the design of the sheet can be numerically calculated when necessary.

4.2.1 Parameter beam length H

Results for the U-model

The following parameters (Tab. 5) stay constant when varying the beam length H.

Table 5: Constant parameters varying H for U-model

E(MPa)	75000
q(N/mm)	0,300
L(mm)	25,00
t(mm)	1,00
Δh(mm)	7,83
-->Δhmax	7,83333
u	2,7923
v	-0,0404
w	1,1849
B	8,3333
n	500

To vary the beam length H, the following values for the changing parameters are found (Tab. 6).

Table 6: Changing parameters varying H for U-model

H1 =	100,00
A1 (Aa)	-0,0783
Δx1 (dxa)	0,200
H2 =	200,00
A2 (Ab)	-0,0392
Δx2 (dxb)	0,400
H3 =	400,00
A3 (Ac)	-0,0196
Δx3 (dxc)	0,800
H4 =	600,00
A4 (Ad)	-0,0131
Δx4 (dxd)	1,200

By applying these values, the resulting variation can be visualised by on the following figure (Fig. 22).

Figure 22: Effect variation of H for the U-model

Results for the U-model with constant base

The following parameters (Tab. 7) stay constant when varying the beam length H.

Table 7: Constant parameters varying H for U-model with constant base

E(MPa)	75000
q(N/mm)	0,300
L(mm)	25,00
L(mm)	8,33
t(mm)	1,00
Δh(mm)	3,09000
-->Δhmax	3,09276
u	-7,1622
v	175,72
w	-774,67
B	11,4233
n	500

To vary the beam length H, the following values for the changing parameters are found (Tab. 8).

Table 8: Changing parameters varying H for U-model with constant base

H1 =	100,00
A1 (Aa)	-0,0309
Δx1 (dxa)	0,200
H2 =	200,00
A2 (Ab)	-0,0155
Δx2 (dxb)	0,400
H3 =	400,00
A3 (Ac)	-0,0077
Δx3 (dxc)	0,800
H4 =	600,00
A4 (Ad)	-0,0052
Δx4 (dxd)	1,200

By applying these values, the resulting variation can be visualised by on the following figure (Fig. 23).
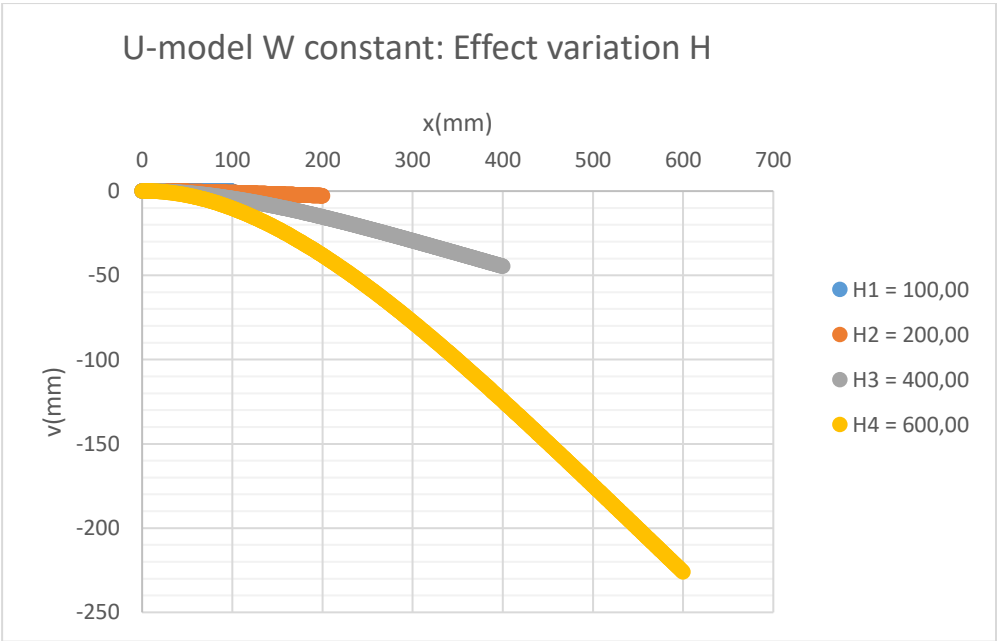
Figure 23: Effect variation of H for the U-model with constant base

Discussion results

For both models, the deformation increases when the beam length increases. This is due to the distributed charge: if the beam length is greater, there is a bigger load on the sheet. Mathematically, this makes sense, but in reality, the charge would be distributed over a bigger surface, decreasing this effect. Therefore, it is preferred to not vary the beam length to affect the deformation, but rather adjust other parameters since the effect of their variations are better modelled in the calculations.

Another factor is the distance between the centre of gravity and the embedding. When this distance increases, the flexural moment on the sheet increases. This is a logical result.

4.2.2 Parameter height difference Δh

Results for the U-model

The following parameters (Tab. 9) stay constant when varying the height difference Δh.

Table 9: Constant parameters varying Δh for U-model

E(MPa)	75000
q(N/mm)	0,300
H(mm)	400,00
L(mm)	25,00
t(mm)	1,00
u	2,7923
v	-0,0404
w	1,1849
n	500
Δx(mm)	0,800

To vary the height difference Δh, the following values for the changing parameters are found (Tab. 10).

Table 10: Changing parameters varying Δh for U-model

Δha =	0,00000
Aa	0,0000
Ba	0,500
Δhb =	2,00000
Ab	-0,0050
Bb	2,5000
Δhc =	4,00000
Ac	-0,0100
Bc	4,500
Δhd =	7,83333
Ad	-0,0196
Bd	8,333

By applying these values, the resulting variation can be visualised by on the following figure (Fig. 24).

Figure 24: Effect variation of Δh for the U-model

Results for the U-model with constant base

The following parameters (Tab. 11) stay constant when varying the height difference Δh.

Table 11: Constant parameters varying Δh for U-model with constant base

E(MPa)	75000
q(N/mm)	0,300
H(mm)	400,00
L(mm)	25,00
W(mm)	8,33
t(mm)	1,00
u	-7,1622
v	175,72
w	-774,67
n	500
Δx(mm)	0,800

To vary the height difference Δh, the following values for the changing parameters are found (Tab. 12).

Table 12: Changing parameters varying Δh for U-model with constant base

Δha =	0,00000
Aa	0,0000
Ba	8,3350
Δhb =	0,50000
Ab	-0,0013
Bb	8,8350
Δhc =	1,00000
Ac	-0,0025
Bc	9,3350
Δhd =	3,09276
Ad	-0,0077
Bd	11,4278

By applying these values, the resulting variation can be visualised by on the following figure (Fig. 25).
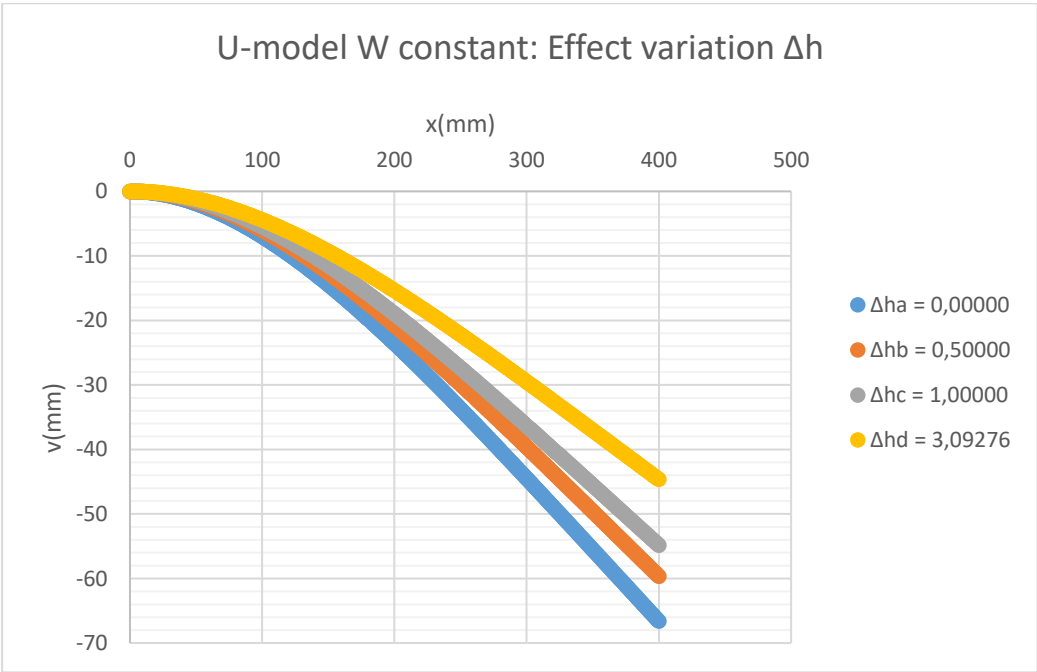
Figure 25: Effect variation of Δh for the U-model with constant base

Discussion results

The height difference seems to have a far greater impact on the U-model. This is due to the great variation in rigidity, because for a height difference of zero the rigidity stays the minimal value. The height difference varies greater for the U-model because the minimal value for the U-model far lower is than for the U-model with constant base. This could be used as a variable design parameter to recreate the deformation, since it is easy to vary this parameter.

4.2.3 Parameter thickness t

Results for the U-model

The following parameters (Tab. 13) stay constant when varying the thickness t.

Table 13: Constant parameters varying t for U-model

E(MPa)	75000
q(N/mm)	0,300
H(mm)	400,00
L(mm)	25,00
Δh(mm)	7,33000
A	-0,0183
n	500
Δx(mm)	0,800

To vary the thickness t, the following values for the changing parameters are found (Tab. 14).

Table 14: Changing parameters varying t for U-model

ta =	0,25
-->Δhmax	8,20833
u	0,6947
v	-0,0006
w	0,0186
Ba	7,455
tb =	0,50
-->Δhmax	8,08333
u	1,3466
v	0,3022
w	-0,2131
Bb	7,58
tc =	1,00
-->Δhmax	7,83333
u	2,7923
v	-0,0404
w	1,1849
Bc	7,83
td =	2,00
-->Δhmax	7,33333
u	5,4527
v	1,3957
w	6,7504
Bd	8,33

By applying these values, the resulting variation can be visualised by on the following figure (Fig. 26).
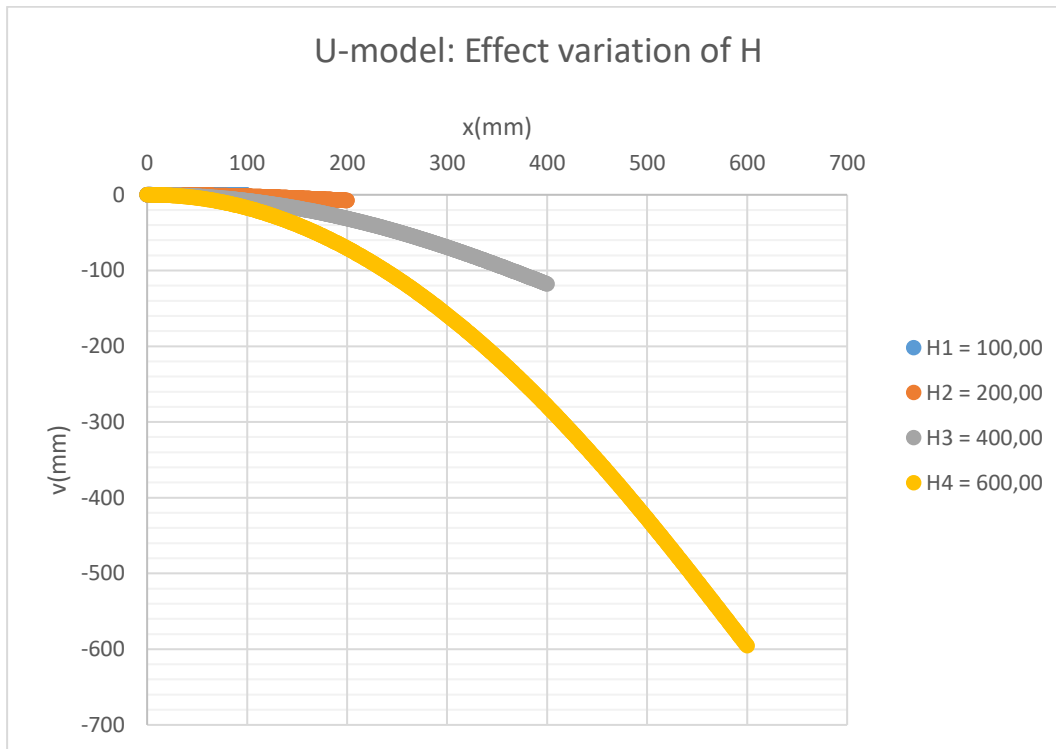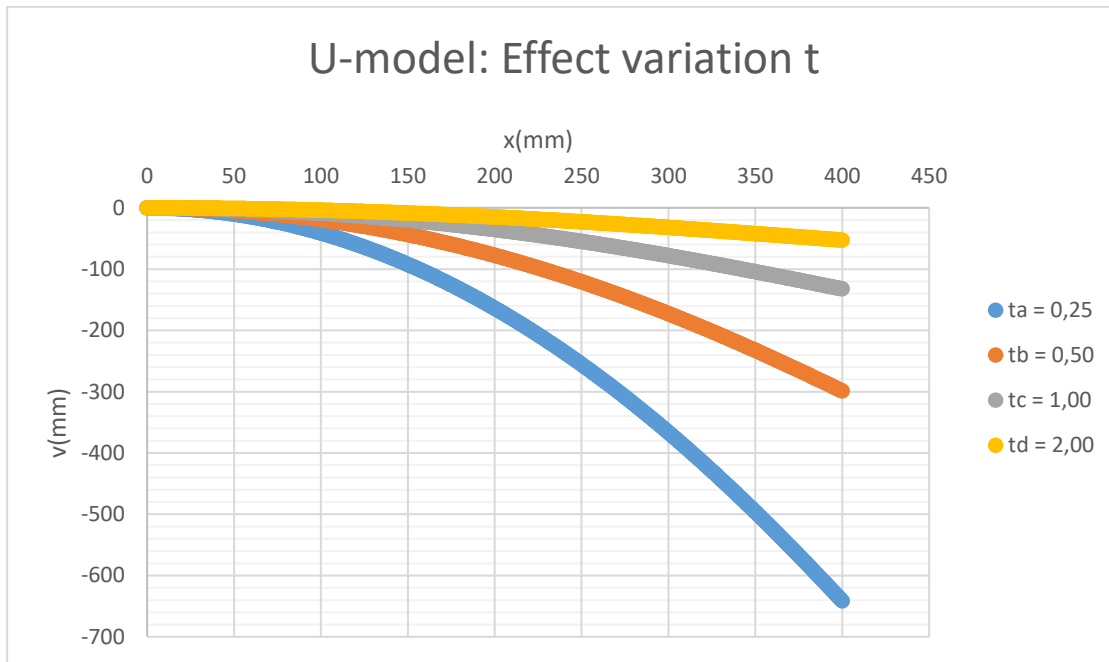

Figure 26: Effect variation of t for the U-model

Results for the U-model with constant base

The following parameters (Tab. 15) stay constant when varying the thickness t.

Table 15: Constant parameters varying t for U-model with constant base

E(MPa)	75000
q(N/mm)	0,300
H(mm)	400,00
L(mm)	25,00
W(mm)	8,33
Δh(mm)	2,72208
A	-0,0068
n	500
Δx(mm)	0,800

To vary the thickness t, the following values for the changing parameters are found (Tab. 16).

Table 16: Changing parameters varying t for U-model with constant base

ta =	0,25
-->Δhmax	3,36306
ua	-2,022
va	48,364
wa	-215,28
Ba	11,0554
tb =	0,50

-->Δhmax	3,27366
ub	-3,8888
vb	93,738
wb	-416,05
Bb	11,0554
tc =	1,00
-->Δhmax	3,09276
uc	-7,1622
vc	175,72
wc	-774,67
Bc	11,0554
td =	2,00
-->Δhmax	2,72208
ud	-11,911
vd	306,1
wd	-1324,8
Bd	11,0554

By applying these values, the resulting variation can be visualised by on the following figure (Fig. 27).
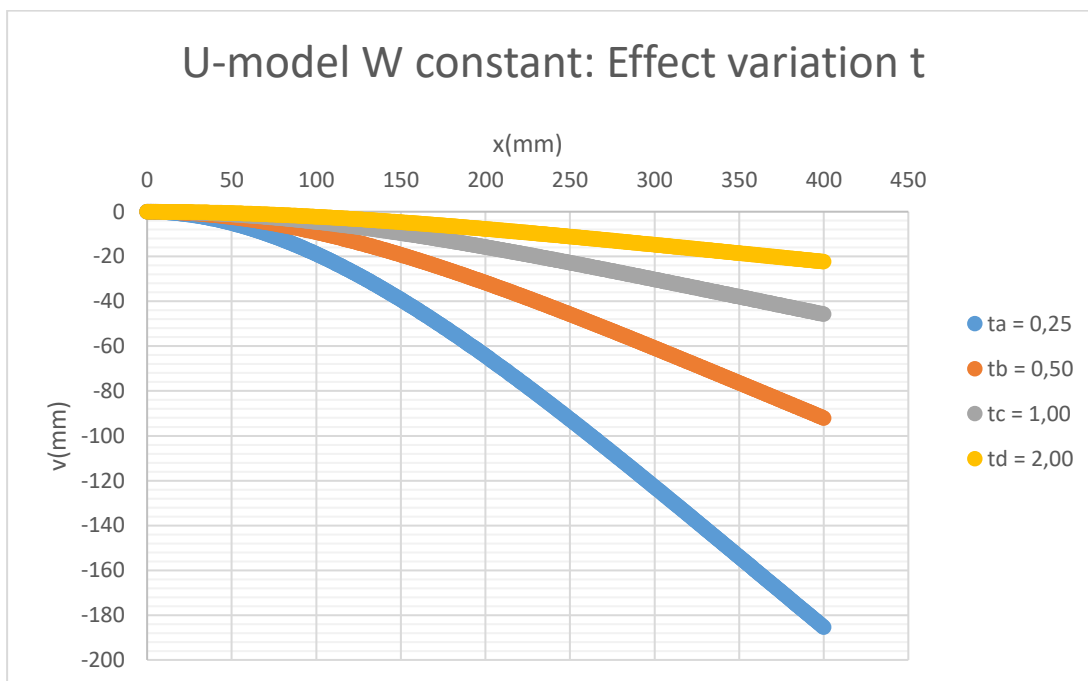
Figure 27: Effect variation of t for the U-model with constant base

Discussion results

For both models, there seems to be an inverse relationship between the deformation and the thickness. When the thickness halves, the deformation seems to double. This is one of the most defining relationships between the sheet design and the deformation and should be taken into consideration when preforming the physical tests.

4.2.4 Parameter length L

Results for the U-model

The following parameters (Tab. 17) stay constant when varying the secton length L.

Table 17: Constant parameters varying L for U-model

E(MPa)	75000
q(N/mm)	0,300
H(mm)	400,00
t(mm)	1,00
Δh(mm)	**2,83300**
A	-0,0071
n	500
Δx(mm)	0,800

To vary the secton length L, the following values for the changing parameters are found (Tab. 18).

Table 18: Changing parameters varying L for U-model

La =	10,00
-->Δhmax	2,83333
ua	1,1497
va	-0,0487
wa	0,4751
Ba	3,3330
Lb =	**20,00**
-->Δhmax	6,16667
ub	2,1617
vb	0,4259
wb	0,4349
Bb	3,3330
Lc =	25,00
-->Δhmax	7,83333
uc	2,7923
vc	-0,0404
wc	1,1849
Bc	3,3330
Ld =	40,00
-->Δhmax	12,83333
ud	4,4535
vd	-0,0401
wd	1,8996
Bd	3,3330

By applying these values, the resulting variation can be visualised by on the following figure (Fig. 28).
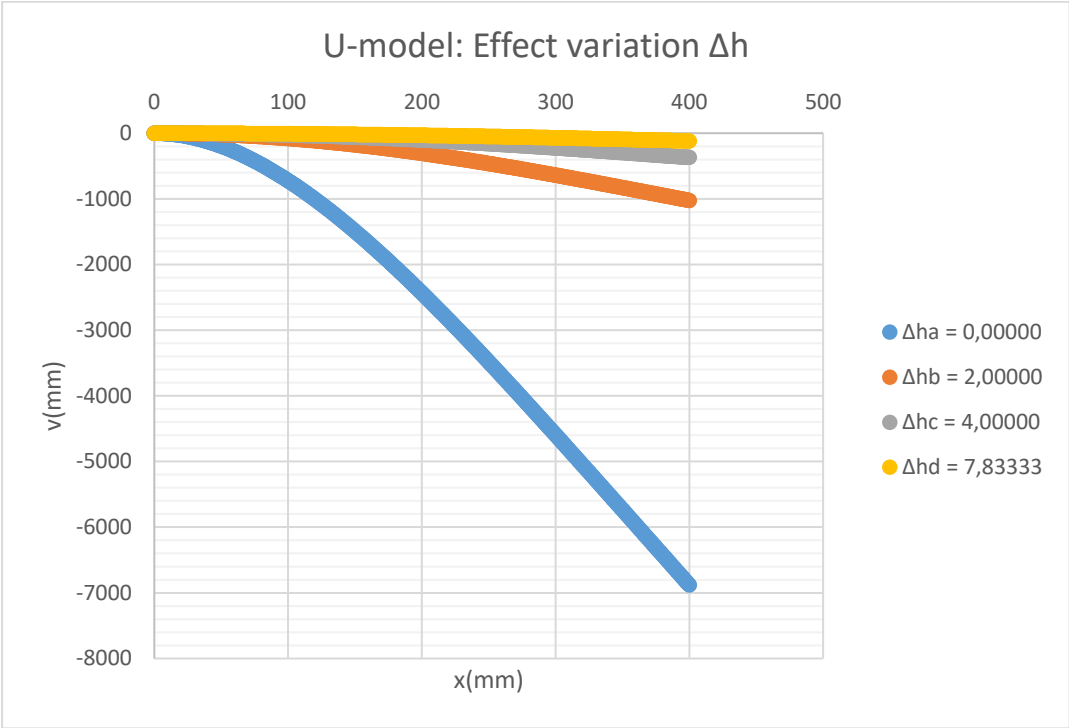

Figure 28: Effect variation of L for the U-model

Results for the U-model with constant base

The following parameters (Tab. 19) stay constant when varying the secton length L.

Table 19: Constant parameters varying L for U-model with constant base

E(MPa)	75000
q(N/mm)	0,300
H(mm)	400,00
W(mm) =	8,33
t(mm)	1,00
Δh(mm)	1,77609
A	-0,0044
n	500
Δx(mm)	0,800

To vary the secton length L, the following values for the changing parameters are found (Tab. 20).

Table 20: Changing parameters varying L for U-model with constant base

La =	10,00
-->Δhmax	1,77541
ua	0,9134
va	0,814
wa	-0,5262
Ba	2,6087

Lb =	20,00
-->Δhmax	2,93054
ub	-4,3099
vb	86,985
wb	-286,97
Bb	8,7639
Lc =	25,00
-->Δhmax	3,09276
uc	-7,1622
vc	175,72
wc	-774,67
Bc	11,4261
Ld =	40,00
-->Δhmax	3,31884
ud	-15,844
vd	618,95
wd	-4752,7
Bd	19,1522

By applying these values, the resulting variation can be visualised by on the following figure (Fig. 29).
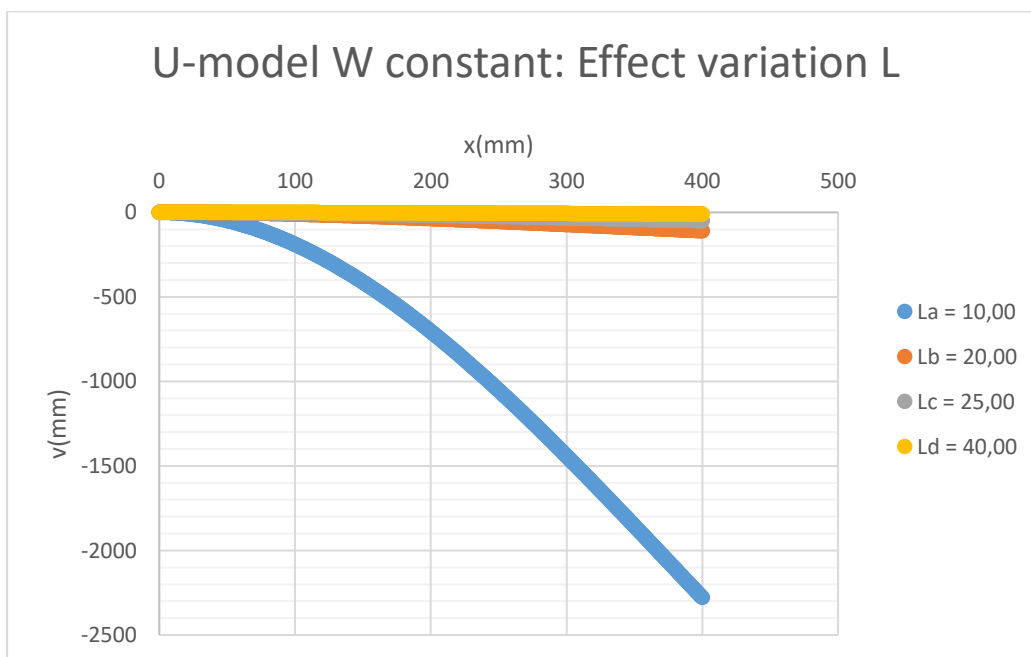
Figure 29: Effect variation of L for the U-model with constant base

Discussion results

The results for the deformation are radically different for the two models. The U-model seems to indicate an inverse relationship between the deformation and the section length. When the section length doubles, the deformation halves.

For the U-model with a constant base, the result seems more unrefined. This is due to the influence of the base W: since W stays constant and the section length changes, the minimal height changes drastically. The lower the section length, the lower the difference between W and L, the higher the deformation.

4.2.5 Parameter width W

Results for the U-model with constant base

The following parameters (Tab. 21) stay constant when varying the base W.

Table 21: Constant parameters varying W for U-model with constant base

E(MPa)	75000
q(N/mm)	0,300
H(mm)	400,00
L(mm) =	25,00
t(mm)	1,00
Δh(mm)	**1,83216**
A	-0,0046
n	500
Δx(mm)	0,800

To vary the base W, the following values for the changing parameters are found (Tab. 22).

Table 22: Changing parameters varying W for U-model with constant base

Wa =	5,00
-->Δhmax	1,83216
ua	-9,5387
va	234,67
wa	-1124,3
Ba	11,8322
Wb =	8,33
-->Δhmax	3,09276
ub	-7,1622
vb	175,72
wb	-774,67
Bb	11,4261
Wc =	10,00
-->Δhmax	3,62430
uc	-5,9681
vc	147,65
wc	-619,29
Bc	11,1243
Wd =	20,00
-->Δhmax	4,83144
ud	0,8227
vd	19,477

wd	-50,475
Bd	7,3314

By applying these values, the resulting variation can be visualised by on the following figure (Fig. 30).
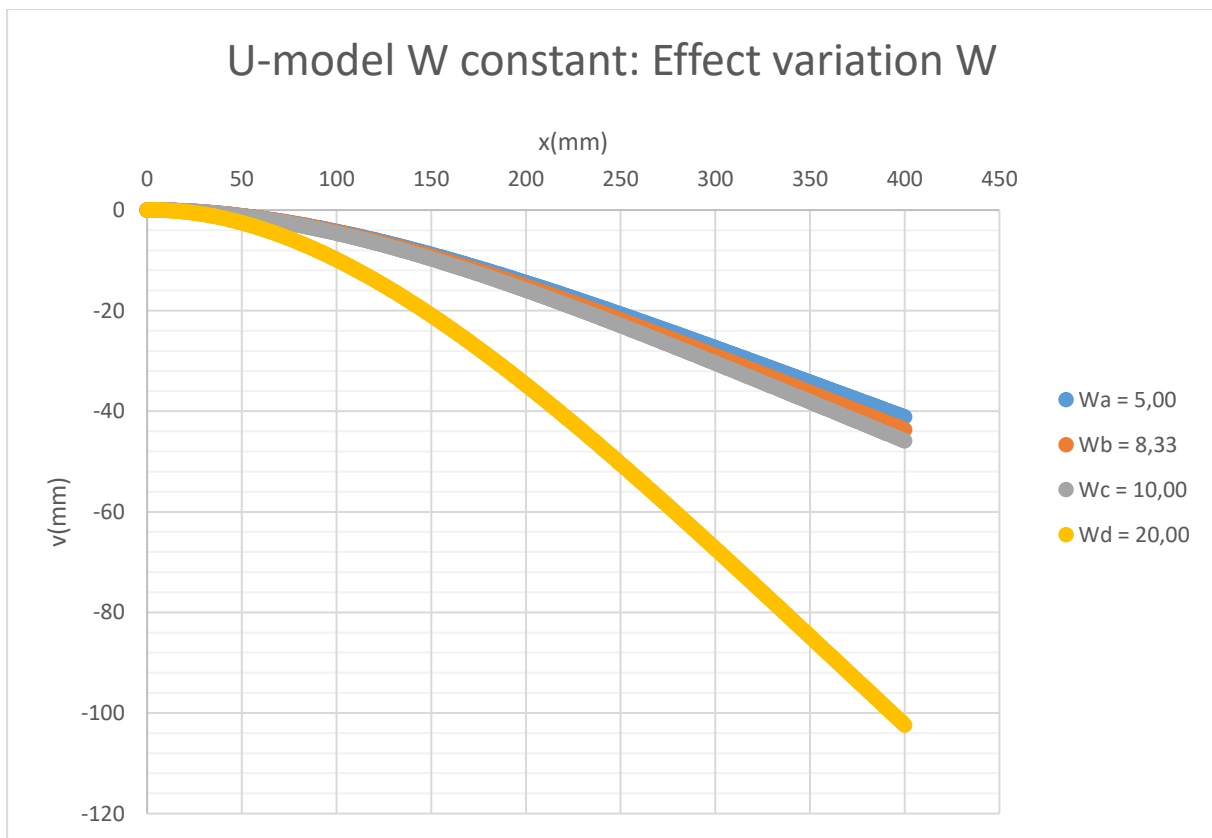
Figure 30: Effect variation of W for the U-model with constant base

Discussion result

The results are similar to the variation of the section length L. The same reasoning applies here as well: the higher the base W, the lower the difference between W and L, the higher the deformation. These last two results prove that to increase the deformation means to increase the difference between L and W for this model.

4.2.6 Parameter charge q

Results for the U-model

The following parameters (Tab. 23) stay constant when varying the charge q.

Table 23: Constant parameters varying q for U-model

E(MPa)	75000
H(mm)	400,00
L(mm)	25,00
t(mm)	1,00
Δh(mm)	7,83000
-->Δhmax	7,83333
u	2,7923
v	-0,0404
w	1,1849
A	-0,0196
B	8,3333
n	500
Δx(mm)	0,800

To vary the charge q, the following values for the changing parameters are found (Tab. 24).

Table 24: Changing parameters varying q for U-model

qa =	0,050
qb =	0,150
qc =	0,300
qd =	0,600

By applying these values, the resulting variation can be visualised by on the following figure (Fig. 31).
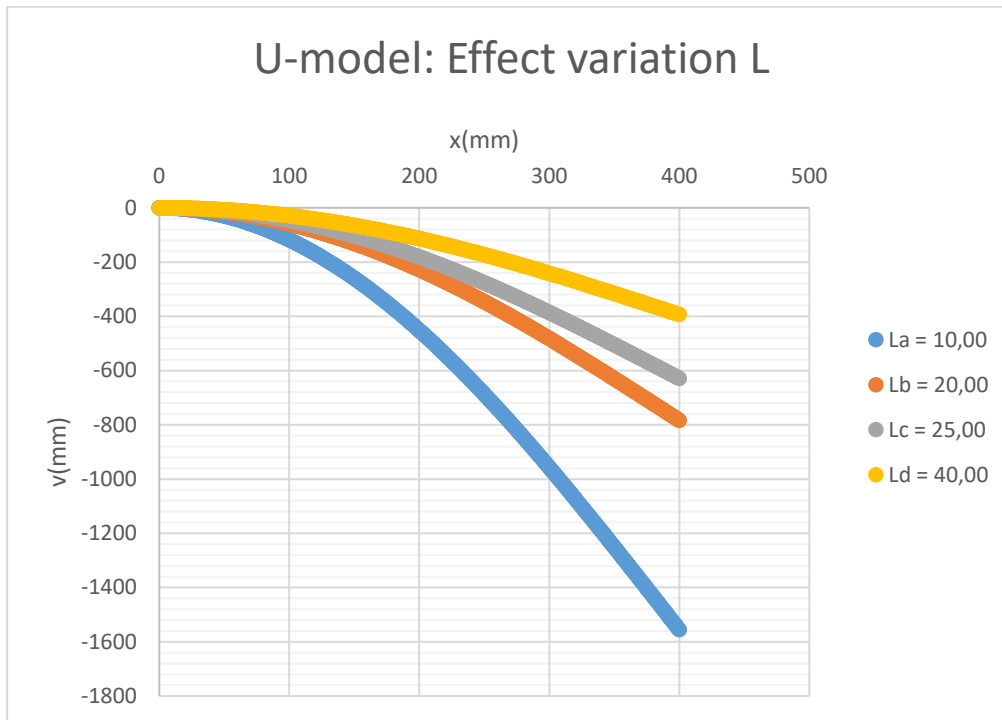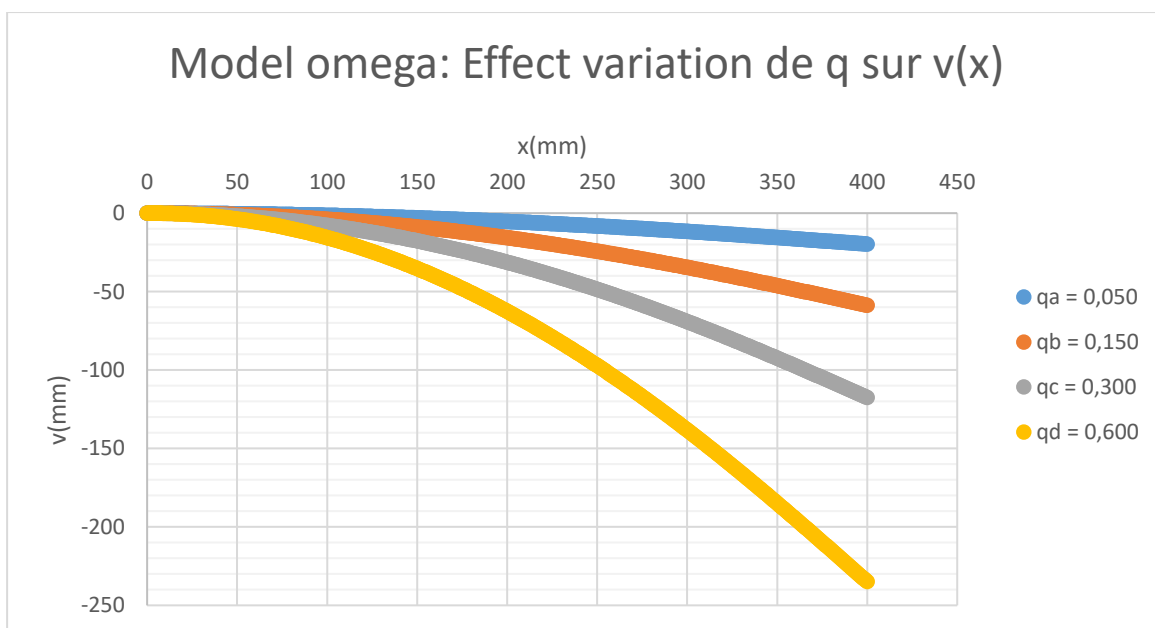

Figure 31: Effect variation of q for the U-model

Results for the U-model with constant base

The following parameters (Tab. 25) stay constant when varying the charge q.

Table 25: Constant parameters varying q for U-model with constant base

E(MPa)	75000
H(mm)	400,00
L(mm)	25,00
W(mm)	8,33
t(mm)	1,00
Δh(mm)	3,09000
-->Δhmax	3,09276
u	-7,1622
v	175,72
w	-774,67
A	-0,0077
B	11,4233
n	500
Δx(mm)	0,800

To vary the charge q, the following values for the changing parameters are found (Tab. 26).

Table 26: Changing parameters varying q for U-model with constant base

qa =	0,050
qb =	0,150
qc =	0,300
qd =	0,600

By applying these values, the resulting variation can be visualised by on the following figure (Fig. 32).
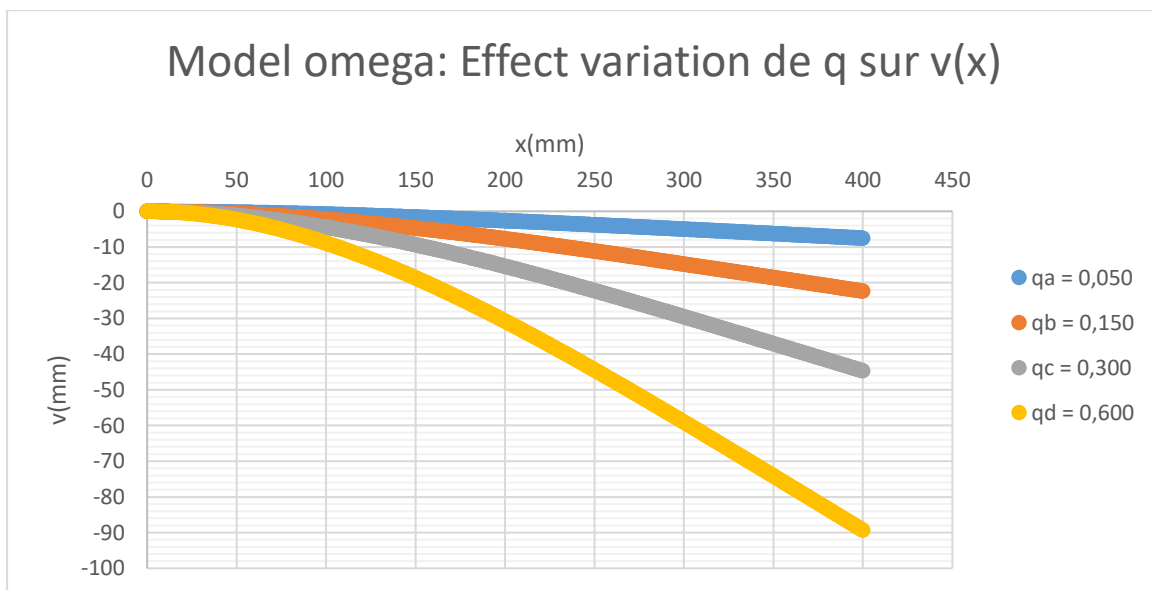
Figure 32: Effect variation of q for the U-model with constant base

Discussion result

The results indicate that there is a linear relationship between the deformation and the charge. If the charge doubles, the deformation doubles. This is correct, since the charge q is a constant factor of the flexural moment M(x) and does not change for a given position. This is only true for a constant charge.

5. Designing the sheet

Since the relationship between the section design and the deformation is found and the effect of each design parameter on the deformation is clear, the sheet can now be calculated based on the desired deformation. The reverse process consists of:

1. Calculating the desired deformation
2. Calculating the sheet parameters based on the moment of inertia equations
3. Designing the prototype and mould in parameters and CAD models

5.1 Calculating the desired deformation

The desired deformation of the elastic bands must be calculated for a single point of the backrest. To keep it simple, the middle of the backrest is used since this part will have the maximum deformation. The sheet will thus try to reproduce the maximum deformation of the elastic bands. The point of reference is shown in the following figure.

Figure 33: Point of reference on the backrest

Since the athlete was filmed during a training session, the maximum deformation can be determined for each stroke. The deformation needs to be calculated based on a reference length at approximately the same distance from the camera. When the actual length of the reference is known, the deformation and the reference are measured on the images. Utilising the reference length, the deformation can be calculated based on a scale factor.

In the following images, the actual height of a side panel is 153 mm. This reference is marked on the images as a yellow rectangle. Another reference is used once to calculate the deformation and control

the other references. This reference is a yellow vertical line and follows a tube of the frame. Each following figure shows the deformation for a different stroke (Fig. 34 – Fig. 38).

Figure 34: Deformation of the first stroke

Figure 35: Deformation of the second stroke with side panel reference (centre) and tube reference (right)

Figure 36: Deformation of the third stroke

Figure 37: Deformation of the fourth stroke

Figure 38: Deformation of the fifth stroke

The deformation is calculated based on the following table (Tab. 27).

Table 27: Calculating the desired deformation

Stroke	Measured reference (cm measured)	Scale factor (mm/cm measured)	Measured deformation (cm measured)	Actual deformation (mm)
()	(measured)	= reference length/measured reference	(measured)	= scale factor * measured deformation
1	2.33	65.7	1.59	104
2	2.17 (side panel) 5.85	66.8 (side panel) 70.5 (tube)	1.25	88.1 (tube)
3	2.24	68.3	1.37	93.6
4	2.63	58.2	2.01	117
5	2.56	59.8	1.72	103

Based from the data in the final column of table 27, the actual deformation can be averaged to find an **estimation for the desired deformation of 101 mm**. However, the (sample) **standard deviation of these results is 11.1 mm** (whilst the population standard deviation is 9.90). This means the **measured deformation should be within the interval of 84.4 and 117.6 mm** (since an uncertainty of three times the standard deviation should include 99.7% of the results, assuming a normal distribution of the results).

5.2 Calculating the design

5.2.1 Calculating section parameters

To calculate the section parameters, the sheet/beam length and the thickness must be determined.

Measuring the thickness t

A reference for the thickness is necessary for the calculations. The thickness of another carbon fibre object (a carbon fibre handle) in the research centre is measured to use as a reference. This is a good estimation since the carbon fibre sheet will likely be made from the same material. The following values were measured for the handle (Tab. 28).

Table 28: Measurements of the carbon fibre handle as reference

Measurement	Measured value (mm)
1	0.44
2	0.36
3	0.32
4	0.44
5	0.33

The average thickness of the measurements is **0.38 mm**. The sample standard deviation is 0.06, thus the realistic thickness has a 99.7% certainty of being within the range of 0.29 and 0.47 mm. Because the thickness is an estimate and will be checked by the physical tests, a value of 0.38 mm will suffice as a reference for the thickness.

Calculating the sheet/beam length H

The current backrest has the following measurements, as shown on figure 39.
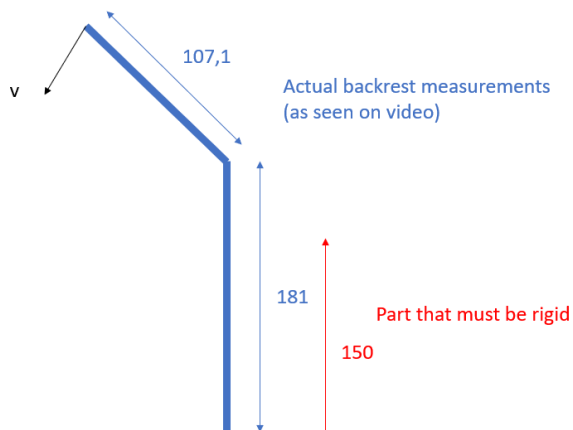
Figure 39: Current measurements backrest in profile

The curved shape of the current backrest makes the calculation of the effective sheet length more complex, but the deformation can be estimated to be equal to the deformation of a straight sheet. Therefore, the shape of the current backrest is transformed to a straight sheet. This principle is shown on the following figure (Fig. 40).
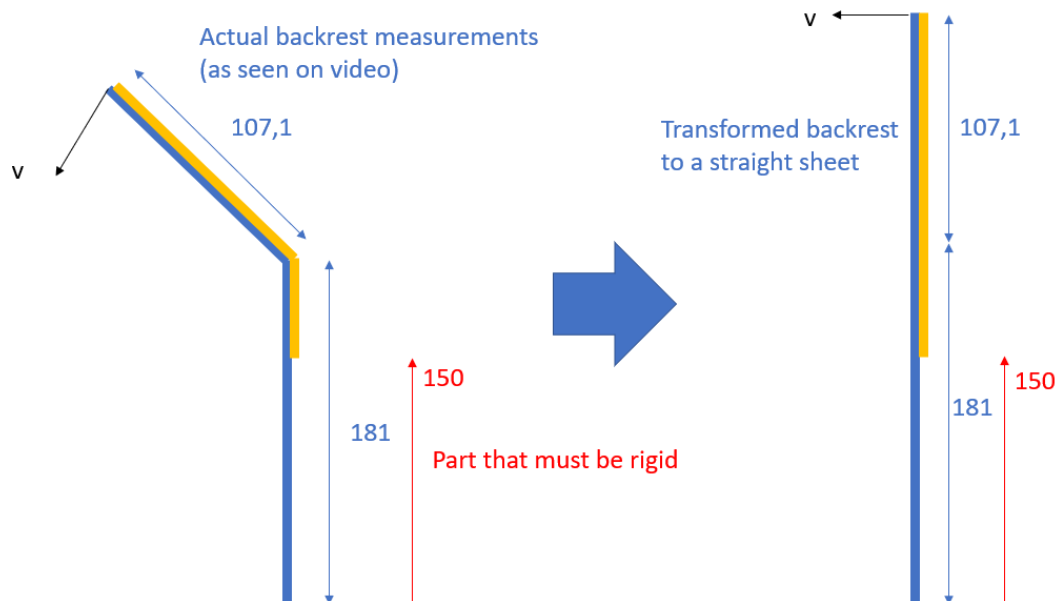
Figure 40: Transformation of the backrest to a straight sheet

This is a good estimation since this value can be used to fabricate the prototype and is easier to test for Measured a single sheet. Worth mentioning is that this transformation is an estimation. The goal is to recreate the deformation and rigidity for estimated values. Because 150 mm from the seat upwards must be rigid, the effective length of the sheet in profile is:

$$H = 107\ mm + 181\ mm - 150\ mm = \mathbf{138\ mm} \tag{5.1}$$

Based on calculation 5.1, the **sheet/beam length is chosen as 138 mm.**

Calculate the design parameters analytically

In theory, the design parameters can be calculated based on the following formula:

$$E * I(x) * \frac{d^2 v(x)}{dx^2} = M(x) \tag{5.2}$$

Because of the constraints of an embedded beam (v(x = 0) = 0; $\frac{dv(x=0)}{dx} = 0$) , the deformation v(x) can be estimated as:

$$v(x) = v_c * x^2 \; with \; v_c \; constant \tag{5.3}$$

Combining 5.2 and 5.3 results in:

$$2 * E * v_c * (\bar{u} * h(x)^2 + \bar{v} * h(x) + \bar{w}) = \frac{-q}{2} * x^2 + q * H * x - \frac{q}{2} * H^2 \tag{5.4}$$

Combining 5.4 and 4.2 results in the following equation (5.5):

$$2 * E * v_c * (\bar{u} * A^2 * x^2 + (2 * \bar{u} * A * B + \bar{v} * A) * x + \bar{u} * B^2 + \bar{v} * B + \bar{w})$$
$$= \frac{-q}{2} * x^2 + q * H * x - \frac{q}{2} * H^2 \tag{5.5}$$

With equation 5.5, the parameters A and B can be analytically calculated in theory. However, since A = -Δh/H and B dependant on L and t (and W), this makes it very difficult to calculate the correct values iteratively. This is because $\bar{u}$, $\bar{v}$ and $\bar{w}$ can only be calculated with a given L and t. This means that L and t must be searched iteratively, whilst satisfying the following system of equations:

$$\bar{u} * A^2 = \frac{-q}{2} \; with \; \bar{u} < 0 \tag{5.6}$$

$$2 * \bar{u} * A * B + \bar{v} * A = q * H \tag{5.7}$$

$$\bar{u} * B^2 + \bar{v} * B + \bar{w} = -\frac{q}{2} * H^2 \tag{5.8}$$

Because of the equation 5.6, $\bar{u}$ must be negative. As shown in figure 17, this is not the case for the U-model, whils this result has been validated as correct by the calculations. This means that the design parameters cannot be calculated analytically.

Tweak the design parameters iteratively

Since the design parameters cannot be calculated analytically, the parameters themselves must be adjusted to fit the desired deformation. In essence, the effects of the design parameters that were discussed in chapter four are utilised to tweak the deformation iteratively until it matches the desired deformation.

Before starting the with tweaking, the fixed parameters are summarised in table 29.

Table 29: Summary fixed parameters

E(MPa)	75 000
q(N/mm)	0,300
H(mm)	138,00
t(mm)	0,38

It is preferred that L > 25 or 30 because it is necessary to produce a prototype sheet.

5.2.2   U-model

Firstly, the section length L is varied for a height difference Δh of 1.30 mm. The utilised section lengths and the deformation results are summarised in table 30.

Table 30:Utilised section lengths and maximal deformation results for U-model

	La =	8,00
	-->Δhmax	2,47667
v$_{max}$a:	ua	0,3403
-382,8685496	va	-0,0022
	wa	0,0208
	Ba	1,4900
	Lb =	**15,00**
	-->Δhmax	4,81000
v$_{max}$b:	ub	0,6347
-204,6360846	vb	-0,0022
	wb	0,0391
	Bb	1,4900
	Lc =	25,00
	-->Δhmax	8,14333
v$_{max}$c:	uc	1,0563
-122,7834718	vc	-0,0022
	wc	0,0653
	Bc	1,4900
	Ld =	30,00
	-->Δhmax	9,81000
v$_{max}$d:	ud	1,2673
-102,3047032	vd	-0,0022
	wd	0,0784
	Bd	1,4900

Table 30 shows that for a section length of 30 mm, the deformation is still a bit higher than the desired deformation. This is ideal for precise tweaking the height difference Δh to match the desired deformation. Therefore, the values for option d are used in the next round of tweaking.

Now the height difference Δh is varied for a section length L of 30 mm. The utilised height differences and the deformation results are summarised in table 31.

Table 31: Utilised height differences and maximal deformation results for U-model

v_maxa:	Δha =	1,30000	
-102,3047032	Aa	-0,0094	=-Δha/H
	Ba	1,490	=t/2 + Δha
v_maxb:	Δhb =	**1,31000**	
-101,0972248	Ab	-0,0095	=-Δhb/H
	Bb	1,5000	=t/2 + Δhb
v_maxc:	Δhc =	1,40000	
-91,12523941	Ac	-0,0101	=-Δhc/H
	Bc	1,590	=t/2 + Δhc
v_maxd:	Δhd =	9,81000	
-2,755947857	Ad	-0,0711	=-Δhd/H
	Bd	10,000	=t/2 + Δhd

Table 31 indicates that a height difference of 1.31 mm can be used to recreate the desired deformation of 101 mm. To test the tweaked values, the whole deformation is recalculated for n is 1000 to see if the result is equivalent. This calculation results in a maximal deformation of **-101,1345852.** Because the result should only contain 3 significant figures, the maximal deformation is exactly equal to -101 and can be recreated by tweaking the design parameters L and Δh.

5.2.3   U-model with constant base

The same methodology as for the U-model is applied here. Firstly, the section length L is varied for a height difference Δh of 0 mm to have the minimal height and thus the maximal possible deformation in consequence of the section length.

The base W is chosen as 15 mm to make sure there is enough room at the sides to bend the sheet. The highest possible minimal height of the section is calculated by the following equation (with L maximally 30 and W minimum 15):

$$\frac{L - W}{2} = \frac{30 - 15}{2}\ mm = 7.5\ mm \tag{5.9}$$

This is the length of the legs of the sheet and the amount of sheet that is allowed to bend. If this number becomes too small, the sheet will be very hard to produce. This should be kept in mind regarding the results.

The utilised section lengths and the deformation results are summarised in table 32.

Table 32: Utilised section lengths and maximal deformation results for U-model with constant base W = 15

	La =		23,00
	-->Δhmax		4,63018
v_{max}a:	ua		-0,7262
-20,02448491	va		20,347
	wa		-60,701
	Ba		4,0000
	Lb =		25,00
	-->Δhmax		4,90454
v_{max}b:	ub		-1,1514
-9,793852444	vb		30,831
	wb		-106,83
	Bb		5,0000
	Lc =		28,00
	-->Δhmax		5,21665
v_{max}c:	uc		-1,8008
-4,452220478	vc		50,215
	wc		-209,53
	Bc		6,5000
	Ld =		30,00
	-->Δhmax		5,38022
v_{max}d:	ud		-2,2386
-2,944409029	vd		65,524
	wd		-303,84
	Bd		7,5000

For the highest possible deformation (because $\Delta h = 0$) given $W = 15$ mm, the deformation of a sheet with section length 23 mm is five times smaller than the desired deformation of -101. The deformation could be increased by increasing W, but this would make the sheet even harder to produce because of the low height of the function. This means the sheet must be bent with legs of less than 7.5 mm, which is too small for its size. It is also required that the section length be minimally 25 mm to fabricate the prototype more easily. This would require significant tweaking and it is uncertain if an ideal design could be reached with this model.

5.2.4 Conclusion calculation results

Because of the low range of section length and deformation of the U-model with constant base, this model will not be used to design the prototype. Therefore, the prototype will be designed with the U-model with the following parameters:

- L = 30
- H = 138
- e = 0.38
- dh = 1.31

5.3 Designing the prototype and mould

To design the prototype and the mould, the CAD software Creo Parametric 7.0.1.0 is utilised to create a 3D model, based on the design specifications found in the previous paragraph. The section design of the U-model in figure 10 should transform based on the calculated height difference and thickness. The transformation of the section is shown in figure 41.
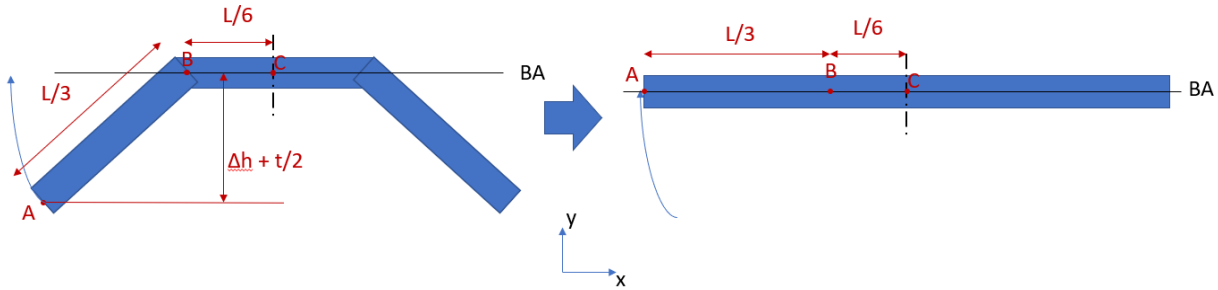
Figure 41: Required transformation of the section for the U-model

It is important to note that the coordinate system in Creo replaces the x-axis as defined in the theoretical background with the z-axis. This has no effect on the actual design or deformation, but reinterprets the insights of the theoretical calculations. For the prototype and mould design and the FEM tests, the following values for the design parameters are used (Tab. 33):

Table 33: Used values for the FEM tests and calculations

E(GPa)	75,00
H(mm)	138,00
L(mm)	30,00
t(mm)	0,38
Δh(mm)	1,31

The actual 3D CAD design is shown in figure 42.

Figure 42: Final design of the prototype with section at the origin.

Figure 41 shows the transformation for z <= 0 to z = H. This is implemented in figure 42. Note that there is a straight section of 50 mm long added for z<0. This part is used to fix the sheet to the backrest. Since it will be fixed, the rigidity is constant.

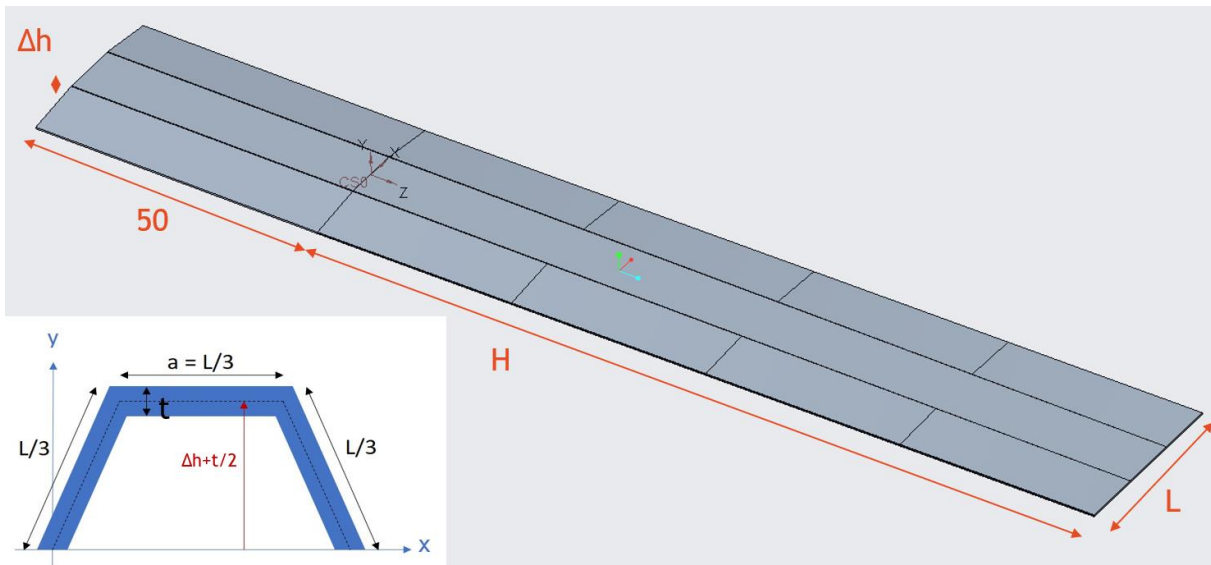Note that there are four separate sections of the carbon fibre sheet which transform in form. This is due to the approximation of the path of the section as shown in figure 41. Since it is hard to exactly approximate this curve, different sketches of the section are linearly swept. This produces a small error in the design of the sheet. This principle is shown in figure 43.
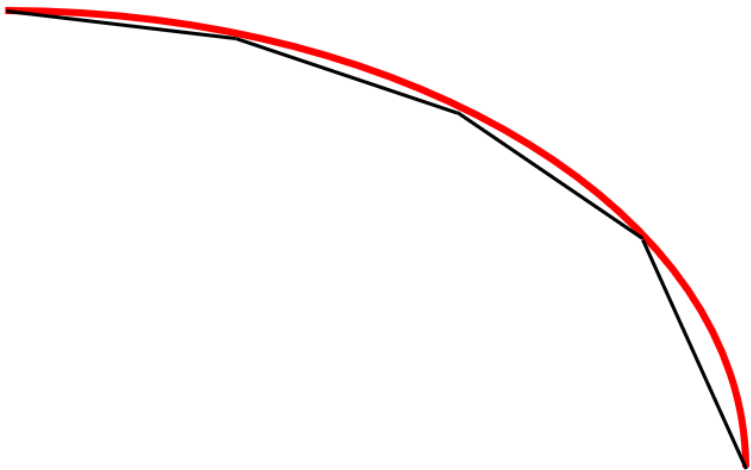
Figure 43: Approximation of the desired movement of point A of the section (red) by linearly connecting certain sections (black)

However, for the design of the mould, the slopes of the varying section can be extended. This means that there will be too much material used for the production of the prototype, but the excess of material can always be removed afterwards. For the mould design, it is also key that the section is t/2 lower for each point than for the neutral line of the section. To be able to manufacture the mould with a CNC machine, the sharp angles of the section need to be rounded (in this case, with a radius of 1 mm). The mould will be manufactured from Aluminium. These design concepts are translated to the mould design, visible on figure 44.

Figure 44: Final design of the mould

6. Virtual testing on the prototype

To check if the preformed calculations and design are correct, Finite Element Analyses are conducted. These analyses are conducted with two different software programs. The linear FEM tests on the deformation are preformed using PTC Creo Simulate. The non-linear FEM tests and the linear FEM test of the bending stress are conducted with Hyperworks, with the solver OptiStruct.
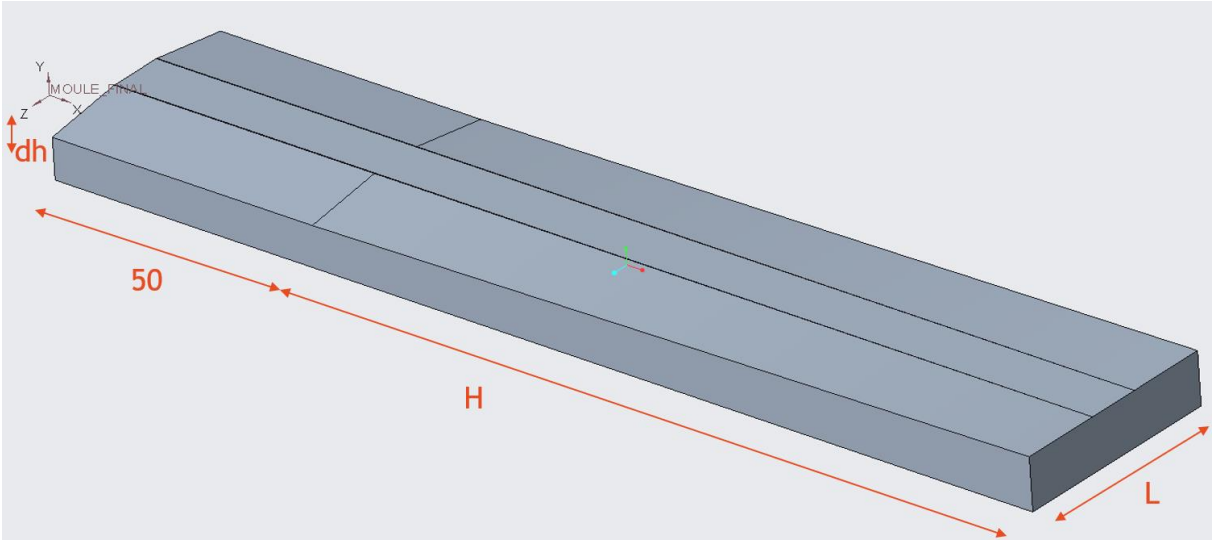
For these tests, simplified models of the prototype will be used. The 50 mm long constant section is removed because this part of the sheet is embedded and will not undergo any displacements. The prototype design is also cut in half because of the symmetry of the section. A Young's Modulus of 75 GPa and a Poisson-coefficient of 0.3 are chosen as the material characteristics of the tests. Because of the low thickness of the sheet(s), the model is simplified by shell elements with a max element size of 1 mm.

6.1 Linear FEM testing of the deformation

To test the linear deformation, three tests are conducted: test one and two measure the displacement for the most extreme forms of the section of the sheet (thus a constant rigidity with the extreme section). This should correspond with the calculated values for the most extreme cases. The final linear test for the deformation is performed on the prototype, to see if the desired deformation can be recreated. For all of the tests, a charge of 300 N/m is applied.

Test 1: Straight sheet

The first design is a straight sheet with section length L = 30 mm and thickness t = 0.38 mm. The resulting mesh consists of 919 tria and 2927 quad elements and a max aspect ratio of 2.86, which is excellent. The resulting deformation is shown in figure 45.

Figure 45: Result linear FEM analysis of the deformation for a straight sheet

The FEA result in a maximum deformation of 1286,95 mm. In the theory, it is calculated that the deformation should be 1323 mm. However, these calculations are based on values with three significant figures, resulting in the value of 132*10 mm. The error is possible due to the Poisson-deformation, which the calculations do not take into a count. However, the relative error is less than

3%, which is a good approximation for such high deformations. There are no displacements in the x- and z- directions of the sheet, which is accurate for this sheet.

Test 2: Bent sheet with constant section

This design consists of a sheet with a constant section as shown on the image below (Fig. 46)
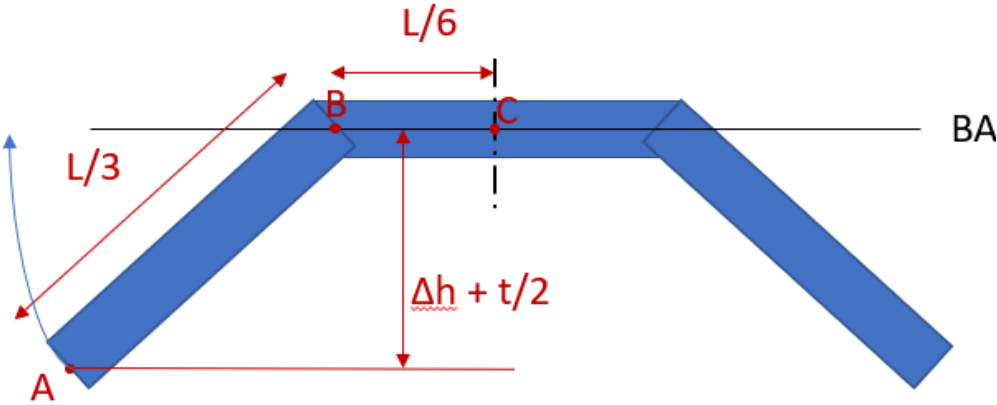
Figure 46: Constant section of bent sheet for FEM test

The resulting mesh consists of 957 tria and 2950 quad elements and a max aspect ratio of 2.7, which is excellent. The resulting deformation is shown in figure 47.

Figure 47: Result linear FEM analysis of the deformation for a bent sheet with constant section

The FEA result in a maximum deformation of 61.1510 mm. In the theory, it is calculated that the deformation should be 62,0. The error is possible due to the Poisson-deformation, which the calculations do not take into a count. The relative error is less than 1.5%, which is a good approximation for such high deformations.

Test 3: Prototype sheet

This FEA tests the prototype sheet to see if the calculated deformation can actually be recreated. The resulting mesh consists of 920 tria and 2934 quad elements and a max aspect ratio of 2.8, which is excellent. The resulting deformation is shown in figure 48.
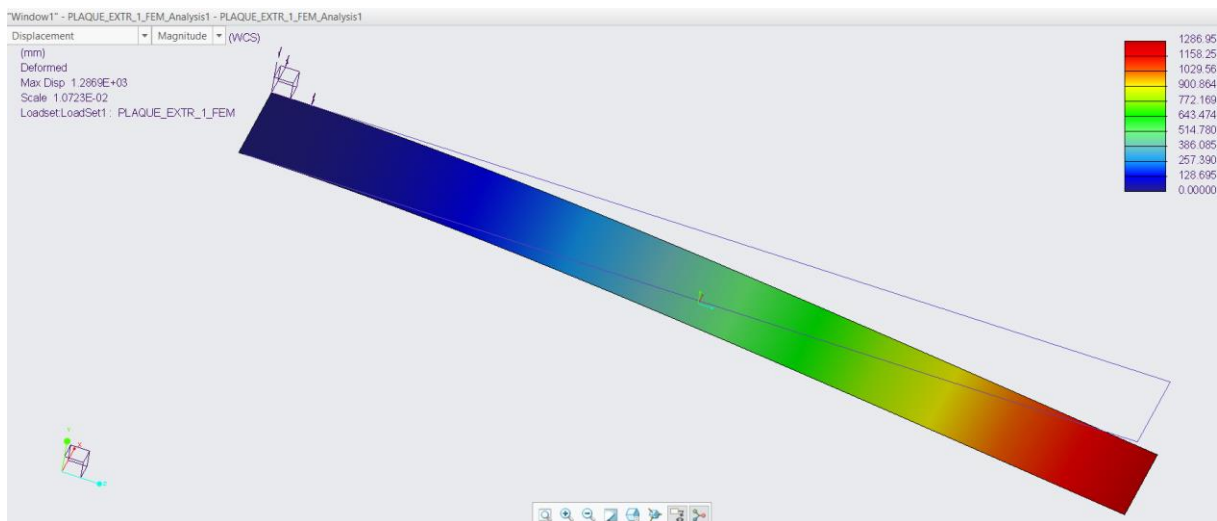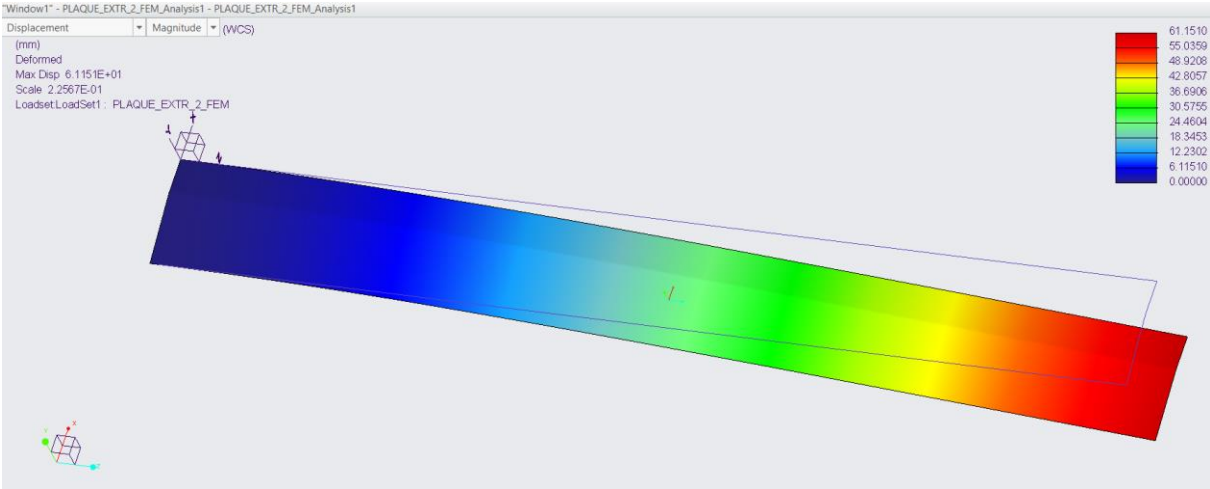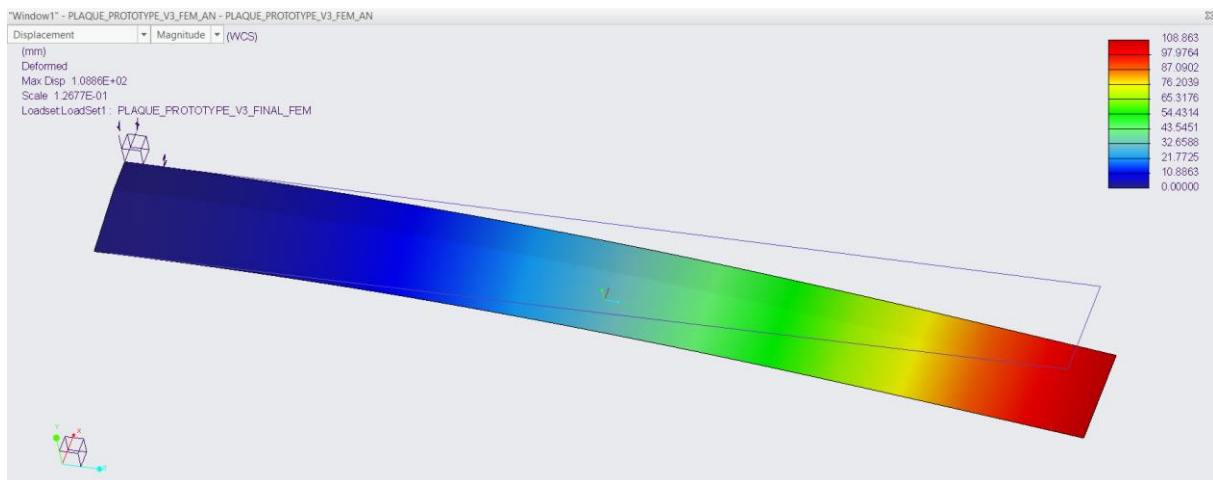

Figure 48: Result linear FEM analysis of the deformation for the designed prototype

The FEA result in a maximum deformation of 108.863 mm. In the theory, it is calculated that the deformation should be 101 mm. The error is possible due to the Poisson-deformation, which the calculations do not take into a count. The relative error is 7%, which seems too big. This is actually a good result for such high deformations because of the high number of estimations and the result falls within the calculated uncertainty (lower than 117.6 mm). The result has the same order of grandeur, which is not simple for such a low difference in height Δh: each small error in the height will result in huge differences in rigidity and deformation.

6.2 Non-linear FEM testing of the deformation

The non-linear FEM calculations are a greater approximation of reality because of the implementation of a non-linear relation between the charge and the deformation: when the deformation is relatively big, the charge can no longer be estimated to be at the original surface. Therefore, an iterative calculation is done to incrementally increase the charge and measure the deformation. Based on that deformation, the charge is applied at that new deformation. This is a closer representation of reality.

Because of the nature of these non-linear calculations, no solution will be found when the deformation becomes too high. For each non-linear FEA, a linear FEA is also calculated to compare the difference in results. This process is repeated for a different charge. The resulting deformations in function of the charge are shown in the following figure (Fig. 49).
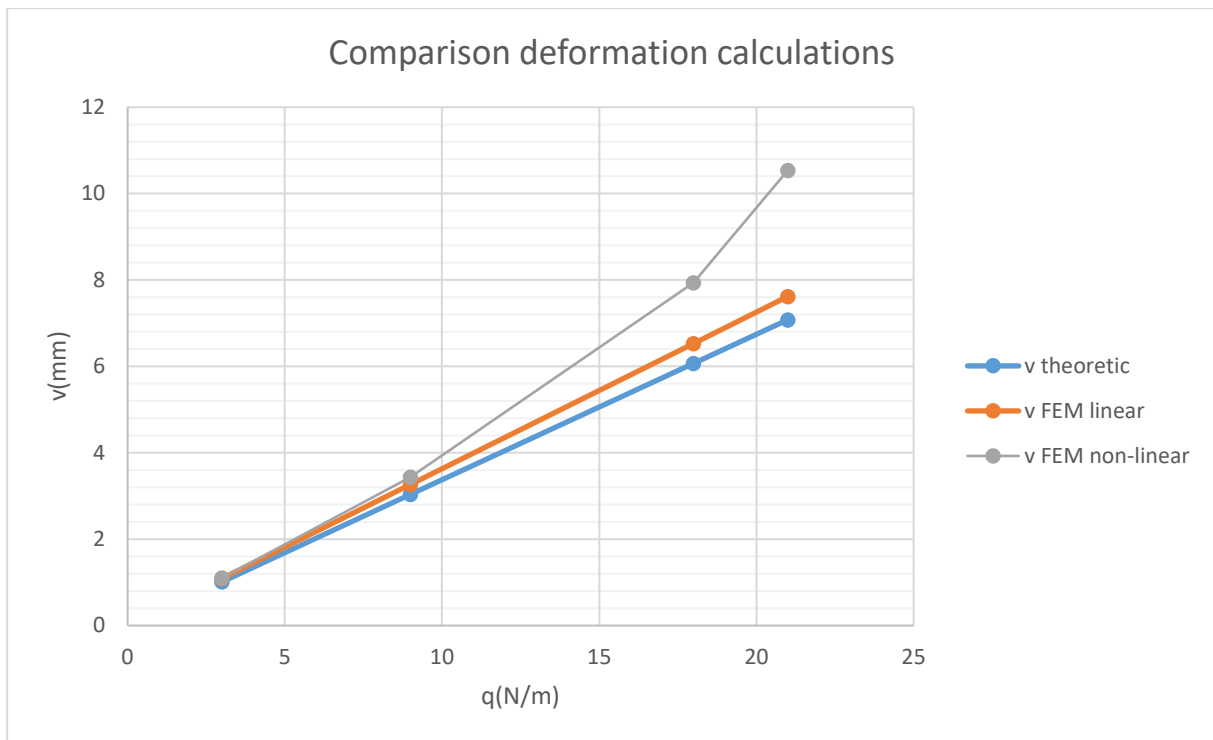
Figure 49: Comparison between the theoretic, linear FEM and non-linear FEM results

Based on these results, it is clear that for a charge q greater than 20 N/m linear calculations no longer apply because of the high relative deformation. From that point onwards, a non-linear model is required to calculate the deformation accurately. However, for lower values of the deformation, the theoretical and non-linear FEM results correspond well. This means the mathematical model is a good representation of the real deformation and rigidity for a limited deformation.

It is also interesting to check the relative difference between the theoretical deformation and the FEM results. In table 34, the relative difference between the theoretical deformation and the linear FEM result is determined.

Table 34: Calculation of the relative difference between the theory and the linear FEA

v theoretic (mm)	v FEM linear (mm)	Δv FEM linear (mm)	rel Δv FEM linear (%)
1,01	1,089	0,078	7,72
3,03	3,266	0,232	7,65
6,07	6,53	0,462	7,61
7,08	7,62	0,541	7,64

As shown in table 34, the relative difference between the linear FEA and the theoretical calculation is constant. This means that there is a key relation between the theoretical and FEA results. It also means that the error linearly increases as the deformation increases.

In table 35, the relative difference between the theoretical deformation and the linear FEM result is determined.

Table 35: Calculation of the relative difference between the theory and the non-linear FEA

v theoretic (mm)	v FEM non-linear (mm)	Δv FEM non-linear (mm)	rel Δv FEM non-linear (%)
1,01	1,10	0,0890	8,80
3,03	3,434	0,400	13,2
6,07	7,932	1,86	30,7
7,08	10,54	3,46	48,9

The results in table 35 show that there is no simple relation between the (relative) difference in calculated values for the theory and the non-linear FEA. The relative error increases greatly when the deformation increases. This could indicate an exponential relationship, but the deformation can no longer be calculated for high deformations.

6.3 Linear FEM testing of the bending stress

Predicting the maximum bending stress

For this paragraph, only the bending stress will be calculated, since this has a direct relation with the applied load. The bending stress in the x-axis can be calculated with the following formula [10]:

$$\sigma_x = \frac{-M}{I_{gz}} * y \tag{6.1}$$

Containing:

σ_x: Bending stress in the x-direction (x for calculations, z for FEA)
M: Flexural moment
I_{gz}:   Moment of inertia in the centre of gravity for the z-direction (z for calculations, x for FEA)
y: Height in the section relative to the centre of gravity

Because the flexural moment M and the moment of inertia are dependent on the position in the x-direction:

$$\sigma_x = \frac{-M(x)}{I_{gz}(x)} * (y) \tag{6.2}$$

For the most extreme values of the tension should be at the embedding (x=0), because the flexural moment there is maximal. This could be compensated if I(x) decrease greater than M(x). A quick calculation of M(x)/I(x) shows that the minimum is indeed at x=0. To attain the maximal possible value for the bending stress, it should be regarded at the two outermost points of the section: the top base and the lower base. Because x=0, the section has the most bent shape possible.

To calculate the height of the centre of gravity, the section of can be split up into three parts. The centre of gravity of each individual part of the section can be visualised in figure 50.
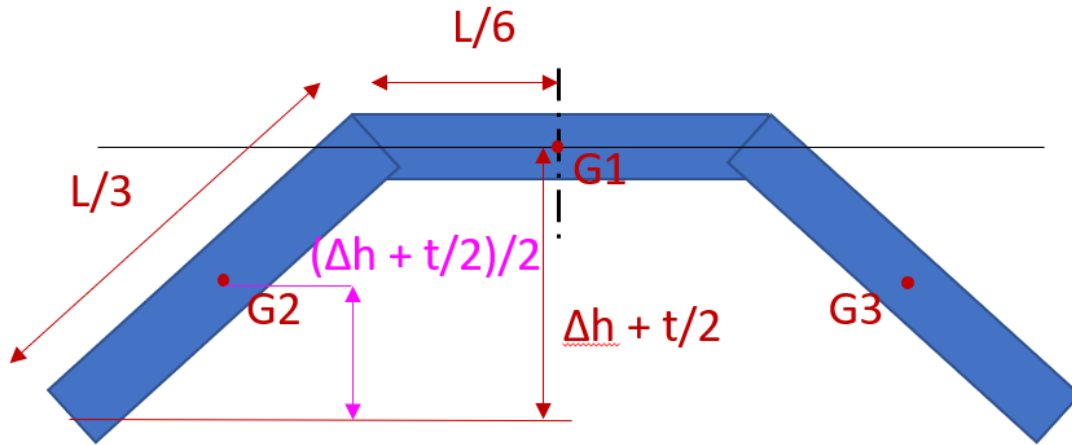
Figure 50:Section with indicated centres of gravity

The centre of gravity of the whole section can be described as:

$$y_G = \frac{\sum S_i * y_i}{\sum S_i} = \frac{2 * \left(\frac{L}{3} * t * \frac{\Delta h + \frac{t}{2}}{2}\right) + \frac{L}{3} * t * \left(\Delta h + \frac{t}{2}\right)}{3 * \frac{L}{3} * t} = \frac{2}{3} * \left(\Delta h + \frac{t}{2}\right) \qquad (6.3)$$

From the solution of equation 6.3, the most extreme bending stresses can be calculated for a charge of 300 N/m:

$$\sigma_{x,top} = \frac{-M(0)}{I(0)} * \left[\frac{1}{3} * \left(\Delta h + \frac{t}{2}\right)\right] = 488 \ MPa \qquad (6.4)$$

$$\sigma_{x,base} = \frac{-M(0)}{I(0)} * \left[-\frac{2}{3} * \left(\Delta h + \frac{t}{2}\right)\right] = -976 \ MPa \qquad (6.5)$$

The maximal value for the bending stress is a little greater than the reference for the flexural strength (950 MPa). These values are checked by a linear FEA.

FEA of the bending stress

In figure 51, the bending stress in the z-direction is calculated, which corresponds with the bending stress in the x-direction for the theoretical calculations.
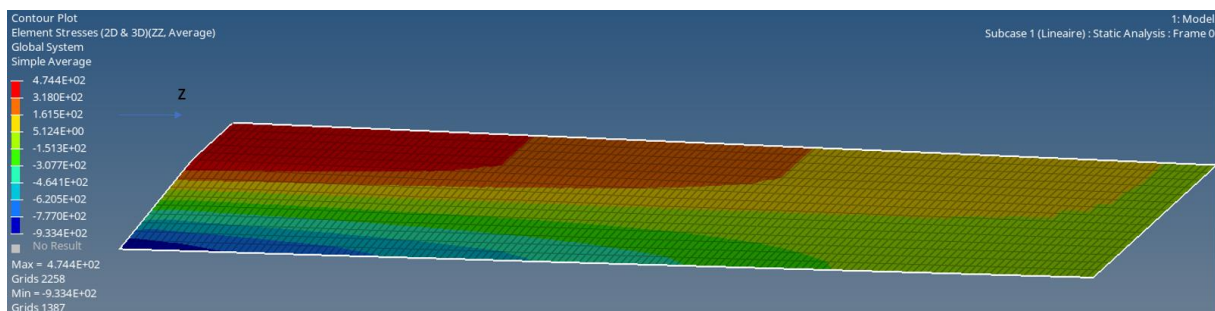

Figure 51: Result linear FEM analysis of the stress for the designed prototype

The maximal stresses as calculated by the FEA are: **474.4 MPa and -933.4 MPa**. These values correspond greatly with the theoretical values. Note that the maximal value is close to the flexural strength for a charge of 300 N/m. If the charge is kept below 20 N/m as calculated in the previous section, the sheet can bear the given uniform load and this prototype is strong enough.

6.4 Conclusions and preparing physical tests

All of the FEM analyses confirm the calculated results with a small margin of error. This means that, for a linear deformation, the desired deformation and rigidity of the elastic bands can be replicated by a carbon fibre sheet.

The FEM analyses also show that the deformation can only be recreated for a limited charge of q. The limit for the given prototype is 20 N/m. The physical tests should subject the produced prototype by this charge.

Preparing the physical tests

To prepare for the physical tests, the mould can be manufactured by a 6-axis CNC milling machine. The cutting process of the CNC-machine is visualised on the following figure (Fig. 52).

Figure 52: The 6-axis CNC-milling machine is milling the mould by repositioning the clamped object

The finished mould is completed and shown in the following image (Fig. 53).

Figure 53: Completed aluminium mould

When the mould is finished, two carbon fibre sheets must be produced: one with the varying section of the mould (the prototype) and one with a constant rectangular section (straight sheet). The straight sheet will be used to determine the thickness, the flexural modulus and the flexural strength. When these parameters are found, the calculations need to be recalibrated with these updated values to accurately predict the deformation of the prototype.

After the calculations are updated, the prototype is tested under a distributed load of 20 N/m maximum. It would be ideal to check the deformations for the charges of figure 49: that way, the non-linear FEA and theoretical deformations can be checked. After these physical tests, it should be clear if the theoretical calculations can recreate the linear deformation of an elastic band…

7. Conclusion

7.1 Evaluation

To evaluate if this master's thesis is a success, conclusions must be drawn from the FEM analyses:

- The difference between the calculated deformation and the linear FEA results for the deformation is small. They confirm the mathematical calculations for the deformation made in this thesis. For a linear analysis, the calculations can predict the deformation.
- The non-linear FEA results for the deformation show that the mathematical model to calculate the deformation is accurate for a distributed charge below 20 N/m. For these charges, the calculations are a good representation of the deformation.
- The linear FEA results for the stress show that flexural stresses in the prototype are close to the flexural strength for a charge of 300 N/m. This means that for a charge of 20 N/m, which is an order of magnitude smaller than 300 N/m, the stress should be below the flexural strength. Therefore, the prototype can resist the load.

The results of the thesis support the calculations made. This means that the prototype should be able to recreate the rigidity of the elastic bands for a limited charge and deformations.

7.2 Relevance

The linear calculations for the rigidity are the base for the whole design of the sheet and the backrest. Of all the rigidities, the base rigidity of the sheet is the most important. If the base rigidity is too high, the backrest will be uncomfortable and result in practically no deformation. If the base rigidity is too low, the athlete will receive no support. That's why this study lays the foundation for calculating the whole backrest.

7.3 Critical remarks

- The constant charge is not an accurate representation of the mechanical situation. This must be replaced by a function of the charge (in function of the position x). Also, a larger beam length results in a bigger deformation because the charge remains fixed. This results in a higher load on the sheet. Ideally, a solution must be found to fix the total load, whilst distributing it accurately over the sheet.
- The calculations of the stresses are hard to validate without concrete values for the flexural strength and the flexural modulus. Therefore, physical tests are a necessity to validate this thesis.
- The creation of the CAD model is based on an approximation, whilst the mould produces the prototype with the actual required variation of the section. This could result in a discrepancy in results during physical tests.
- The FEA for the stress is calculated solely for a charge of 300 N/m. It would also be advisable to check which stresses exactly develop for a charge of 20 N/m.
- The time of the deformation for the elastic bands should also be taken in consideration. This is an important aspect in recreating the whole elastic backrest.
- The athlete must receive an equal amount of momentum. Therefore, the elastic deformation should also be calculated based on the energy of the deformation.
- In this study, the charge was calculated and focussed on only one sheet. In reality, there are multiple carbon fibre sheets bearing the load and distributing the charge.

- The deformation is used to calculate if the rigidity can be replicated, but that is not a correct assumption. The rigidity of the elastic bands is unknown. But this study does prove that the deformation of the elastic bands can be recreated by a carbon fibre sheet. To definitively recreate the rigidity, more research about the mechanics of the elastic bands is required.

7.4 Prospects

First and foremost, the prototype must be physically tested. The calculations in this thesis were time consuming. Therefore, the mould and prototype could not be completed within a three-month period.

The physical tests do not only need to verify the calculations, they also are a means to optimise the values of the flexural modulus and the thickness. When these values are found, the deformation can be more accurately calculated and checked with the results of the physical tests.

A 3D scan to find the deformations and charge on the actual backrest is also preferred to use in the calculations. These could be used to expand the model for non-linear deformations and calculating the required rigidity for the more flexible parts.
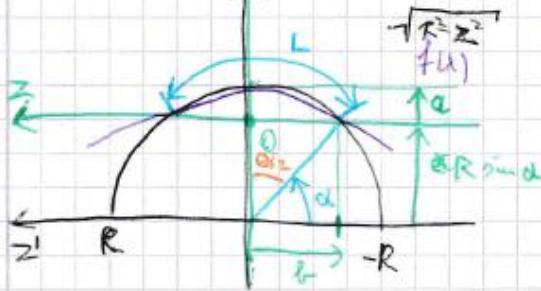
Reference list

[1]   M. Lambrecht, "Internal report: Optimisation of wheelchairs for paralympic athletes," Katholieke Universiteit Leuven/Université Toulouse III - Paul Sabatier, 2021.

[2]   Wikipedia, "Euler–Bernoulli beam theory," 2021. https://en.wikipedia.org/wiki/Euler–Bernoulli_beam_theory (accessed Jun. 06, 2021).

[3]   M. Hamzah and A. Gatta, "Design of a Novel Carbon-Fiber Ankle-Foot Prosthetic using Finite Element Modeling," *IOP Conf. Ser. Mater. Sci. Eng.*, vol. 433, p. 012056, Nov. 2018, doi: 10.1088/1757-899X/433/1/012056.

[4]   Wikipedia, "Bending stiffness," 2021. https://en.wikipedia.org/wiki/Bending_stiffness (accessed Jun. 07, 2021).

[5]   R. C. Hibbeler, *Sterkteleer*, 9th ed. Amsterdam: Pearson Benelux, 2017.

[6]   A. K. Veerapaneni and M. Dandu, "Characterisation of PAN Carbon Fabric/ Epoxy Resin for Structural Materials," *Procedia Mater. Sci.*, vol. 10, pp. 760–767, 2015, doi: 10.1016/j.mspro.2015.06.092.

[7]   C. Dong, "Flexural properties of symmetric carbon and glass fibre reinforced hybrid composite laminates," *Compos. Part C Open Access*, vol. 3, p. 100047, Nov. 2020, doi: 10.1016/j.jcomc.2020.100047.

[8]   P. Dawkins, "Calculus II - Arc Length," *Lamar University*, 2018. https://tutorial.math.lamar.edu/classes/calciii/LineIntegralsPtI.aspx (accessed Apr. 05, 2021).

[9]   M. E. Lemonis, "Calc Resource: Moment of Inertia of a Trapezoid," 2020. https://www.calcresource.com/moment-of-inertia-trap.html (accessed Apr. 13, 2021).

[10]   M. Sudre, "Conception et Calcul de Structures: Poutres." Université Toulouse III Paul Sabatier, p. 44, 2020, [Online]. Available: http://www.mastercalcul.fr.

Dériver modèle pour 2ième

$$L = \theta \cdot R \implies \theta = \frac{L}{R}$$

$a = R - R\sin\alpha$

$ = R(1 - \sin\alpha)$

$ = R\left[1 - \sin\left(90° - \frac{\theta}{2}\right)\right]$

$ = R\left(1 - \cos\frac{\theta}{2}\right)$

$$\boxed{a = R\left[1 - \cos\left(\frac{L}{2R}\right)\right]}$$

$\lim\limits_{R \to \infty} a = 0 \;\checkmark$

$b = R\cos\alpha$

$ = R\cos\left(90° - \frac{\theta}{2}\right)$

$ = R\sin\frac{\theta}{2}$

$$\boxed{b = R \cdot \sin\left(\frac{L}{2R}\right)}$$

$\lim\limits_{R \to \infty} b = L/2 \;\checkmark$

$\sqrt{R^2 - z^2}$
$f(x)$

$\sqrt{R^2 - z^2}$
$f(x) = Az^2 + B$

$\sin 90° - \gamma = \cos\gamma$

$\cos 90° - \gamma = \sin\gamma$
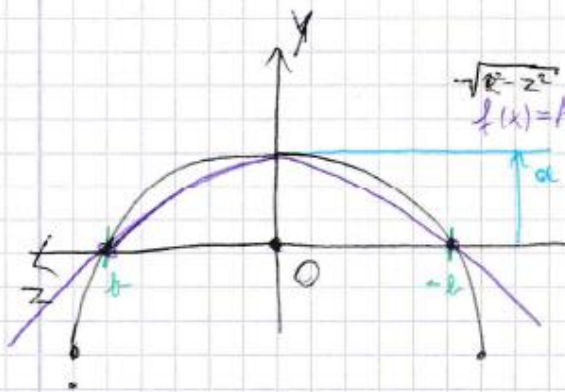
Trouver $f(z)$:

$f(0) = a \implies A\cdot 0 + B = a \implies \boxed{B = a}$

$f(b) = 0 \implies A\cdot b^2 + B = 0$

$A = \dfrac{-B}{b^2}$

$\boxed{A = \dfrac{-a}{b^2}}$

$\implies \boxed{f(z) = \dfrac{-a}{b^2}\cdot z^2 + a}$

$$\ell = \int d\ell = L \, d\ell$$

$$f(x) = \frac{-a}{b^2} z^2 + a$$
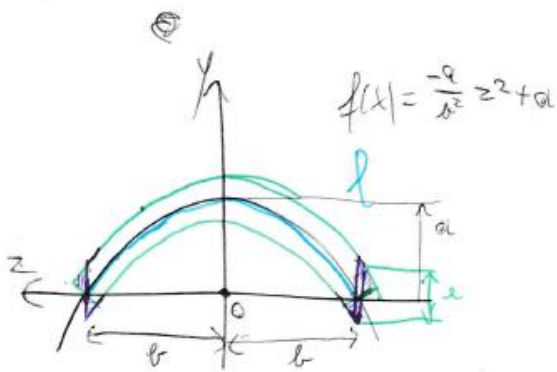
$$dS = d\ell \, dy \qquad \text{avec } d\ell = \sqrt{1 + \left(\frac{dy}{dz}\right)^2} \, dz$$

$$= \sqrt{1 + \left(\frac{dy}{dz}\right)^2} \, dz \, dy$$

$$\boxed{dS = \sqrt{1 + \left(\frac{dy}{dz}\right)^2} \, dy \, dz}$$

→ normalement doive se composer

$$S = \iint dS$$

$$= \int_{-b}^{b} \int_{f(z)-\frac{e}{2}}^{f(z)+\frac{e}{2}} \sqrt{1 + \left(f'(x)\right)^2} \, dy \, dz$$

$$= \int_{-b}^{b} \int_{-\frac{a}{b^2} z^2 + a - \frac{e}{2}}^{-\frac{a}{b^2} z^2 + a + \frac{e}{2}} \sqrt{1 + \left(\frac{d}{dz}\left(-\frac{a}{b^2} z^2 + a\right)\right)^2} \, dy \, dz$$

$$= \int_{-b}^{b} \int_{-\frac{a}{b^2} z^2 + a - \frac{e}{2}}^{-\frac{a}{b^2} z^2 + a + \frac{e}{2}} \sqrt{1 + \left(\frac{d}{dz}(y)\right)^2} \, dy \, dz$$

$$\boxed{S = 2 \, b \cdot e} \qquad \rightarrow \text{ne semble pas correct}$$

$$I_{oz} = \iint y^2 \, dS$$

$$I_{oz} = \int_{-b}^{b} \int^{-\frac{a}{b^2} z^2 + a + e} \cdots$$

$$I_{oz} = \int_{-b}^{b} \int^{-\frac{a}{b^2} z^2 + a +} \cdots$$

$$I_{oz} = \int_{-b}^{b} \int_{f(z)-\frac{e}{2}}^{f(z)+\frac{e}{2}} y^2 \cdot \sqrt{1 + \left(\frac{dy}{dz}\right)^2} \, dy \, dz$$

$$I_{oz} = \frac{5}{\cancel{36}\,32} \frac{\left(a^2 + 5e^2\right) b \, e}{30}$$
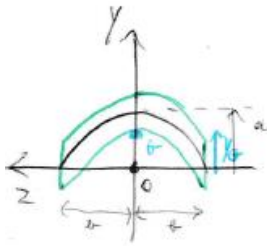
$$\lim_{R \to \infty} I_{oz} = \lim_{\substack{a \to 0 \\ b \to 4L}} I_{oz} = \frac{\left(0 + 5e^2\right) \cdot \frac{L}{2} \cdot e}{30} = \frac{1}{6} \cdot \frac{L}{2} \cdot e^3 = \frac{L e^3}{12} \checkmark$$

Si $f(z) = \frac{-a}{b^2} z^2 + a$

Pour
$\begin{cases} S = 2 b \cdot l \\ I_{oz} = \dfrac{(32a^2 + 5e^2) b \cdot l}{30} \end{cases}$
$\Rightarrow \begin{cases} S = 2 \cdot R \cdot \sin\left(\frac{L}{2R}\right) \\ \vdots \\ I_{oz} \end{cases}$ Désol.

avec $\begin{cases} b = R \sin\left(\frac{L}{2R}\right) \\ a = R\left(1 - \cos\left(\frac{L}{2R}\right)\right) \end{cases}$

$Y_G = \dfrac{\iint y \, dS}{\iint dS} = \dfrac{\displaystyle\int_{-b}^{b} \int_{f(z)-\frac{s}{2}}^{f(z)+\frac{s}{2}} y \sqrt{1 + \left(\frac{dy}{dz}\right)^2} \cdot dy \, dz}{2 b \cdot l}$

$Y_G \Big|_{f(z) = \frac{-a}{b^2}z^2 + a} = \dfrac{\frac{4 a b l}{3}}{2 b l} = \frac{2}{3} a$

$\Rightarrow \lim_{R \to \infty} Y_G = \lim_{a \to 0} Y_G = 0$ ✓

$I_{GZ} = I_{oz} - S \cdot Y_G^2 = \dfrac{(32a^2 + 5e^2) b \cdot l}{30} - 2 b l \cdot \left(\frac{2}{3} a\right)^2$

$I_{oz} = \dfrac{(16a^2 + 15e^2) b \cdot l}{90}$

$\lim_{R \to \infty} I_{oz} = \lim_{\substack{a \to 0 \\ b \to \frac{L}{2}}} I_{GZ} = \dfrac{(0 + 15e^2)\frac{L}{2} \cdot l}{90} = \frac{1}{6} \cdot \frac{L}{2} \cdot l^3$

$\lim_{R \to \infty} I_{GZ} = \dfrac{L \, l^3}{12}$ ✓

$\Rightarrow \begin{cases} L = \dfrac{\ln\left(\sqrt{4a^2 + b^2} \cdot b + 2 a b\right)}{2a} + \sqrt{4a^2 + b^2} + \dfrac{\ln\left(\frac{1}{b}\right) b^2}{2a} \\ S = 2 b \cdot l \\ I_{GZ} = \dfrac{(16a^2 + 15e^2) b \cdot l}{90} \end{cases}$

avec $\begin{cases} a = R\left(1 - \cos\left(\frac{L}{2R}\right)\right) \\ b = R \sin\left(\frac{L}{2R}\right) \\ f(z) = \frac{-a}{b^2} z^2 + a \end{cases}$

Par Limites $\begin{array}{l} \lim_{R \to \infty} L = \text{indéf} \times \\ \lim_{R \to \infty} S = L \cdot l \checkmark \\ \lim_{R \to \infty} I_{oz} = \frac{L l^3}{12} \checkmark \end{array}$

$\Rightarrow I_{GZ} \sim \left[R^2\left(1 - \cos\frac{L}{2R}\right)^2 + \frac{15 e^2}{15}\right] R \sin\frac{L}{2R}$

Calcule I du trapèze $f(x) = \dfrac{H}{B/2} \cdot x$

1)

$\dfrac{H}{B/2} = \dfrac{H-h}{b/2} \Rightarrow H\left(\dfrac{1}{B} - \dfrac{1}{b}\right) = \dfrac{h}{b/2}$

$\tan \sigma = \dfrac{h}{B/2 - b/2}$

$H = \dfrac{2h}{2b\left(\frac{1}{b} - \frac{1}{B}\right)}$

$H = \dfrac{h}{b\left(\frac{1}{b} - \frac{1}{B}\right)} = \dfrac{-h \cdot B}{b - B}$

$$I_{o3x} = \left(\int_0^{B/2} \int_0^{\frac{H}{B/2} \cdot x} y^2\, dy\, dx - \int_{B/2 - b/2}^{B/2} \int_h^{\frac{H}{B/2} \cdot x} y^2\, dy\, dx\right) \cdot 2$$

$$I_{o3x} = \dfrac{3b \cdot h^3}{12} + \dfrac{B \cdot h^3}{12}$$

contrôle: $= 2\left(\int_0^{\frac{B}{2} - \frac{b}{2}} \int_0^{\frac{H}{B/2} \cdot x} y^2\, dy\, dx + \int_{\frac{B}{2} - \frac{b}{2}}^{B/2} \int_0^h y^2\, dy\, dx\right)$ ✓

Contrôle 1

1) calculer pour trapèze
2) l'utiliser pour calculer I_{ox}
3) calcule I_{o2}

$f_1(x) = \dfrac{H}{B/2} \cdot x$

$f_2(x) = \dfrac{-H}{b/2} \cdot x + 2H$

$\dfrac{H}{B/2} = \dfrac{H-h}{b/2}$

$\Rightarrow H = \dfrac{h}{b\left(\frac{1}{b} - \frac{1}{B}\right)} = \dfrac{-hB}{b-B}$

$$I_{ox\,\square} = I_{①} + I_{②} + I_{③}$$

$= \dfrac{b \cdot h^3}{3} + \dfrac{(b-B)^4 \cdot H^3}{12 B^3}$

$H = \dfrac{-h \cdot B}{b - B}$

$= \dfrac{3b \cdot h^3}{12} + \dfrac{B \cdot h^3}{12}$ ✓

$$I_{①} = \int_0^{B/2 - b/2} \int_0^{\frac{H}{B/2} \cdot x} y^2\, dy\, dx$$

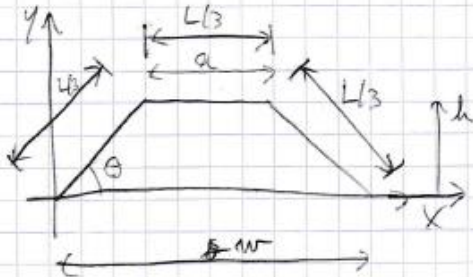$= \dfrac{(b-B)^4 \cdot H^3}{24 B^3}$

$$I_{②} = \int_{B/2 - b/2}^{B/2 + b/2} \int_0^h y^2\, dy\, dx$$

$= \dfrac{b \cdot h^3}{3}$

$$I_{③} = \int_{B/2 + b/2}^{B} \int_0^{\frac{-H}{B/2} \cdot x + 2H} y^2\, dy\, dx$$

$= \dfrac{(b-B)^4 \cdot H^3}{24 B^3}$

Calculer $I_{ox}\,\Omega$

1) écrire a & θ en fonction du h

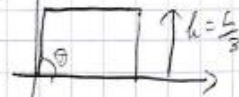2) l'utiliser pour trouver $I_{ox}\,\Omega$

$$a = L/3$$

$$\sin\theta = \frac{h}{L/3}$$

$$\Rightarrow \sin\theta = \frac{3h}{L} \quad\text{ou}\quad \theta = \sin^{-1}\left(\frac{3h}{L}\right)$$

contrôle:

$$\frac{L-a}{2} = \frac{L}{3}$$

$$L - \frac{L}{3} = \frac{2L}{3} \checkmark$$

contrôle: $\quad h = \frac{L}{3}$

$$\sin\theta = \frac{3h}{L} = \frac{3}{4} \cdot \frac{L}{3} = 1$$

$$\theta = 90° \checkmark$$
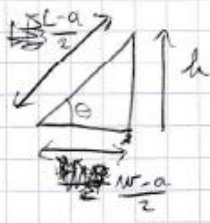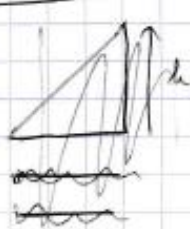
contrôle:

$$w = \frac{L}{3} + 2\frac{L}{3}\cdot\cos\theta$$

$$= \frac{L}{3} + 2\cdot\left(\frac{w - \left(\frac{L}{3}\right)}{2}\right)$$

$$w = w \checkmark$$
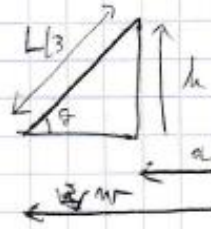
$$\cos\theta = \frac{\frac{w - a}{2}}{\left(\frac{L}{3}\right)} = \frac{\frac{w - \left(\frac{L}{3}\right)}{2}}{\left(\frac{L}{3}\right)}$$

$$w = \frac{L}{3} + 2\cdot\frac{L}{3}\cdot\cos\theta$$

$$w = \frac{L}{3}(1 + 2\cos\theta)$$

contrôle: $\theta = 90° \Rightarrow w = \frac{L}{3}(1+0) = \frac{L}{3}$

$\theta = 0° \Rightarrow w = \frac{L}{3}(1+2) = L$

86
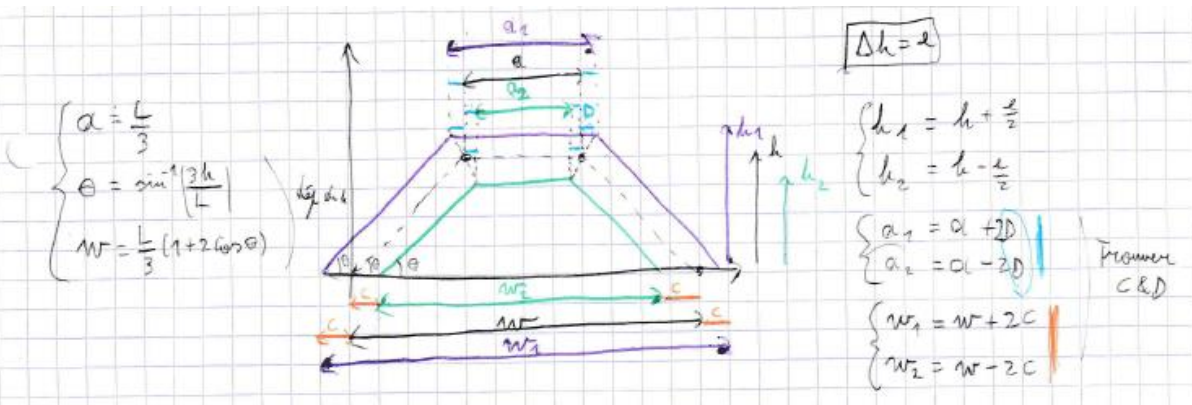
$$\begin{cases} a = \dfrac{L}{3} \\ \theta = \sin^{-1}\left(\dfrac{3h}{L}\right) \\ w = \dfrac{L}{3}(1 + 2\cos\theta) \end{cases}$$
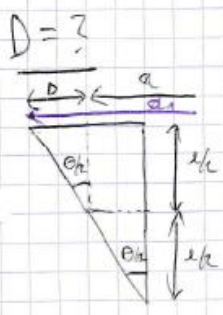
$\boxed{\Delta h = e}$

$$\begin{cases} h_1 = h + \dfrac{e}{2} \\ h_2 = h - \dfrac{e}{2} \end{cases}$$

$$\begin{cases} a_1 = a + 2D \\ a_2 = a - 2D \end{cases} \quad \text{Trouver } C \& D$$

$$\begin{cases} w_1 = w + 2C \\ w_2 = w - 2C \end{cases}$$

w_2 w_1

$D = ?$ $C = ?$

$\alpha = 90° - \theta$

$D < \dfrac{e}{2}$

$\sin\theta = \dfrac{e/2}{C}$

$\tan\dfrac{\theta}{2} = \dfrac{D}{e/2}$

$\boxed{D = \dfrac{e}{2}\tan\dfrac{\theta}{2}}$

$C = \dfrac{e/2}{\sin\theta} \quad \sin\theta = \dfrac{3h}{L}$

$C = \dfrac{e}{2}\cdot\dfrac{L}{3h}$

Controle: $\dfrac{a_1 - a}{2} = D$

$a_1 = a + 2D \checkmark$

Controle: $\dfrac{w_1 - w}{2} = C$

$$\begin{cases} a_1 = a + e\tan\dfrac{\theta}{2} \\ a_2 = a - e\tan\dfrac{\theta}{2} \end{cases}$$

$w_1 = w + 2C \checkmark$

$$\boxed{\begin{cases} a_1 = \dfrac{L}{3} + e\cdot\tan\dfrac{\theta}{2} \\ a_2 = \dfrac{L}{3} - e\cdot\tan\dfrac{\theta}{2} \end{cases}}$$

$$\begin{cases} w_1 = w + 2\cdot\dfrac{e}{2}\cdot\dfrac{L}{3h} = w + \dfrac{e}{\sin\theta} \\ w_2 = w - 2\cdot\dfrac{e}{2}\cdot\dfrac{L}{3h} = w - \dfrac{e}{\sin\theta} \end{cases}$$

$$\boxed{\begin{cases} w_1 = w + \dfrac{eL}{3h} \\ w_2 = w - \dfrac{eL}{3h} \end{cases}}$$

Controle: Si $\theta = 0° \Rightarrow a_1 = \dfrac{L}{3} + e\cdot\tan 0°$

$a_1 = \dfrac{L}{3} = a_2 \checkmark \quad \Delta a = e \checkmark$

$\theta = 90° \Rightarrow a_1 = \dfrac{L}{3} + e\cdot\tan 45°$

$a_1 = \dfrac{L}{3} + e$

$a_2 = \dfrac{L}{3} - e$

$\Delta a = 2e \checkmark$

Controle: Si $\theta \approx 0° \Rightarrow h_2 = 0$
$h = \dfrac{e}{2} \Rightarrow w = L$

controle:
$\theta \approx 0° \Rightarrow h = \dfrac{e}{2}$
$h = \dfrac{e}{2} \Rightarrow h_2 = 0$
$\Rightarrow \theta = \sin^{-1}\left(\dfrac{3e}{2L}\right)$
$\sin\theta = \dfrac{3e}{2L}$
$\theta \approx 0 \Rightarrow \theta \approx \dfrac{3e}{2L}$
$w = \dfrac{L}{3}(1 + 2\cos\theta)$
$w_1 = w + \dfrac{3e}{2}\cdot\dfrac{2}{e}$

$\theta = 90° \Rightarrow h = \dfrac{L}{3}$
$w = \dfrac{L}{3}$
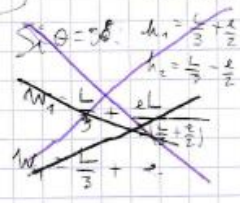
Domaine de h : $h \in \left[\frac{e}{2}, \frac{L}{3}\right]$ $\bigtriangledown$

Y_G, S & I_{ox} du model Ω
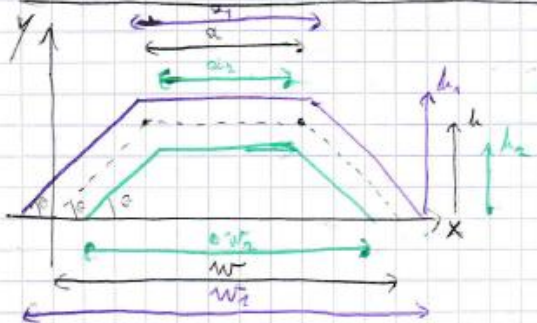
$$\begin{cases} S_1 = \frac{1}{2} h_1 (a_1 + w_1) \\ S_2 = \frac{1}{2} h_2 (a_2 + w_2) \end{cases}$$

$$\boxed{S = S_1 - S_2}$$

$$\begin{cases} Y_{G1} = \frac{1}{3} h_1 \left(\frac{2a_1 + w_1}{a_1 + w_1}\right) \\ Y_{G2} = \frac{1}{3} h_2 \left(\frac{2a_2 + w_2}{a_2 + w_2}\right) \end{cases}$$

$$\boxed{Y_G = \frac{S_1 \cdot Y_{G1} - S_2 \cdot Y_{G2}}{S_1 - S_2}}$$

$$\begin{cases} I_{ox1} = \frac{3a_1 h_1^3}{12} + \frac{b_1 h_1^3}{12} \\ I_{ox2} = \frac{3a_2 h_2^3}{12} + \frac{b_2 h_2^3}{12} \end{cases}$$

$$\boxed{I_{ox} = I_{ox1} - I_{ox2}}$$

$$\boxed{I_{Gx} = I_{ox} - S \cdot Y_G^2}$$

Breu tableau d'organe control

$$Y_G = \frac{1}{3} h \cdot \left(\frac{2a + b}{a + b}\right)$$

$$S = \frac{1}{2} h \cdot (a + b)$$

Mes calculer :
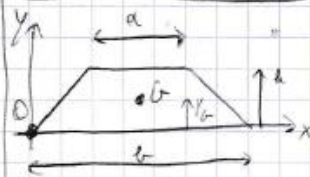
$$I_{ox\square} = \frac{3a \cdot h^3}{12} + \frac{b \cdot h^3}{12}$$

RVW :

1) $h \in \left[\frac{e}{2}, \frac{L}{3}\right]$

2) $\begin{cases} a = \frac{L}{3} \end{cases}$

3) $L \gg e > 0$

4) $h_2 > 0$; $h \geqslant \frac{e}{2}$; $\theta \in [0, 90°]$

Récapitulatif

$h = $ un paramètre variable $h \in \left[\frac{e}{2}, \frac{L}{3}\right]$

$a = \frac{L}{3}$

$\sin \theta = \frac{3h}{L}$ ou $\theta = \sin^{-1}\left(\frac{3h}{L}\right)$

$w = \frac{L}{3} \cdot (1 + 2\cos\theta)$

$$\begin{cases} h_1 = h + \frac{e}{2} \\ h_2 = h - \frac{e}{2} \end{cases}$$

$$\begin{cases} a_1 = \frac{L}{3} + e \cdot \tan\left(\frac{\theta}{2}\right) \\ a_2 = \frac{L}{3} - e \cdot \tan\left(\frac{\theta}{2}\right) \end{cases}$$

$$\begin{cases} w_1 = w + \frac{eL}{3h} = w + \frac{e}{\sin\theta} \\ w_2 = w - \frac{eL}{3h} = w - \frac{e}{\sin\theta} \end{cases}$$

Calculses de Contrôle

$L = 30$
$e = 1$

$h = 0,5 = \frac{e}{2}$

$\Rightarrow h \in [0,5 \; ; 10]$

$h = 0,5$
$\Rightarrow a = \frac{L}{3} = 10$

$\theta = \sin^{-1}\left(\frac{3h}{L}\right) =$

$\theta = \frac{3 \cdot 0,5}{30}$

$\theta = \sin^{-1}\left(\frac{3 \cdot 0,5}{30}\right)$

$\theta = 2,87° = 0,05002 \; rad$

$\sin\theta = \frac{3 \cdot 0,5}{30} = 0,05 \approx \sin\theta$

$W = \frac{L}{3} \cdot (1 + 2 \cdot \cos\theta)$

$= \frac{30}{3} \cdot (1 + 2 \cdot \cos(2,87°))$

$W = 29,97$

Contrôle w_1 & w_2

~~$0,5 \sin\theta \; \sin\theta = \frac{3h}{L}$~~
~~mais~~ $\sin\theta \approx \frac{3h}{L}$

$w_1 \neq w + \frac{e}{2\sin\theta}$

$w_2 \approx w + \frac{e}{\sin\theta}$

$\begin{cases} h_1 = \cancel{0,5} \; 0,5 + \frac{1}{2} = 1 \\ h_2 = 0,5 - \frac{1}{2} = 0 \end{cases}$ $\Big| \Delta h = 1 = e \; \checkmark$

$\begin{cases} a_1 = \frac{30}{3} + 1 \cdot \tan\left(\frac{2,87°}{2}\right) = 10,03 \\ a_2 = \frac{30}{3} - 1 \cdot \tan\left(\frac{2,87°}{2}\right) = 9,97 \end{cases}$ $\Delta a \approx 0 \; \checkmark$

$\begin{cases} w_1 = 29,97 + \frac{1 \cdot 30}{3 \cdot 0,5} = 49,97 \; ▲ \\ w_2 = 29,97 - \frac{1 \cdot 30}{3 \cdot 0,5} = 9,97 \approx a_2 \; \checkmark \end{cases}$

$S_1 = \frac{1}{2} \cdot 1 \cdot (10,03 + 49,97) = 30$

$S_2 = \frac{1}{2} \cdot 0 \cdot (\ldots) = 0$

$\boxed{S = S_1 - S_2 = 30}$

Contrôle

$Y_{G1} = \frac{1}{3} \cdot 1 \cdot \left(\frac{2 \cdot 10,03 + 49,97}{10,03 + 49,97}\right) = \cancel{0,7836} \; \cancel{0,7836}$
$= 0,3891$

$Y_{G2} = \frac{1}{2} \cdot 0 (\ldots) = 0$
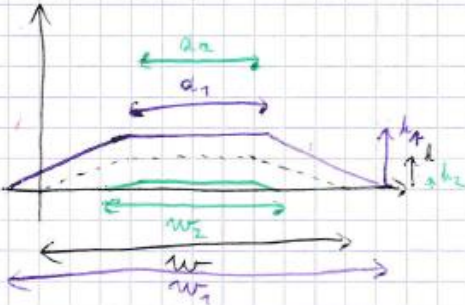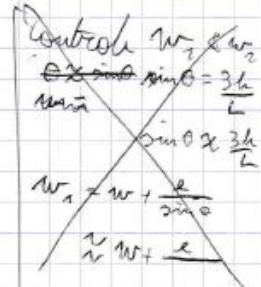
$Y_G = \frac{S_1 \cdot Y_{G1} - S_2 \cdot Y_{G2}}{S_1 - S_2}$ $\Big| \begin{array}{c} S_2 = 0 \\ Y_{G2} = 0 \end{array}$

$\boxed{Y_G = \frac{0,3891}{\cancel{0,7836}}}$

$I_{0x1} = \frac{3 \cdot 10,03 \cdot 1^3}{12} + \frac{49,97 \cdot 1^3}{12} = 6,672 \; mm^4$

$I_{0x2} = \frac{\ldots \cdot 0^3}{12} + \frac{\ldots \cdot 0^3}{12} = 0$

$\boxed{I_{0x} = I_{0x1} - \underset{=0}{I_{0x2}} = 6,672 \; mm^4}$

$I_{Gx} = I_{0x} - S \cdot Y_0^2$

$I_{Gx} = 6,672 - 30 \cdot (\underset{0,3891}{\cancel{0,7836}})^2$

$\boxed{I_{Gx} = 2,130}$ Contrôle avec interssource. com \ moment-of-inertia-trap. html $\checkmark$

Calculer erreur avec plaque droit
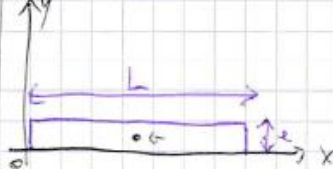
$I_{Gx} = \frac{L \cdot e^3}{12} = \frac{30 \cdot 1}{12}$

$I_{Gx} = 2,5 \; mm^4$

$I_{0x} = 2,5 + 30 \cdot 0,5^2 = 10 \; mm^4$

Erreur $I_{Gx} = \frac{\Delta I_{Gx}}{I_{Gx}} = \frac{2,5 - 2,130}{2,5}$

Erreur $I_{Gx} = 0,148 = 14,8\%$

$$L = 30$$
$$e = 1$$

$$h = 10 = \frac{L}{3}$$

$$h = 10 = \frac{30}{3}$$

$$a_L = \frac{30}{3} = 10$$

$$\sin\theta = \frac{3 \cdot 10}{30} = 1 \Rightarrow \theta = 90°$$

$$w = \frac{30}{3}(1 + 2 \cdot \cos 90°)$$

$$w = 10$$

$$\begin{cases} h_1 = 10 + 0{,}5 = 10{,}5 \\ h_2 = 10 - 0{,}5 = 9{,}5 \end{cases} \Delta h = 1 = e \checkmark$$

$$\begin{cases} a_1 = \frac{30}{3} + 1 \cdot \tan 45° = 11 \\ a_2 = \frac{30}{3} - 1 \tan 45° = 9 \end{cases} \Delta a = 2 = 2e \checkmark$$

$$\begin{cases} w_1 = 10 + \frac{1 \cdot 30}{3 \cdot 10} = 11 = a_1 \checkmark \\ w_2 = 10 - \frac{1 \cdot 30}{3 \cdot 10} = 9 = a_2 \checkmark \end{cases}$$

$$\begin{cases} S_1 = \frac{1}{2} \cdot 10{,}5 \cdot (11 + 11) = 115{,}5 \checkmark \\ S_2 = \frac{1}{2} \cdot 9{,}5 \cdot (9 + 9) = 85{,}5 \checkmark \end{cases}$$
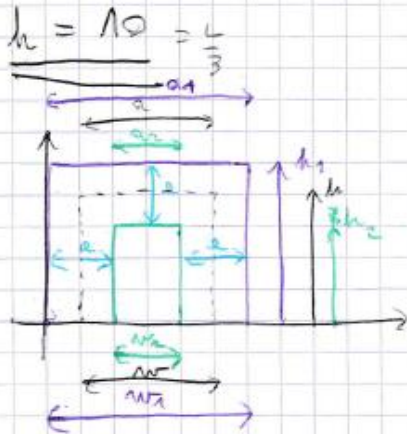
$$\boxed{S = S_1 - S_2 = 30} = S|_{h=0,5} \checkmark$$

$$\begin{cases} y_{G1} = \frac{1}{3} \cdot 10{,}5 \cdot \left(\frac{2 \cdot 11 + 11}{11 + 11}\right) = 5{,}25 \checkmark = h_1/2 \\ y_{G2} = \frac{1}{3} \cdot 9{,}5 \cdot \left(\frac{3 \cdot 9}{2 \cdot 9}\right) = 4{,}75 = h_2/2 \checkmark \end{cases}$$

$$\boxed{y_G = \frac{115{,}5 \cdot 5{,}25 - 85{,}5 \cdot 4{,}75}{30} = 6{,}675} \checkmark$$

$$I_{0x1} = \frac{3 \cdot 11 \cdot 10{,}5^3}{12} + \frac{11 \cdot 10{,}5^3}{12} = 4244{,}63 \checkmark$$

$$I_{0x2} = \frac{3 \cdot 9 \cdot 9{,}5^3}{12} + \frac{9 \cdot 9{,}5^3}{12} = 2572{,}13 \checkmark$$

$$\boxed{I_{0x} = I_{0x1} - I_{0x2} = 1672{,}50 \ mm^4} \checkmark$$

$$I_{Gx} = I_{ox} - S \cdot y_0^2$$

$$= 1672{,}5 - 30(6{,}675)^2$$

$$\boxed{I_{Gx} = 335{,}83} \checkmark$$

Contrôl fait dans ~~model Ω √6~~

model Ω base (1² √2

$$\Rightarrow I_{Ox} = 1672{,}5 \checkmark$$

$$\Rightarrow I_{Gx} = 335{,}831 \checkmark$$

Contrôle pour $\theta \to 90°$

$L = 2h + w$

$a = w$

$\theta \to \pi \to D$

$\overline{}$ Preuve: $a_1 = a + D = a + \frac{e}{2}$

$a_2 = a - D = a - \frac{e}{2}$

$W_1 = w + 2C = w + e$

$W_2 = w + 2C = w + e$

$\boxed{\text{Donc}: D = \frac{e}{2}}$

$C = \frac{e}{2}$

1) $\theta = 90°$

$D = \frac{e}{2} \tan\left(\frac{\theta}{2}\right)$

$= \frac{e}{2} \tan(45°)$ $\tan 45° = 1$

$\boxed{D = \frac{e}{2}} \checkmark$

2) $\theta = 90°$

$C = \frac{e(L-a)}{4h}$ $\begin{vmatrix} L = 2h + w \\ a = w \end{vmatrix}$

$= \frac{e(2h + w - w)}{2 \cdot 2h}$

$\boxed{C = \frac{e}{2}} \checkmark$

contrôle $\theta = 90°$:

$\theta = ?$

$\sin\theta = \frac{2h}{L-a}$ $\begin{vmatrix} L = 2h + w \\ a = w \end{vmatrix}$

$\sin\theta = \frac{2h}{2h + w - w}$

$\sin\theta = \frac{2h}{2h} = 1$

$\Rightarrow \theta = 90° \checkmark$

Récapitulatif

$C = \frac{e(L-a)}{4h}$

$D = \frac{e}{2}\tan\frac{\theta}{2}$

$E \cdot \frac{d\vec{v}}{dx} = \frac{M(x)}{I(x)}$

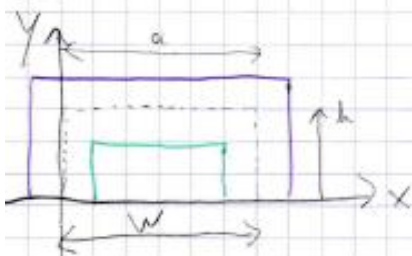$\begin{cases} h_1 = h + \frac{e}{2} \\ h_2 = h - \frac{e}{2} \\ W_1 = w + \frac{e(L-a)}{2h} = w + 2C \\ W_2 = w - \frac{e(L-a)}{2h} = w - 2C \\ a_1 = a + \frac{e}{2}\tan\frac{\theta}{2} = a + D \\ a_2 = a - \frac{e}{2}\tan\frac{\theta}{2} = a - D \end{cases}$

avec: L, E, W & e donné

$\theta = \sin^{-1}\left(\frac{2h}{L-a}\right)$

variable a variable h

$h = \sqrt{\left(\frac{L-a}{2}\right)^2 - \left(\frac{W-a}{2}\right)^2}$ $a = \frac{L^2 - W^2 - 4h^2}{2(L-w)}$

Domaine de α ℓ h

q_{max}

RVW: $L > W$

$$\boxed{a_{max} = W}$$

$$L = 2h + W$$

$$\boxed{h_{ex1} = \frac{L-W}{2}} \Rightarrow RVW: h_{ex1} > \frac{\ell}{2} \, !$$

Contrôle $h_{ex1} = \sqrt{\left(\frac{L-W}{2}\right)^2 - \left(\frac{W-W}{2}\right)^2}$

$$h_{ex1} = \sqrt{\left(\frac{L-W}{2}\right)^2} \checkmark$$

Contrôle que $h_{ex1} < h_{ex2}$

$$\frac{L-W}{2} < \sqrt{\left(\frac{L-a_{min}}{2}\right)^2 - \left(\frac{W-a_{min}}{2}\right)^2}$$

$\Downarrow$ assumption $a_{min} = \frac{\ell}{2}\tan\frac{\theta}{2} \approx 0$

$$\left\{\frac{L-W}{2}\right\}^{II} < \sqrt{\left(\frac{L}{2}\right)^2 - \left(\frac{W}{2}\right)^2}$$

$$\left(\frac{L-W}{2}\right)^2 \overset{II}{<} \left(\frac{L}{2}\right)^2 - \left(\frac{W}{2}\right)^2$$

$$\left(\frac{L}{2}\right)^2 - \frac{3}{2}LW + \frac{W}{2}\right)^2 \overset{II}{<} \left(\frac{L}{2}\right)^2 - \left(\frac{W}{2}\right)^2$$

$$2\left(\frac{W}{2}\right)^2 - LW < 0$$

$$\frac{W^2}{2} - LW < 0$$

$$W\left(\frac{W}{2} - L\right) < 0 \checkmark$$
$$\Rightarrow \text{parce que } L > W$$

$a = 0$ si $\theta = 0$
$\theta = 0$ si $h = 0$
$\Rightarrow$ pas possible

$a_2 = \alpha$ & θ

$a_2\,min = 0$

$\alpha = a_2 + \frac{\ell}{2}\tan\frac{\theta}{2}$

$$\boxed{\alpha_{min} = \frac{\ell}{2}\tan\frac{\theta}{2}}$$

$\Rightarrow \theta = \sin^{-1}\left(\frac{2h}{L-a}\right) \approx \sin^{-1}\left(\frac{2h}{L-a_2}\right)$

$\approx \frac{2h}{L}$

$$h_{ex2} = \sqrt{\left(\frac{L - \frac{\ell}{2}\tan\frac{\theta}{2}}{2}\right)^2 - \left(\frac{W - \frac{\ell}{2}\tan\frac{\theta}{2}}{2}\right)^2}$$

$\Rightarrow$ pas simplifiable

$$\boxed{h_{ex2} = \sqrt{\left(\frac{L-\alpha_{min}}{2}\right)^2 - \left(\frac{W-\alpha_{min}}{2}\right)^2}}$$

$\alpha \in \left[\frac{\ell}{2}\tan\frac{\theta_{min}}{2}, W\right]$

$h \in \left[\frac{L-W}{2}, \sqrt{\left(\frac{\frac{\ell}{2}\tan\frac{\theta}{2}}{2}\right)^2 - \dots}\right]$

ou $h \in \left[\frac{L-W}{2}, \sqrt{\left(\frac{L-a_{min}}{2}\right)^2 - \dots}\right]$

avec $\theta = \sin^{-1}\left(\frac{2h}{L-a}\right)$

$a_{min} = \frac{\ell}{2}$

$d_2 = 0$

$a - \frac{e}{2}\tan\frac{\theta}{2} = 0$

$\frac{e}{2}\tan\frac{\theta}{2} = a$

$\tan\frac{\theta}{2} = \frac{2a}{e}$

$\tan 2\alpha = \frac{2\tan\alpha}{1-\tan^2\alpha}$

$\Downarrow \quad \alpha = \frac{\theta}{2}$

$\tan\frac{\theta}{2} = \frac{2a}{e}$

(1) $\quad \tan\theta = \dfrac{\frac{2a}{e}}{1-\frac{4a^2}{e^2}}$

$\tan\theta = \frac{2h}{?}$

(2) $\quad \tan\theta = \dfrac{h}{\frac{w-a}{2}} = \dfrac{2h}{w-a}$

(1)=(2)

$\dfrac{2h}{w-a} = \dfrac{\frac{1}{2}\cdot\frac{4}{e}a}{\frac{1}{e^2}(e^2-4a^2)}$

(3) $\quad h = \dfrac{4\,a\cdot e}{e^2-4a^2}\cdot\dfrac{w-a}{2}$

(4) $\quad h^2 = \left(\dfrac{L-a}{2}\right)^2 - \left(\dfrac{w-a}{2}\right)^2$

$(3) \Rightarrow (4)$

$\left(\dfrac{L-a}{2}\right)^2 - \left(\dfrac{w-a}{2}\right)^2 = \left(\dfrac{4\,a\,e}{e^2-4a^2}\right)^2\cdot\left(\dfrac{w-a}{2}\right)^2$

$\left(\dfrac{L-a}{2}\right)^2 = \left(\left(\dfrac{4\,a\,e}{e^2-4a^2}\right)^2+1\right)\left(\dfrac{w-a}{2}\right)^2$

$\Downarrow$

$\dfrac{\left(\frac{L-a}{2}\right)^2}{\left(\frac{w-a}{2}\right)^2} = \dfrac{\frac{(L-a)^2}{4}}{\frac{(w-a)^2}{4}} = \dfrac{(L-a)^2}{(w-a)^2}$

(5) $\quad \left(\dfrac{L-a}{w-a}\right)^2 = \left(\dfrac{4\,a\,e}{e^2-4a^2}\right)^2 + 1$

Cepend((5))

Solve((5), a) $\Rightarrow$ rien

$\Rightarrow$ Trop difficile de calculer ~~la limite~~ a_{min}

approx $\Rightarrow$ $a = \frac{e}{2}\tan\frac{\theta}{2}$ avec $\theta < 90°$

$\Rightarrow \theta \leq 90° \Rightarrow \frac{\theta}{2}\leq 45° \Rightarrow \boxed{\tan\frac{\theta}{2}\leq 1}$

pour θ

estimation : $\boxed{a = \frac{e}{2}}$

$\boxed{h = \sqrt{\left(\frac{L-\frac{e}{2}}{2}\right)^2 - \left(\frac{w-\frac{e}{2}}{2}\right)^2}}$

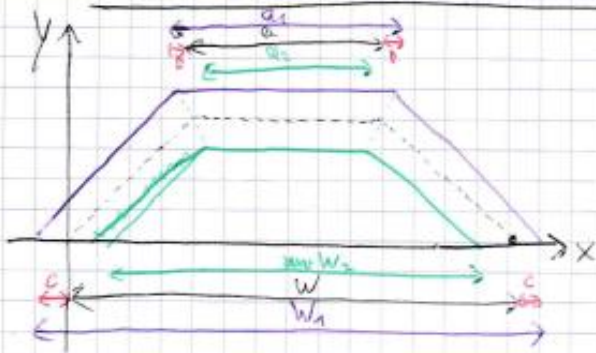$\boxed{\tan\theta = \dfrac{2h}{w-\frac{e}{2}}}$

$a_{min} = \frac{e}{2}$

$h_{max} = \sqrt{\left(\frac{L-\frac{e}{2}}{2}\right)^2 - \left(\frac{w-\frac{e}{2}}{2}\right)^2}$

$\Rightarrow \begin{cases} a \in \left[\frac{e}{2}, W\right] \\ h \in \left[\frac{L-W}{2}, \sqrt{\left(\frac{L-\frac{e}{2}}{2}\right)^2 - \left(\frac{w-\frac{e}{2}}{2}\right)^2}\right] > \frac{e}{2} \end{cases}$

y_G, S & I_{GX} du modèle Ω base c^{te}

$$S \stackrel{?}{=} S_1 = \frac{1}{2} h_1 (a_1 + W_1)$$

$$S_2 = \frac{1}{2} h_2 (a_2 + W_2)$$

$$\boxed{S = \frac{1}{2} h_1 (a_1 + W_1) - \frac{1}{2} h_2 (a_2 + W_2) = S_1 - S_2}$$

$$y_{G1} = \frac{1}{3} h_1 \left(\frac{2 a_1 + W_1}{a_1 + W_1} \right)$$

$$y_{G2} = \frac{1}{3} h_2 \left(\frac{2 a_2 + W_2}{a_2 + W_2} \right)$$

$$\boxed{y_G = \frac{S_1 \cdot y_{G1} - S_2 \cdot y_{G2}}{S_1 - S_2}}$$

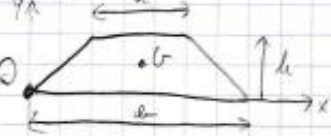$$I_{\alpha x 1} = \frac{3 a_1 \cdot h_1^3}{12} + \frac{W_1 \cdot h_1^3}{12}$$

$$I_{\alpha x 2} = \frac{3 a_2 \cdot h_2^3}{12} + \frac{W_2 \cdot h_2}{12}$$

$$\boxed{I_{0x} = I_{0x1} - I_{0x2}}$$

$$\boxed{I_{Gx} = I_{0x} - S \cdot y_G^2}$$

Right column:

Bon bidouleur

Trapezoïde

$$y_G = \frac{3h}{3} \left(\frac{2a + b}{a + b} \right)$$

$$y_G = \frac{1}{3} \cdot h \cdot \left(\frac{2a + b}{a + b} \right)$$

$$S = \frac{1}{2} h \cdot (a + b)$$

Mes calculs

$$I_{0x} \; \square = \frac{3 \cdot a \cdot h^3}{12} + \frac{b \cdot h^3}{12}$$

$$\boxed{R/W : \text{si } L > W, \text{ pas } L = W!}$$

2) L & $W >> e$
   $\Rightarrow$ contrainte : $h_{min} < h_{max}$

3) $\theta \geq 90° \;\; \theta \in [0, \frac{\pi}{2}]$

4) $h > \frac{e}{2}$
   $\Rightarrow \boxed{L > W + e}$!

$$\left(I_{Gx} + y_G^2 \cdot S = I_{0x} \right)$$

Avec

$$h_1 = h + \frac{e}{2}$$

$$h_2 = h - \frac{e}{2}$$

$$W_1 = W + \frac{e(L - a)}{2h}$$

$$W_2 = W - \frac{e(L - a)}{2h}$$

$$a_1 = a + \frac{e}{2} \tan \frac{\theta}{2}$$

$$a_2 = a - \frac{e}{2} \tan \frac{\theta}{2}$$

$$\theta = \sin^{-1} \left(\frac{2h}{L - a} \right)$$

var a : $h = \sqrt{\left(\frac{L-a}{2}\right)^2 - \left(\frac{W-a}{2}\right)^2}$

var h : $a = \frac{L^2 - W^2 - 4h^2}{2(L - W)}$

pour a : $a \in [0, W]$

pour h : $h \in \left[\frac{L - W}{2}, \sqrt{\left(\frac{L}{2}\right)^2 - \left(\frac{W}{2}\right)^2} \right]$

e, L & W donné

$\begin{cases} \text{pour } a : & a \in \left[\frac{a}{2}, W \right] \\ \text{pour } h : & h \in \left[\frac{L-W}{2}, \sqrt{\left(\frac{L}{2}\right)^2 - \left(\frac{W}{2}\right)^2} \right] \\ & h_{min} \qquad h_{max} \end{cases}$

94

Calculs de controle

$L = 30$ $a \in [e, W]$

$W = 10$ $h \in [h_{min}, h_{max}]$

$e = 1$

$\Rightarrow a \in [1 ; 10]$

$\Rightarrow h \in [10 ; \sqrt{130}]$

$h_{min} = \frac{L-W}{2} = \frac{30-10}{2}$
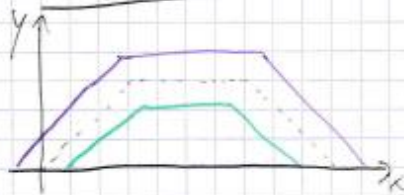
$\qquad = 20/2 = 10$

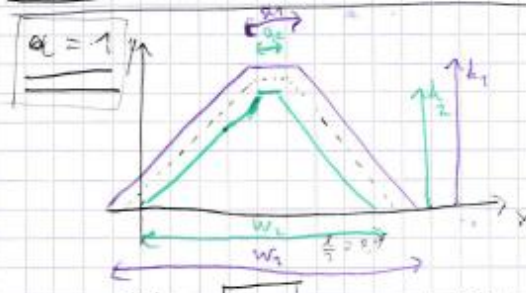$h_{max} = \sqrt{\left(\frac{L-e}{2}\right)^2 - \left(\frac{W-e}{2}\right)^2}$

$\frac{L-e}{2} = \frac{29}{2} (= 14,5)$

$\frac{W-e}{2} = \frac{9}{2} (= 4,5)$

$h_{max} = \sqrt{\left(\frac{29}{2}\right)^2 - \left(\frac{9}{2}\right)^2}$

$h_{max} = \sqrt{130}$

$h_{max} \approx 13,784$

$a = 1$

$h = h_{max}$

$h = \sqrt{130}$

$\theta = \sin^{-1}\left(\frac{2\sqrt{130}}{30-1}\right)$

$\theta = 1,255 \text{ rad} = 71,92°$

$h_1 = \sqrt{130} + 0,5 = 14,284$

$h_2 = \sqrt{130} - 0,5 = 13,284$

$\Delta h = 1 = e \checkmark$

Controle :

$a = \frac{L^2 - W^2 - 4h^2}{2(L-W)}$

$= \frac{30^2 - 10^2 - (2\sqrt{130})^2 \cdot 4}{2(30-10)}$

$= 1,00013 \checkmark$

$\begin{cases} a_1 = 1 + 1 \cdot \tan\left(\frac{71,92°}{2}\right) = 1,726 \\ a_2 = 1 - 1 \cdot \tan\left(\frac{71,92°}{2}\right) = 0,275 \end{cases}$ $|\Delta a \leqslant 2e \checkmark$

$W_1 > W_2$

$W_1 = 10 + \frac{1(30-1)}{2 \cdot \sqrt{130}} = 11,052$

$W_2 = 10 - \frac{1(30-1)}{2 \cdot \sqrt{130}} = 8,948$ $\Delta W \geqslant 2e \checkmark$

$S_1 = \frac{1}{2} \cdot 14,284 \cdot (1,726 + 11,052) = 91,261$

$S_2 = \frac{1}{2} \cdot 13,284 \cdot (0,275 + 8,248) = 61,259$
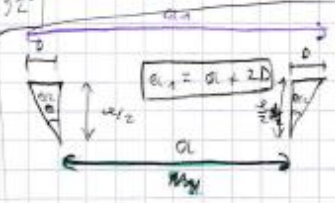
$S = S_1 - S_2 = 30,002 = L \cdot e$

$y_{G1} = \frac{1}{3} \cdot 14,284 \cdot \frac{2 \cdot 1,726 + 11,052}{1,726 + 11,052} = 5,404$

$y_{G2} = \frac{1}{3} \cdot 13,284 \cdot \frac{2 \cdot 0,275 + 8,248}{0,275 + 8,248} = 4,560$

$y_G = \frac{S_1 y_{G1} - S_2 y_{G2}}{(S_1 - S_2) = S} = \frac{91,261 \cdot 5,404 - 61,259 \cdot 4,560}{30,002}$
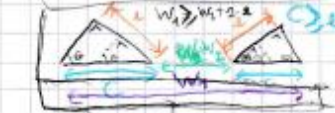
$y_G = 7,127 \rightarrow$ à l'aire de trou

$I_{0x1} = \frac{3 \cdot a_1 h_1^3}{12} + \frac{W_1 h_1^3}{12} = \frac{3 \cdot 1,726 \cdot 14,284^3}{12} + \frac{11,052 \cdot 14,284^3}{12}$

$I_{0x2} = \frac{3 \cdot a_2 h_2^3}{12} + \frac{W_2 h_2^3}{12} = \frac{3 \cdot 0,275 \cdot 13,284^3}{12} + \frac{8,248 \cdot 13,284^3}{12}$

$I_{0x1} = 3741,73 \text{ mm}^4$

$I_{0x2} = 1909,12 \text{ mm}^4$

$a_1 = a + 2D$

$\tan\frac{\theta}{2} \leqslant 1$

$D \leqslant \frac{e}{2} \Rightarrow 2D \leqslant e$

$a_1 = a_2 + 4D$

$\Delta a = 4D$

$\boxed{\Delta a \leqslant 2e}$

$W_1 \geqslant W_2 + 2 \cdot e$

$I_{0x} = I_{0x1} - I_{0x2}$

$I_{0x} = 2032,61 \text{ mm}^4$

$I_{Gx} = I_{0x} - S \cdot y_G^2$

$= 2032,61 - 30,002 \cdot (7,127)^2$

$I_{Gx} = 508,69 \text{ mm}^4$

Petit controle

$I_{0x1} = \frac{W_1}{36} \cdot 11,052 \cdot (14,284)^3 + \frac{11,052}{2}(14,284)^3 \cdot \frac{1}{3}$

$I_{0x2} = \frac{1}{36} \cdot 8,948 \cdot 13,284^3 + \frac{8,248}{2}(13,284)^3 \cdot \frac{1}{3}$

$I_{0x1} = 3741,9 \text{ mm}^4 < 3745 \checkmark$

$I_{0x2} = 1746,96 < 1909 \checkmark$

$$\boxed{a = W = 10}$$
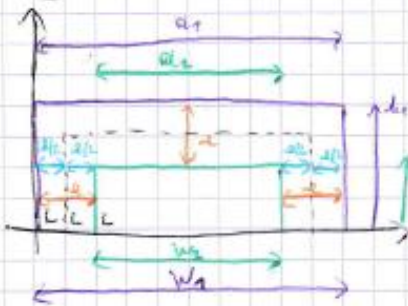
$L = 30$
$W = 10$
$\ell = 1$

$$\boxed{h = \frac{L-W}{2} = 10}$$

Contrôle : $\Theta = \sin^{-1}\left(\frac{2h}{L-a}\right)$
$= \sin^{-1}\left(\frac{2 \cdot 10}{30-10}\right)$
$= \sin^{-1}\left(\frac{20}{20}\right)$
$\Theta = \sin^{-1}|1| = \frac{\pi}{2} = 90° \checkmark$

$$a = \frac{L^2 - W^2 - 4h^2}{2(L-W)}$$
$$= \frac{30^2 - 10^2 - 4 \cdot 10^2}{2(30-10)}$$
$$= 10 \checkmark$$

$\begin{cases} h_1 = 10+0,5 = 10,5 \\ h_2 = 10-0,5 = 9,5 \end{cases}$ $\Delta h = 1 = e \checkmark$

$\begin{cases} 2a_1 = 10 + 1 \cdot \tan 45° = 11 \\ a_2 = 10 + 1 \cdot \tan 45° = 9 \end{cases}$ $2a = 2 = 2e \checkmark$

$\begin{cases} W_1 = 10 + \frac{1 \cdot (30-10)}{2 \cdot 10} = 11 = a_1 \checkmark \\ W_2 = 10 - \frac{1 \cdot (30-10)}{2 \cdot 10} = 9 = a_2 \checkmark \end{cases}$

$\begin{cases} S_1 = \frac{1}{2} \cdot 10,5 \cdot (11+11) = 115,5 = a_1 \cdot h_1 \checkmark \\ S_2 = \frac{1}{2} \cdot 9,5 \cdot (9+9) = 85,5 = a_2 \cdot h_2 \checkmark \end{cases}$

$$\boxed{S = S_1 - S_2 = 30} = S|_{a=e} \Rightarrow \text{si l'aire reste } L \cdot e = c^{te}$$
$$S = L \cdot e \checkmark$$

$y_{G1} = \frac{1}{3} \cdot 10,5 \cdot \left(\frac{11 \cdot 2 + 11}{11+11}\right) = 5,25 \left(= \frac{h_1}{2} \checkmark\right)$

$y_{G2} = \frac{1}{3} \cdot 9,5 \cdot \left(\frac{2 \cdot 9 + 9}{9+9}\right) = 4,75 \left(= \frac{h_2}{2} \checkmark\right)$

$y_G = \frac{S_1 y_{G1} - S_2 y_{G2}}{S}$

$y_G = \frac{115,5 \cdot 5,25 - 85,5 \cdot 4,75}{30}$

$$\boxed{y_G = 6,675} \Rightarrow \text{a l'air de rouge}$$

$\begin{cases} I_{ox1} = \frac{3 \cdot a_1 \cdot h_1^3}{12} + \frac{w_1 \cdot h_1^3}{12} = \frac{3 \cdot 11 \cdot (10,5)^3}{12} + \frac{11 \cdot (10,5)^3}{12} \\ I_{ox2} = \frac{3 \cdot a_2 \cdot h_2^3}{12} + \frac{w_2 \cdot h_2^3}{12} = \frac{3 \cdot 9 \cdot (9,5)^3}{12} + \frac{9 \cdot (9,5)^3}{12} \end{cases}$

$I_{ox1} = 4249,63 \text{ mm}^4$

$I_{ox2} = 2572,13 \text{ mm}^4$

$$\boxed{I_{ox} = I_{ox1} - I_{ox2} = 1672,50 \text{ mm}^4}$$

$$\boxed{I_{Gx} = I_{ox} - S \cdot y_G^2}$$

$= 1672,50 - 30 \cdot 6,675^2$

$$\boxed{I_{Gx} = 335,83 \text{ mm}^4}$$

$y_{G1} = h_1/2$
$y_{G2} = h_2/2$

$I_{9x1} = \frac{w_1 \cdot h_1^3}{12} + w_1 \cdot h_1 \left(\frac{h_1}{2}\right)^2$
$= \frac{11 \cdot 10,5^3}{12} + 11 \cdot 10,5 \cdot \frac{10,5^2}{4}$

$I_{ox1} = 4244,63 \checkmark$

$I_{ox2} = \frac{w_2 \cdot h_2^3}{12} + w_2 \cdot h_2 \left(\frac{h_2}{2}\right)^2$
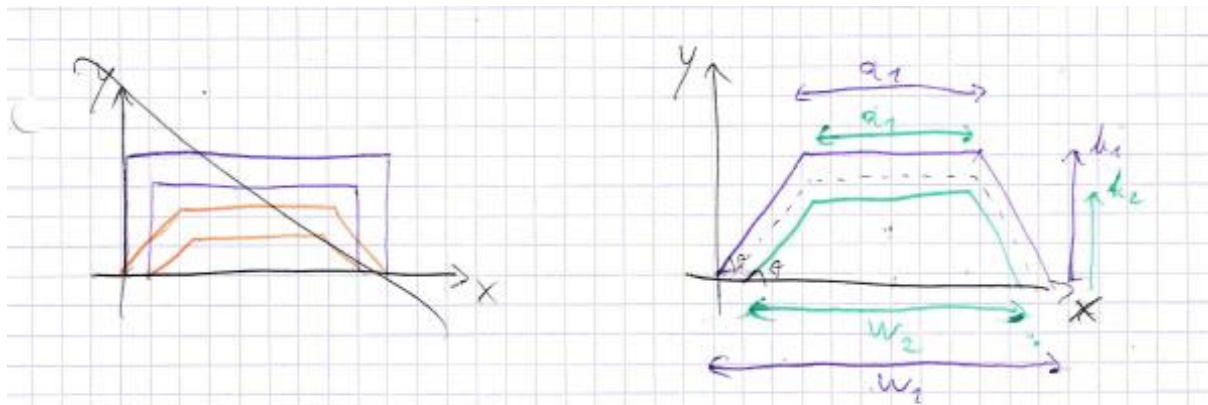$= \frac{9 \cdot 9,5^3}{12} + \frac{9 \cdot 9,5^3}{4}$

$I_{ox2} = 2572,13 \text{ mm} \checkmark$

$I_{ox} = 1672,50 \checkmark$

$I_{Gx} = I_{ox} - S \cdot y_G^2$ $S = h_1 \cdot w_1 - h_2 \cdot w_2$

$= 1672,50 - (10,5 \cdot 11 - 9,5 \cdot 9) \cdot \left(\frac{\frac{10,5 \cdot 10,5}{2} - 9,5 \cdot \frac{9,5}{2}}{115,5 - 9,25}\right)^2$

$$\boxed{I_{Gx} = 335,83 \text{ mm}^4 \checkmark}$$

Pour tous : $L = 30$
$\ell = 1$

Model $\Sigma \Sigma$ | $\alpha = 1$ ① $h_1 = 14,284$ $\theta = 71,92°$
base c^{te} $h_2 = 13,284$
                                     $a_1 = 1,726$ $\Rightarrow I_{Gx} = 508,69 \text{ mm}^4$
                                     $a_2 = 0,275$ $Ig = 507,96 \text{ mm}^4$
                                     $W_1 = 11,052$
                                     $W_2 = 8,948$ $S = 30 \text{ mm}^2$
                                                          $Y_G = 7,123 \text{ mm}$

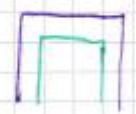   ② $h_1 = 10,5$ $\theta = 90°$
                                     $h_2 = 9,5$
                                     $a_1 = 11$ $\Rightarrow \tilde{I}_{Gx} = 335,83 \text{ } 1 \text{ mm}^4$
                                     $a_2 = 9$
                                     $W_1 = 11$ $Ig = 335,031 \text{ mm}^4$
                                     $W_2 = 9$ $S = 90 \text{ mm}^2$
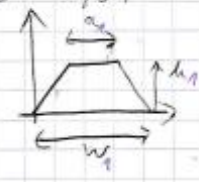 $Y_G = 6,675$

Model Ω ③ $\begin{cases} h_2 = 0 \\ a_2 = 0 \\ w_2 = 0 \end{cases}$ $\theta = 2,87°$
$\rightarrow$ Trapèze
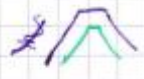
                                     $h_1 = X = 1$
                                     $a_1 = a = 10,03$ $\Rightarrow I_{Gx} = 2,136 \text{ mm}^4$
                                     $w_1 = W = 49,98$
                                     $= 50,985 \text{ mm}$
                                                               $I_G = 2,131 \text{ mm}^4$
Prochain fois : $S = 30,005 \text{ mm}^2$
Calculer entre les deux états 4, 5 $Y_G = 0,983 \text{ mm}$
  $\Rightarrow$ W entre 4 et 5
    $\Rightarrow$ pour a_i tout
  4) $a = 5$
  5) $h = 5$
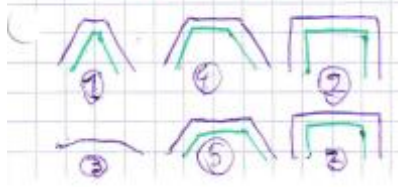
Appendix E: MATLAB code to calculate the deformation analytically

Code:

```
clc
clear

%Function M(x) = 2nd order polyn
syms q;
syms H;
syms x;

M(x) = -q/2*(x^2) + q*H*x - q*H^2/2;
fprintf('M(x) = ');
disp(M(x));

%Function I(x) = 2nd order polyn
syms h;
syms u;
syms v;
syms w;
%syms L;
%syms W;
%syms dh;

syms A;
syms B;
%In excel: A & B used as simplificaitons, calculate for the
functions

I(h) = u*(h^2) + v*h + w;
fprintf('I(h) = ');
disp(I(h));

I(x) = I(A*x + B);
fprintf('I(x) = ');
disp(I(x));

%Function f(x) = M(x)/I(x) = E*d²v/dx²
f(x) = M(x)/I(x);
fprintf('f(x) = ');
disp(f(x));

syms C1;
ff(x) = int(f(x),x) + C1;
fprintf('ff(x) = ');
disp(ff(x));

syms C2;
fff(x) = int(ff(x),x) + C2;
fprintf('fff(x) = ');
disp(fff(x));
```

Results from command window:
```
M(x) = H*q*x - (q*x^2)/2 - (H^2*q)/2

I(h) = u*h^2 + v*h + w
```

```
I(x) = w + v*(B + A*x) + u*(B + A*x)^2

f(x) = -((q*H^2)/2 - q*H*x + (q*x^2)/2)/(w + v*(B + A*x) + u*(B +
A*x)^2)

ff(x) = C1 - (log(u*A^2*x^2 + 2*u*A*B*x + v*A*x + u*B^2 + v*B +
w)*(- 16*H*q*w*A^4*u^2 + 4*H*q*A^4*u*v^2 - 16*B*q*w*A^3*u^2 +
4*B*q*A^3*u*v^2 - 8*q*w*A^3*u*v + 2*q*A^3*v^3))/(2*(16*w*A^6*u^3 -
4*A^6*u^2*v^2)) - (q*x)/(2*A^2*u) - (q*atan((v + 2*B*u +
2*A*u*x)/(4*u*w - v^2)^(1/2))*(2*A^2*H^2*u^2 + 4*A*B*H*u^2 +
2*A*H*u*v + 2*B^2*u^2 + 2*B*u*v - 2*w*u + v^2))/(2*A^3*u^2*(4*u*w -
v^2)^(1/2))

fff(x) = C2 - x*((- 2*C1*A^4*u^2 + 2*H*q*A^2*u + 4*B*q*A*u +
2*q*v*A)/(2*A^4*u^2) - (q*(4*B*A^3*u^2 + 2*v*A^3*u))/(4*A^6*u^3)) -
(log(((q*x*(A^2*H^2*u^2 + 4*A*B*H*u^2 + 2*A*H*u*v + 3*B^2*u^2 +
3*B*u*v - w*u + v^2))/(2*A^2*u^2) - ((v + 2*B*u + 2*A*u*x)*(q*v^2 +
3*B^2*q*u^2 + A^4*u^3*(-(q^2*(2*A^2*B*H^2*u^3 + A^2*H^2*u^2*v +
4*A*B^2*H*u^3 + 4*A*B*H*u^2*v - 4*w*A*H*u^2 + 2*A*H*u*v^2 +
2*B^3*u^3 + 3*B^2*u^2*v - 6*w*B*u^2 + 3*B*u*v^2 - 3*w*u*v +
v^3)^2)/(A^8*u^6*(- v^2 + 4*u*w)))^(1/2) - q*u*w + A^2*H^2*q*u^2 +
3*B*q*u*v + 2*A*H*q*u*v + 4*A*B*H*q*u^2))/(4*A^3*u^3) + (q*(v +
2*B*u + 2*A*H*u)*(u*B^2 + v*B + w))/(2*A^3*u^2))*((q*x*(A^2*H^2*u^2
+ 4*A*B*H*u^2 + 2*A*H*u*v + 3*B^2*u^2 + 3*B*u*v - w*u +
v^2))/(2*A^2*u^2) - ((v + 2*B*u + 2*A*u*x)*(q*v^2 + 3*B^2*q*u^2 -
A^4*u^3*(-(q^2*(2*A^2*B*H^2*u^3 + A^2*H^2*u^2*v + 4*A*B^2*H*u^3 +
4*A*B*H*u^2*v - 4*w*A*H*u^2 + 2*A*H*u*v^2 + 2*B^3*u^3 + 3*B^2*u^2*v
- 6*w*B*u^2 + 3*B*u*v^2 - 3*w*u*v + v^3)^2)/(A^8*u^6*(- v^2 +
4*u*w)))^(1/2) - q*u*w + A^2*H^2*q*u^2 + 3*B*q\\r\n*u*v +
2*A*H*q*u*v + 4*A*B*H*q*u^2))/(4*A^3*u^3) + (q*(v + 2*B*u +
2*A*H*u)*(u*B^2 + v*B + w))/(2*A^3*u^2)))*(- 8*q*A^6*H^2*u^3*w +
2*q*A^6*H^2*u^2*v^2 - 32*q*A^5*B*H*u^3*w + 8*q*A^5*B*H*u^2*v^2 -
16*q*A^5*H*u^2*v*w + 4*q*A^5*H*u*v^3 - 24*q*A^4*B^2*u^3*w +
6*q*A^4*B^2*u^2*v^2 - 24*q*A^4*B*u^2*v*w + 6*q*A^4*B*u*v^3 +
8*q*A^4*u^2*w^2 - 10*q*A^4*u*v^2*w + 2*q*A^4*v^4))/(2*(16*w*A^8*u^4
- 4*A^8*u^3*v^2)) - (q*x^2)/(4*A^2*u) + (x*log(u*A^2*x^2 + 2*u*A*B*x
+ v*A*x + u*B^2 + v*B + w)*(8*H*q*A^4*u^3 + 8*B*q*A^3*u^3 +
4*q*v*A^3*u^2))/(16*A^6*u^4) - (x*atan((v + 2*B*u + 2*A*u*x)/(4*u*w
- v^2)^(1/2))*(2*q*A^2*H^2*u^2 + 4*q*A*B*H*u^2 + 2*q*A*H*u*v +
2*q*B^2*u^2 + 2*q*B*u*v - 2*q*w*u + q*v^2))/(2*A^3*u^2*(4*u*w -
v^2)^(1/2)) - (q*atan((v + 2*B*u + 2*A*u*x)/(4*u*w -
v^2)^(1/2))*(2*A^2*B*H^2*u^3 + A^2*H^2*u^2*v + 4*A*B^2*H*u^3 +
4*A*B*H*u^2*v - 4*w*A*H*u^2 + 2*A*H*u*v^2 + 2*B^3*u^3 + 3*B^2*u^2*v
- 6*w*B*u^2 + 3*B*u*v^2 - 3*w*u*v + v^3))/(2*A^4*u^3*(4*u*w -
v^2)^(1/2))
```